Effective Field Theories for Generalized Spin Ladders

Vom Fachbereich Physik der Universität Hannover

zur Erlangung des Grades
Doktor der Naturwissenschaften
– Dr. rer. nat. –

genehmigte Dissertation

von

M. Sc. Teimuraz Vekua
geboren am 23.05.1976 in Tbilissi, Georgien

2003

Referent:	Prof. Dr. H.-J. Mikeska
Korreferent:	Prof. Dr. O. Lechtenfeld
Tag der Promotion:	15. Juli 2003

Effektive Feldtheorien für verallgemeinerte Spinleitern

Kurzzusammenfassung

Thema der vorliegenden Arbeit ist die Untersuchung des Phasendiagramms verallgemeinerter Spinleitern mit effektiver feldtheoretischer Beschreibung. Zwei verschiedene Spin Systeme werden untersucht. Im ersten Teil der Doktorarbeit wird eine antiferromagnetische SU(2)-symmetrische Spinleiter mit zusätzlicher zyklischer Vier-Spin-Wechselwirkung (Ringaustausch) untersucht. Das Hauptziel dieses Teiles der Doktorarbeit ist die Erklärung des Frustrationseffektes produziert durch Ringaustausch auf dem Grundzustandsphasendiagramm und des Verhaltens des Modelles bei endlichen Temperaturen.

Die Bosonisierung-Fermionisierungsmethode wird verwendet für die Beschreibung der niederenergetischen Anregungen der Spinleiter mit den massiven, schwach wechselwirkenden Majorana Fermionen. Diese Methode ermöglicht auch einen Teil des Grundzustandsphasendiagramms für genügend starke Frustration zu bekommen. Der gewöhnliche Sprossensinglett-Grundzustand der Spinleiter geht durch einen Quantenphasenübergang in eine spontan dimerisierte Phase mit zunehmendem Ringaustausch über. Eine weitere Transformation zu zweidimensionalen Ising Variablen wird benutzt, um Korrelationsfunktionen des Modells mit 2D Ising Korrelationsfunktionen in Verbindung zu bringen, die analytisch nicht nur im kritischen Punkt sondern auch in der massiven Phase bekannt sind. Die quasiteilchen-ähnliche Anregung (Magnon) verschwindet aus dem niederenergetischen Anregungsspektrum. Die letztere ist aus einem Kontinuum von Dimerisierungskinks zusammengesetzt, die zwischen zwei degenerierten Vacua des spontan dimerisierten Grundzustands interpolieren. Die fermionische Beschreibung niederenergetischer Freiheitsgrade ermöglicht uns sowohl Thermodynamik als auch endlich-temperaturdynamisches Verhalten des Modelles zu studieren. Die Temperaturabhängigkeit verschiedener Responsefunktionen, Suszeptibilitäten, der Spezifische Wärme und der kernmagnetischen Resonanz-Relaxationsrate werden mit konformer Feldtheorie und Matsubara-Formalismus berechnet.

In dem zweiten Teil der Doktorarbeit wird das Grundzustandsphasendiagramm von zwei ferromagnetiesches Spin 1/2 Ketten untersucht, die mit bilinearen Kopplungen von beliebigem Vorzeichen gekoppelt sind. Das Hauptziel dieses Teils ist, die Auswirkungen der Anisotropien in sowohl Holm- als auch in Sprossenkopplungen über das Grundzustandsphasendiagramm zu beschreiben. Man bekommt ein extrem reiches Phasendiagram für das Modell. Alle Phasen der Spin 1 Kette mit zusätzlicher singleionischer Anisotropie können (XY1, XY2, Haldane, Starke D, Ferromagnetisch) realisiert werden für verschiedene Werte der Anisotropie. Zusätzlich bekommt man weniger bekannte Phasen, die nicht bei Spin 1 Ketten vorkommen.

Der Bosonisierungs-Formalismus wird durch die Kombinierung exakter (nichtperturbativer) für isolierte Ketten verfügbarer Methoden mit einem linearisierten Ausdruck für die Wechselwirkung zwischen Ketten zum ferromagnetischen Instabilitätspunkt für eine isolierte Kette hin erweitert. Zusätzlich zur Bosonisierung werden Spinwellen und starke Sprossenkopplungsentwicklung benützt, um die exakte Grenze der ferromagnetischen Phase zu bekommen. Grundzustandskorrelationsfunktionen werden überall auf der Phasendiagramme berechnet.

Schlagworte: Spinleitern, Bosonisierung, Phasendiagramm

Effective Field Theories for Generalized Spin Ladders

Abstract

In the present work generalized spin $1/2$ ladder systems are investigated using the continuum limit of the effective field theory description.
Two different spin ladder systems are considered: first part of the thesis is concerned with the study of a $SU(2)$ antiferromagnetic ladder with additional four-spin ring interactions. The main aim of this part of the thesis is to study the effects of frustration produced by additional biquadratic terms on the ground state phase diagram as well as the finite temperature behavior of the model.
The bosonization- fermionization approach is used to describe the low energy excitations of the model in terms of weakly interacting massive Majorana fermions. This allows us to obtain a part of the ground state phase diagram for sufficiently strong frustration. We found that the ordinary rung singlet phase of the pure antiferromagnetic ladder undergoes a quantum phase transition to a spontaneously dimerized phase with increasing ring exchange. Further transformation to two dimensional Ising variables is used to relate correlation functions of the model with the 2D Ising correlation functions that are known analytically both at and off criticality. The single magnon that is a well defined particle like excitation in the ordinary ladder disappears from the low energy excitation spectrum. The latter is exhausted by the continuum of incoherent dimerization kinks interpolating between two degenerate vacua of a spontaneously dimerized state. The fermionic representation of the low energy degrees of freedom allows us to study thermodynamics as well as a dynamical behavior of the model at finite temperature. The temperature dependence of various response functions, susceptibilities, specific heat, and nuclear magnetic resonance relaxation rate is calculated using the conformal field theory and the finite temperature Matsubara formalism.
In the second part of the thesis we study the ground state phase diagram of two spin $1/2$ ferromagnetic chains coupled by the exchange interactions of arbitrary sign. The aim is to describe the effects of the anisotropies both in intra and interchain interactions on the ground state phase diagram of the spin ladder. All known phases for the spin 1 chain with additional single ion anisotropy are realized for various values of anisotropies ($XY1$, $XY2$, Haldane like, large D, ferromagmetic phases). In addition less conventional phases are obtained that are not encountered in the analysis of spin 1 chain and thus are genuine to ladder systems. By combining exact (nonperturbative) results, available for the single chain, with linearized expressions for interchain interaction the bosonization formalism is extended to approach the single chain ferromagnetic instability point. In addition to the bosonization analysis spin wave calculations and large rung coupling expansions are carried out to obtain the exact boundary of the ferromagnetic phase. The ground state correlation functions are calculated throughout the phase diagram.

keywords: Spin Ladders, Bosonization, Phase Diagrams

Contents

Introduction

The study of magnetic properties of systems with reduced dimensionality has gained new interest and strength after the discovery of high $\mathrm{T_c}$ superconductivity[1] in materials showing a layered structure with superconducting planes alternating with non superconducting blocks. After it was realized that the celebrated BCS picture of superconductivity, based on phonon mediated pairing of electrons, failed to account for the properties of high $\mathrm{T_c}$ materials there was a need to find a new mechanism responsible for it. One of the universal features of copper-oxide compounds is the antiferromagnetic ordering of the copper spins in the $\mathrm{CuO_2}$ planes. A strong superexchange interaction (via oxygen ions) of the order 1500 K between hole spins at the copper sites gives rise to a three-dimensional long range AFM order with high Néel temperature up to 500K. The long-range AFM order disappears in the metallic and superconducting phase, but strong dynamical spin fluctuations with a wide spectrum of excitations are observed at temperatures exceeding 100K.[2,3] This fact has led to a number of hypothesis on the possible electron pairing in copper-oxide compounds via the magnetic degrees of freedom. One, probably the most famous scenario, namely that doped spin liquid state favors superconductivity, belongs to Anderson.[4] The first work on doped spin ladders were done by Rice et al.[5–7] It turns out that only a doped spin ladder of the Haldane type exhibits strongly enhanced superconducting fluctuations. The physics is very simple to understand in the limit when rung exchange is much bigger than exchange along the chains. The holes tend to stay on the same rung of the ladder in order not to break the spin singlet and to gain the energy of the order of the spin gap. Thus strong AFM exchange interaction provides with a pairing mechanism to holes. These pairs of holes behaving like bosons with the hard core can propagate along the ladder. The pairing susceptibility is diverging indicating that the finite three dimensional interaction between the ladders can stabilize quasi long range superconductivity order.

Apart from the relevance for high T_c superconductivity theoretical understanding of the properties of quantum spin ladder systems has attracted a lot of current interest for a number of other reasons as well. On the one hand they possess very rich and interesting ground state phase diagrams. On the other hand since a spin-S chain can be described as a $2S$-leg ladder with spin $S = 1/2$, provided the interchain coupling is appropriately chosen[27–29] the even- or odd-leg ladder systems are an excellent demonstration for Haldane's conjecture[32] as generalized to $S = 1/2$ ladders: the *antiferromagnetic* spin ladder with an even number of legs corresponds to a spin chain with integer spin and is predicted to have a gap, while a ladder with an odd number of legs has a gapless excitation spectrum. The two-leg antiferromagnetic ladder is presumably the simplest spin system which allows to follow the continuous evolution between the spin $S = 1/2$ and $S = 1$ antiferromagnetic chains nearly exactly.[29,31] Low energy excitations of separate spin 1/2 chains are decoupled spinons with quantum number spin 1/2. Although flipping one spin at least two spinons are created they can propagate independently. In a ladder system dynamical confinement of spinons occurs into magnons, particle like excitations with spin 1. In measurements of the dynamical spin susceptibility

by neutron scattering the emission of a magnon in a ladder system is seen as a sharp peak, in contrast to the incoherent two-spinon tail that is seen for separate chains. How does an arbitrary small interaction between the chains modify the low energy excitation spectrum so dramatically? How do even tiny interchain interactions serve as confining potential between the spinons? Where do such strong correlations come from? One explanation is that separate chains are critical, that is they possess no intrinsic scales, so the word weak or tiny looses its sense. There always exist length scales for which any weak interaction becomes confining. For infinitesimally weakly coupled chains we can go to still smaller energies and yet will discover particle like excitation.

In one dimension spin 1/2 systems could be equally well described in terms of spinless fermions by Jordan- Wigner transformation.[8] Thus studying strongly correlated electron systems in 1D we can unveil physics of much more complicated nonlinear objects – spins. Condensed matter physics in one spatial dimension is physics of strongly correlated systems. In contrast to the standard three dimensional fermi-liquid picture, in one dimensional Fermi systems with arbitrary weak bare interaction infrared orthogonality catastrophe[9](orthogonality catastrophe means that the ground state wave function of an electron gas perturbed by a local potential becomes orthogonal to the unperturbed ground state in thermodynamic limit, thus making inapplicable conventional perturbation theory) removes single-fermion quasiparticles from excitation spectrum. The low energy spectrum turns out to be purely bosonic. This bosonic modes are called Tomonaga bosons[10] and represent well defined quasiparticles made of electron-hole pairs. In any real system excitations always come in pairs, but in higher dimensions they decay into independently propagating fermionic quasiparticles. In one dimension there is a strong correlation between electrons and holes forbidding independent propagation. The fact that in 1D Fermi systems particle-hole excitations with small energy and momentum form well defined bosonic modes is a consequence of a drastic reduction of available phase space. For a long wavelength density excitations, both particle and hole must be in the vicinity of one and the same Fermi point. Since close to Fermi points the spectrum is almost linear, it turns out that for such particle-hole pairs conservation of momentum automatically implies conservation of the energy. As a result the particle-hole excitation energy depends only on the relative momentum. In contrast in higher dimensions the energy of the electron-hole pair depends also on the orientation of the particle-hole relative momentum with respect to the Fermi surface. Thus crucial difference from higher dimensions stems from the absence of a finite dimensional Fermi surface in one dimension. It is a remarkable feature of one dimensional interacting electron systems that the low energy excitations are *exhausted* by bosonic modes. Bosonization is an approach when one tries to reformulate complicated fermionic interacting models in terms of Tomonaga modes (term plasmon, or zero sound for interacting systems could equally be used) in such a way that they become weakly interacting. The simplest example demonstrating the power of bosonization is manifested when applied to the Tomonaga-Luttinger model, that is the model of interacting electrons without backscattering. The forward scattering term is trivially handled in the bosonic picture. Bosonization[12] provides a convenient basis for the theory of strongly correlated electron systems in one spatial dimension. It became a universal effective field theoretical language for describing Luttinger liquids, one dimensional counterparts of Fermi liquids. The reason why bosonization is so powerful in one dimension and less useful in higher dimensions results also from the fact that the effective field theories obtained with

the help of bosonization apart of diagrammatic perturbative treatments are amenable to rigorous truly non-perturbative treatments such as current algebra and Bethe ansatz calculation. These methods fail to deal with higher dimensional problems. Even if the 1D effective field theory obtained this way does not admit exact solutions, further mappings e.g. refermionization, passing to Ising variables could be used to analyze it. These latter mappings will be extensively used in the first part of the thesis, which deals with the study of frustrated spin ladder systems.

The advantage of bosonization manifests itself particularly when applied to frustrated systems. While quasiclassical approaches need some kind of at least locally ordered basis to expand on, bosonization does not need some a priori assumption on the spin basis. What really matters is that interactions in spin systems should be weak compared to intrachain exchange.

In the first part of the thesis, using bosonization- fermionization approach together with mapping to Ising variables, we will show how the phase diagram for spin ladder system with additional four-spin plaquette ring exchange can be derived. The above mentioned methods will allow us also to study the finite temperature thermodynamics of the model as well as its dynamical behavior.

In the second part of the thesis we analyze ferromagnetic spin chains coupled by a ladder type of interaction of arbitrary sign. Here we will see how the effective field theory description using bosonization can be used to obtain phase diagrams for various anisotropies both in interchain and intrachain couplings.

A chapter on methods used in effective field theory approach precedes the main part of the thesis. The technical calculations of physical quantities are given in detail in appendices A-E.

CHAPTER 1

Methods

In this chapter we will recapitulate on the formalism of quantum field theory of massless scalar field in 1+1 dimensions.

1.1 Massless Scalar Field in 1+1 Dimensions

Rather than choosing Hilbert space operator formalism (so called second or canonical quantization) we will follow as described in the book by Polchinski[20] path integral formalism for free scalar field theory in 2 D. The Euclidean action for massless scalar field (Gaussian field) in 2 D reads:

$$S = \frac{1}{2}\int d\tau dx \left[v^{-1}(\partial_\tau \phi(x,\tau))^2 + v(\partial_x \phi(x,\tau))^2\right] \tag{1.1}$$

where $\tau = it$ is Euclidean time and we used a normalization factor of $\frac{1}{2}$ in front of the action. Conveniently regularized Green's function could be evaluated directly by functional integral method (detailed and rigorous calculation involving special treatment of zero mode could be found in[17]):

$$\langle \phi(x,\tau)\phi(0,0)\rangle = \left(\int D\phi e^{-S}\right)^{-1} \int D\phi e^{-S}\phi(x,\tau)\phi(0,0) = -\frac{1}{4\pi}\ln\frac{x^2+v^2\tau^2+a^2}{R^2} \tag{1.2}$$

where R stands for system size and a for ultraviolet cutoff.

It is convenient to adopt complex coordinates:

$$z = x - iv\tau,\ \bar{z} = x + iv\tau \tag{1.3}$$

For these coordinates we have:

$$\partial_z := \partial = \frac{1}{2}(\partial_x + iv^{-1}\partial_\tau),\ \partial_{\bar{z}} =: \bar{\partial} = \frac{1}{2}(\partial_x - iv^{-1}\partial_\tau) \tag{1.4}$$

and for measure we adopt $d^2z := dzd\bar{z} = 2vdxd\tau$. Action in new coordinates will take form:

$$S = \int d^2z \partial\phi\bar{\partial}\phi \tag{1.5}$$

Classical equation of motion follows directly:

$$\partial\bar{\partial}\phi(z,\bar{z}) = 0 \tag{1.6}$$

meaning in particular, that $\partial\phi$ is analytic function of z, while $\bar{\partial}\phi$ is analytic function of $\bar{z}$. From above follows that classical solution could be decomposed as sum of analytic and antianalytic parts (under Minkovski continuation $t = -i\tau$ analytic field is function of only $x+vt$, thus is left-moving, while antianalytic field is function of $x-vt$ thus is right-moving).

$$\phi(x,t) = \phi_L(x+vt) + \phi_R(x-vt) \tag{1.7}$$

We will show, that the same decomposition holds for quantum case. In path integral formalism we are dealing with expectation values of various quantities defined as:

$$\langle F[\phi]\rangle = \left(\int D\phi e^{-S}\right)^{-1} \int D\phi e^{-S} F[\phi] \tag{1.8}$$

where $F[\phi]$ stands for general functional of field ϕ. We will use the fact, that path integral of total derivative is zero:

$$\begin{aligned} 0 &= \left(\int D\phi e^{-S}\right)^{-1} \int d\phi \frac{\delta}{\delta\phi(z,\bar{z})} e^{-S} \\ &= -\left(\int D\phi e^{-S}\right)^{-1} \int d\phi e^{-S} \frac{\delta S}{\delta\phi(z,\bar{z})} \\ &= -\left\langle \frac{\delta S}{\delta\phi(z,\bar{z})} \right\rangle = 2\left\langle \partial\bar{\partial}\phi(z,\bar{z})\right\rangle \end{aligned} \tag{1.9}$$

Exactly the same calculation is applicable when arbitrary additional insertions are present in path integral as long as they are not at point z.

$$\left\langle \partial\bar{\partial}\phi(z,\bar{z})\ldots\right\rangle = 0 \tag{1.10}$$

Above dots implicitely mean that insertions are located away from z. Such statements in path integral formalism are referred as operator equations. One can view this as Ehrenfest's quantum counterpart of classical equation of motion or quantum left-right decomposition. From (1.2) one can see that Green's function in new coordinates look:

$$\langle\phi(z,\bar{z})\phi(0,0)\rangle = -\frac{1}{4\pi}\ln|z|^2 \tag{1.11}$$

(for the moment for the sake of simplicity we don't bother with regularization of the Green's function at small and large distances). From above we can deduce Green's function for the chiral left- right components of the quantum field:

$$\langle\phi_L(z)\phi_L(0)\rangle = -\frac{1}{4\pi}\ln z \tag{1.12}$$

and

$$\langle\phi_R(\bar{z})\phi_R(0)\rangle = -\frac{1}{4\pi}\ln\bar{z} \tag{1.13}$$

1.2 Normal Ordering V Operator Product Expansion

In bosonization formalism we are dealing with e.g. expectation values of exponentials of quantum fields. So we have to consider situations when there are insertions that coincide with z. This statement is equivalent of adopting some ordering that renders ill defined products of quantum fields at coinciding points manageable. Convenient way is to adopt normal ordering that comes naturally from 'insertions' formalism.

$$\begin{aligned} 0 &= \left(\int D\phi e^{-S}\right)^{-1} \int d\phi \frac{\delta}{\delta\phi(z,\bar{z})}\left(e^{-S}\phi(z',\bar{z}')\right) \\ &= -\left(\int D\phi e^{-S}\right)^{-1} \int d\phi e^{-S}\left[\delta^2(z-z',\bar{z}-\bar{z}') + 2\phi(z',\bar{z}')\partial_z\partial_{\bar{z}}\phi(z,\bar{z})\right] \\ &= \left\langle\delta^2(z-z',\bar{z}-\bar{z}')\right\rangle + 2\partial_z\partial_{\bar{z}}\left\langle\phi(z',\bar{z}')\phi(z,\bar{z})\right\rangle \end{aligned} \tag{1.14}$$

The same is true for arbitrary insertion away from z, z'

$$2\partial_z\partial_{\bar{z}}\left\langle\phi(z',\bar{z}')\phi(z,\bar{z})\ldots\right\rangle = -\left\langle\delta^2(z-z',\bar{z}-\bar{z}')\ldots\right\rangle \tag{1.15}$$

(this statement holds, since as above dots imply that we exclude possibility that other insertions coincide with z, in contrary for $\phi(z',\bar{z}')$ such possibility was not excluded). Above means operator equation:

$$2\partial_z\partial_{\bar{z}}\phi(z',\bar{z}')\phi(z,\bar{z}) = -\delta^2(z-z',\bar{z}-\bar{z}') \tag{1.16}$$

Now we introduce very important notion of normal ordering denoted by $:A:$.

$$\begin{aligned} &:\phi(z,\bar{z}) := \phi(z,\bar{z}) \\ &:\phi(z,\bar{z})\phi(0,0) := \phi(z,\bar{z})\phi(0,0) + \frac{1}{4\pi}\ln|z|^2 \end{aligned} \tag{1.17}$$

The reason for this kind of definition is the property:

$$\partial_z\partial_{\bar{z}} :\phi(z,\bar{z})\phi(0,0) := 0 \tag{1.18}$$

that follows from operator equation (1.15) and the following differential equation:

$$\partial\bar{\partial}\ln|z|^2 = 2\pi\delta(z,\bar{z}) \tag{1.19}$$

From vacuum average (1.11) of course one recognizes in $::$ usual normal ordering in the sense of creation- annihilation operators. When carrying out perturbative R.G. procedure one has to deal with products of fields at the close points (we remind, that in R.G. one has to integrate out short wavelength degrees of freedom). Below we will see that for free field theories normal ordering renders product of operators at coinciding point well-defined. Since throughout the thesis we discuss asymptotically (ultraviolet) free theories, we can use ope of underlying free theory e.g. for R.G. calculation. Equation (1.18) states not only that **normal product satisfies naive equation of motion**, but more importantly that it is a **harmonic function**. It is well known from complex analysis that a harmonic function is

locally the sum of an analytic and antianalytic functions. In particular it means that it is nonsingular when $z \to 0$ and can be freely Taylor expanded in z and $\bar{z}$. The definition of normal ordering for arbitrary numbers of fields is given recursively:

$$: \phi(z_1, \bar{z}_1) \dots \phi(z_n, \bar{z}_n) := \phi(z_1, \bar{z}_1) \dots \phi(z_n, \bar{z}_n) + \sum \text{subtractions} \tag{1.20}$$

(the sum runs over all ways of choosing one, two, or more pairs of fields from the product and replacing them with propagator (1.11). In this way defined normal ordered product of any number of fields retains desired property of **satisfying equation of motion** that is tantamount of being **harmonic function**, thus it is Taylor expandable at any point. Compact formula for bringing any functional of the field to the normal ordering is:

$$: F[\phi(z, \bar{z})] := exp \left\{ \int d^2z' d^2z'' \frac{1}{4\pi} \ln |z' - z''| \frac{\delta}{\delta\phi(z', \bar{z}')} \frac{\delta}{\delta\phi(z'', \bar{z}'')} \right\} F[\phi(z, \bar{z})] \tag{1.21}$$

The most simple tool for the calculation to render product of normal ordered operators under the single normal ordering is to use the following formula:

$$\begin{aligned} &: F[\phi(z, \bar{z})] :: G[\phi(w, \bar{w})] : \\ &= exp \left\{ - \int d^2z' d^2z'' \frac{1}{4\pi} \ln |z' - z''|^2 \frac{\delta_F}{\delta\phi(z', \bar{z}')} \frac{\delta_G}{\delta\phi(z'', \bar{z}'')} \right\} : F[\phi(z, \bar{z})] G[\phi(w, \bar{w})] : \end{aligned} \tag{1.22}$$

Above functional derivatives act respectively only on F or G functionals. (To apply this rule for chiral operators we have to change $-\frac{1}{4\pi} \ln |z' - z''|^2$ by the appropriate propagators (1.12) and (1.13)). Using this practical tool we apply it on probably the most relevant to our case:

$$: e^{i\alpha\phi(z,\bar{z})} :: e^{i\beta\phi(0,0)} := |z|^{\alpha\beta/2\pi} : e^{i\alpha\phi(z,\bar{z}) + i\beta\phi(0,0)} : \tag{1.23}$$

To derive **ope** we have to Taylor expand inside the normal ordering (Taylor procedure is applicable after normal ordering) to express everything in terms of **local operators** at 0 and put the most singular terms first.

$$: e^{i\alpha\phi(z,\bar{z})} :: e^{i\beta\phi(0,0)} := |z|^{\alpha\beta/2\pi} : e^{i(\alpha+\beta)\phi(0,0)} [1 + O(z, \bar{z})] : \tag{1.24}$$

1.2.1 Some Frequently Used OPE-s

Applying rules from Eq. (1.22) we write out some of the most frequently used in bosonization formalism operator product expansions.

$$
\begin{aligned}
&:\partial\phi(z)\partial\phi(z)::\partial\phi(0)\partial\phi(0):=\frac{1}{8\pi^2 z^4}-\frac{1}{\pi z^2}:(\partial\phi(0))^2:-\frac{1}{\pi z}:\partial^2\phi(0)\partial\phi(0):+\cdots\\
&:\partial\phi(z)\bar{\partial}\phi(\bar{z})::\partial\phi(0)\bar{\partial}\phi(0):=\frac{1}{16\pi^2|z|^4}-\frac{1}{4\pi z^2}:\left(\bar{\partial}\phi(0)\right)^2:-\frac{1}{4\pi\bar{z}^2}:(\partial\phi(0))^2:+\\
&\qquad\qquad -\frac{1}{4\pi z}:\bar{\partial}^2\phi(0)\bar{\partial}\phi(0):-\frac{1}{4\pi\bar{z}}:\partial^2\phi(0)\partial\phi(0):+\cdots\\
&\partial\phi(z):e^{i\alpha\phi(0,0)}:=-\frac{i\alpha}{4\pi z}:e^{i\alpha\phi(0,0)}:+:\partial\phi(0)e^{i\alpha\phi(0,0)}:+\cdots\\
&\partial\phi(z):\cos\alpha\phi(0,0):=\frac{\alpha}{4\pi z}:\sin\alpha\phi(0,0):+:\partial\phi(0)\cos\alpha\phi(0,0):+\cdots\\
&:\partial\phi(z)\bar{\partial}\phi(\bar{z})::\cos\alpha\phi(0,0):=-\frac{\alpha^2}{(4\pi)^2|z|^2}:\cos\alpha\phi(0,0):+\cdots\\
&:\cos\alpha\phi(z,\bar{z})::\cos\alpha\phi(0,\bar{0}):=\frac{1}{2}|z|^{\alpha^2/2\pi}:\cos 2\alpha\phi(0,0):-\frac{1}{2}|z|^{-\alpha^2/2\pi}\\
&-\frac{\alpha^2}{2}|z|^{\frac{4\pi-\alpha^2}{2\pi}}:\partial\phi(0)\bar{\partial}\phi(0):-\frac{\alpha^2}{4}\left[z^{\frac{4\pi-\alpha^2}{2\pi}}\left(\bar{\partial}\phi(0)\right)^2+\bar{z}^{\frac{4\pi-\alpha^2}{2\pi}}\left(\partial\phi(0)\right)^2\right]+\cdots
\end{aligned}
\tag{1.25}
$$

dots in above formulas dots stand either for less singular or regular for $z\to 0$ terms. On the example of free scalar field in 2D we have demonstrated 'by hand' general property of conformally invariant field theories in 2D, and namely possibility of operator product expansion. The latter states that a product of two local operators close to each other can be approximated to arbitrary accuracy by a sum of local operators:

$$A_i(z)A_j(0)=\sum_k c_{ijk}(z)A_k(0) \tag{1.26}$$

above coefficient functions c_{ijk} are called ope coefficients. They govern one loop R.G. equations (see Appendix D) and are very important to our calculational purposes.

1.2.2 Correlation Functions of Vertex Operators

Now we want to discuss the correlation functions of conformally invariant theories. Scale invariance alone is enough to fix the two-point correlation function of fields in the infinite z-plane:

$$\langle\phi(z_1,\bar{z}_1)\phi(z_2,\bar{z}_2)\rangle=\frac{1}{(z_1-z_2)^{-2\triangle}(\bar{z}_1-\bar{z}_2)^{-2\bar{\triangle}}} \tag{1.27}$$

quantities $\triangle$ and $\bar{\triangle}$ are called left an right conformal weights. Their sum and difference are called the conformal dimension and the conformal spin of the ϕ field.

$$d=\triangle+\bar{\triangle},\quad S=\triangle-\bar{\triangle} \tag{1.28}$$

Let's return to the Eq. (1.23). From that equation we see, that:

$$: e^{i\alpha\phi(z_1,\bar{z}_1)} :: e^{i\beta\phi(z_2,\bar{z}_2)} :=: e^{i\alpha\phi(z_1,\bar{z}_1)+i\beta\phi(z_2,\bar{z}_2)} : e^{-\alpha\beta\langle\phi(z_1,\bar{z}_1)\phi(z_2,\bar{z}_2)\rangle} \tag{1.29}$$

With the help of the Green's function $G(z_1, z_2) = \langle\phi(z_1, \bar{z}_1)\phi(z_2, \bar{z}_2)\rangle = -\frac{1}{4\pi}\ln|z_1 - z_2|^2$ we can evaluate the two point correlation function of the normal ordered exponentials:

$$\left\langle : e^{i\alpha\phi(z_1,\bar{z}_1)} :: e^{i\beta\phi(z_2,\bar{z}_2)} : \right\rangle = e^{-\alpha\beta G(z_1,z_2)} = \left(|z_1 - z_2|^2\right)^{\alpha\beta/4\pi} \tag{1.30}$$

From this equation follow the conformal dimensions of bosonic exponents (in addition correlator is nonzero only if $\alpha = -\beta$ so called neutrality condition).

$$\triangle = \bar{\triangle} = \frac{\alpha^2}{8\pi},\ d = \frac{\alpha^2}{4\pi},\ S = 0 \tag{1.31}$$

Although the neutrality condition does not follow directly from (1.30) , because it requires special treatment of the zero mode, we can prove neutrality condition by noting, that the correlation function should enjoy symmetry $\phi \to \phi + const$, since action as well as path integral measure (apparently) enjoy this symmetry. Everywhere in the text we will have in mind the normal ordered exponents, even if normal ordering sign will be suppressed.

1.3 Weak Coupling Effective Field Theory for Spin Ladders

In this section we derive effective field theory for weakly coupled $S = 1/2$ chains. Lattice Hamiltonian of general anisotropic spin ladder Fig.(1.1) reads:

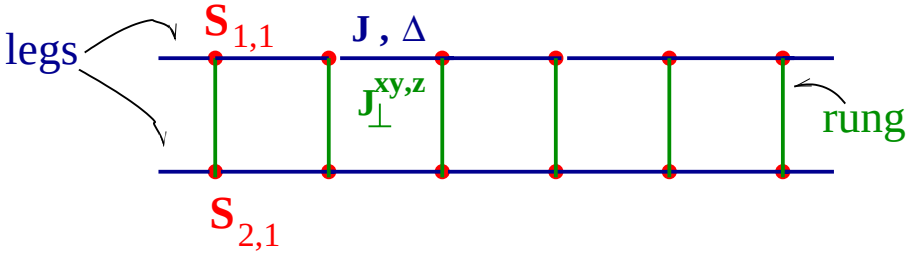

FIGURE 1.1: Structure of the Spin Ladder

$$\hat{H} = H^1_{leg} + H^2_{leg} + H_\perp\,, \tag{1.32}$$

where the Hamiltonian for leg $\alpha = 1, 2$ is

$$\begin{aligned} H^\alpha_{leg} &= -J\sum_{j=1}^{N}\left(S^x_{\alpha,j}S^x_{\alpha,j+1} + S^y_{\alpha,j}S^y_{\alpha,j+1}\right. \\ &+ \left.\Delta\, S^z_{\alpha,j}S^z_{\alpha,j+1}\right), \end{aligned} \tag{1.33}$$

and the interleg coupling is given by

$$\begin{aligned} H_\perp &= J_\perp^{xy} \sum_{j=1}^{N} \left(S_{1,j}^x S_{2,j}^x + S_{1,j}^y S_{2,j}^y \right) \\ &+ J_\perp^z \sum_{j=1}^{N} S_{1,j}^z S_{2,j}^z \,. \end{aligned} \tag{1.34}$$

Here $S_{\alpha,j}^{x,y,z}$ are spin $S = 1/2$ operators at the j-th rung. We start with two critical $S = 1/2$ chains and treat the interleg coupling as a perturbation assuming $|J_\perp^z|, |J_\perp^{xy}| \ll J$. The anisotropic spin $S = 1/2$ Heisenberg chain with $|\Delta| < 1$ is known to be critical. The long wavelength excitations are described by the standard Gaussian theory.[12] Therefore we start with two Gaussian Hamiltonians and simply will attach a leg index $\alpha = 1, 2$ to the fields.

$$\mathcal{H}_{leg} = \frac{u}{2} \int dx \, [(\partial_x \phi)^2 + (\partial_x \theta)^2]. \tag{1.35}$$

$\phi(x)$ and $\theta(x)$ are dual bosonic fields, $\partial_t \phi = u \partial_x \theta$, and satisfy the following commutational relation

$$\begin{aligned} [\phi(x), \theta(y)] &= i\Theta(y - x) \,, \\ [\phi(x), \theta(x)] &= i/2 \,. \end{aligned} \tag{1.36}$$

u stands for the velocity of spin excitation and is fixed from the Bethe ansatz solution as[12]

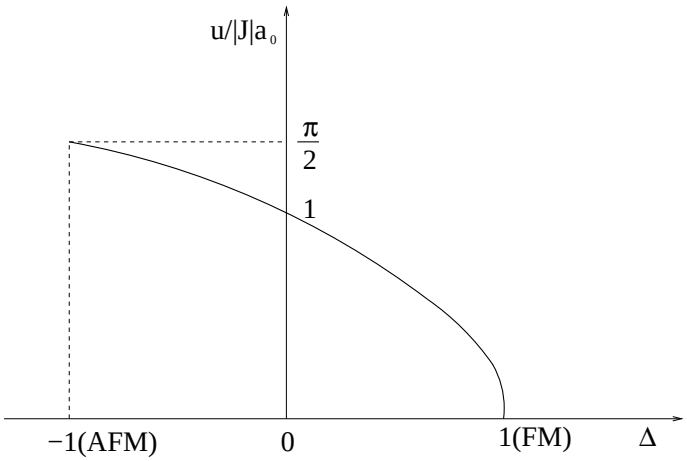

FIGURE 1.2: Spin wave velocity as function of anysotropy parameter (from Bethe Ansatz).

$$u = J \frac{K}{2K - 1} \sin(\pi/2K) \,, \tag{1.37}$$

where K is Luttinger liquid parameter known from comparison with the exact solution of the XXZ chain:

$$K = \frac{\pi}{2 \arccos \Delta} \,. \tag{1.38}$$

Thus the parameter K increases monotonically along the XXZ critical line $-1 < \Delta < 1$ from its minimal value $K = 1/2$ at $\Delta = -1$ (isotropic antiferromagnetic chain), is equal to unity at $\Delta = 0$ (the XY chain) and $K \to \infty$ at $\Delta \to 1$. At $\Delta = 1$ the spin excitation velocity vanishes, $u = 0$. This corresponds to the *ferromagnetic instability* point of a single chain. To obtain the bosonized version of the ladder Hamiltonian we need the explicit bosonized expressions of the spin operators. To classify the operators which originate from interchain coupling it is convinient to write the spin operators on each chain in terms of their smooth and staggered parts in vector denotions:

$$\mathbf{S}_{1,2}(x) = \mathbf{J}_{1,2}(x) + (-1)^x \mathbf{n}_{1,2}(x). \tag{1.39}$$

Where $\mathbf{J}_{1,2} = J_{1,2} + \bar{J}_{1,2}$ are sum of analityc and antianalytic currents and represent generators of $SU(2)$ rotations on each chain. The interchain coupling:

$$H_\perp = J_\perp \left[\mathbf{J}_1(x)\mathbf{J}_2(x) + \mathbf{n}_1(x)\mathbf{n}_2(x)\right] \tag{1.40}$$

is expressed in terms of slowly varying and staggered spin densities. Using bosonic representation of spin operators from Appendix (A) we obtain the following bosonic Hamiltonian density:

$$\begin{aligned}
\mathcal{H} &= \frac{u}{2}[(\partial_x\theta_1(x))^2 + (\partial_x\phi_1(x))^2] + \frac{u}{2}[(\partial_x\theta_2)^2 + (\partial_x\phi_2(x))^2] \\
&+ J_\perp^z \left(\frac{K}{\pi}\partial_x\phi_1(x)\partial_x\phi_2(x) + \frac{a^2}{\pi^2}\sin\sqrt{4\pi K}\phi_1(x)\sin\sqrt{4\pi K}\phi_2(x)\right) \\
&+ J_\perp^{xy}\left[\frac{c^2}{2\pi}\left(\cos\sqrt{\frac{\pi}{K}}\theta_1\,\cos\sqrt{\frac{\pi}{K}}\theta_2 + \sin\sqrt{\frac{\pi}{K}}\theta_1\,\sin\sqrt{\frac{\pi}{K}}\theta_2\right)\right. \\
&- \frac{b^2}{2\pi}\left(\sin\sqrt{4\pi K}\phi_1\,\sin\sqrt{\frac{\pi}{K}}\theta_1\,\sin\sqrt{4\pi K}\phi_2\,\sin\sqrt{\frac{\pi}{K}}\theta_2\right. \\
&\left.\left. + \sin\sqrt{4\pi K}\phi_1\,\cos\sqrt{\frac{\pi}{K}}\theta_1\,\sin\sqrt{4\pi K}\phi_2\,\cos\sqrt{\frac{\pi}{K}}\theta_2\right)\right]
\end{aligned} \tag{1.41}$$

We note, that above expression is strictly valid for easy plane regime, that is when $|\Delta| < 1$. The reason is that when we include all the effect of Z part of interaction in renormalization of Luttinger liquid parameter K and of nonuniversal constants we assume that S^ZS^Z interaction is irrelevant. This assumption is valid for easy plane regime. At $SU(2)$ AFM point S^ZS^Z interaction is marginally irrelevant. To be rigorous we have to add to the above effective Hamiltonian terms originating from single chain S^ZS^Z interaction, which are responsible for Néel transition into the easy axis regime (see formulas (3.16) and (3.17) and discussion below them). The rigorous derivation of these terms are possible by nonabelian bosonzation[61] starting from Hubbard Hamiltonian and are given by the current-current interaction within the single chain $\frac{U}{t}\mathbf{J}_L\mathbf{J}_R$. U stands for the positive onsite repulsion of the underlying Hubbard model and t is nearest neighbour hopping. In the abelian bosonization approach close to $SU(2)$ AFM point ($\Delta = -1$) these terms have the following form:

$$U\left(-(\Delta+2)\frac{\partial_x\phi_{\alpha,L}(x)\partial_x\phi_{\alpha,R}(x)}{\pi} + \frac{\cos\sqrt{8\pi\phi_\alpha}}{2\pi^2}\right) \tag{1.42}$$

In the following we will suppress these terms, having in mind to recover them when discussing $SU(2)$ AFM point. Now we want to analyse Hamiltonian (1.41). To get rid of operator $\partial_x\phi_1(x)\partial_x\phi_2(x)$ and simplify the Hamiltonian we introduce symmetric and antisymmetric combinations of the bosonic fields:

$$\phi_\pm = \sqrt{\frac{1}{2\Lambda_\pm}}\left(\phi_1 \pm \phi_2\right) , \theta_\pm = \sqrt{\frac{\Lambda_\pm}{2}}\left(\theta_1 \pm \theta_2\right), \tag{1.43}$$

where

$$\Lambda_\pm = \left(1 \mp \frac{1}{2\pi}\frac{J_\perp^z}{J_{eff}}\right)$$

and

$$J_{eff} = \frac{u}{K} = J\frac{1}{2K-1}\sin\frac{\pi}{2K}.$$

Using above transformation we obtain straightforwardly the following bosonic Hamiltonian density for symmetric and antisymmetric fields:

$$\mathcal{H} = \mathcal{H}^+ + \mathcal{H}^- + \mathcal{H}^\pm_{int}, \tag{1.44}$$

$$\begin{aligned}\mathcal{H}^+ &= \frac{u_+}{2}[(\partial_x\theta_+)^2 + (\partial_x\phi_+)^2] \\ &- \frac{\mathcal{J}_\perp^z}{2\pi}\cos\sqrt{8\pi K_+}\phi_+(x),\end{aligned} \tag{1.45}$$

$$\begin{aligned}\mathcal{H}^- &= \frac{u_-}{2}[(\partial_x\theta_-)^2 + (\partial_x\phi_-(x))^2] \\ &+ \frac{\mathcal{J}_\perp^z}{2\pi}\cos\sqrt{8\pi K_-}\phi_-(x) \\ &+ \frac{\mathcal{J}_\perp^{xy}}{2\pi}\cos\sqrt{\frac{2\pi}{K_-}}\theta_-(x) \\ &- \frac{\tilde{\mathcal{J}}_\perp^{xy}}{2\pi}\cos\sqrt{\frac{2\pi}{K_-}}\theta_-(x)\cos\sqrt{8\pi K_-}\phi_-(x),\end{aligned} \tag{1.46}$$

$$\mathcal{H}^\pm_{int} = \frac{\mathcal{J}_{+-}}{2\pi}\cos\sqrt{\frac{2\pi}{K_-}}\theta_-(x)\cos\sqrt{8\pi K_+}\phi_+(x). \tag{1.47}$$

Here

$$u_\pm = \frac{u}{\Lambda_\pm} \simeq u\left(1 \pm \frac{1}{2\pi}\frac{J_\perp^z}{J_{eff}}\right) \tag{1.48}$$

$$K_\pm = K\cdot\Lambda_\pm \simeq K\left(1 \mp \frac{1}{2\pi}\frac{J_\perp^z}{J_{eff}}\right), \tag{1.49}$$

and we have introduced the following coupling constants:

$$\mathcal{J}_\perp^z = J_\perp^z/\pi\,, \tag{1.50}$$

for $\Delta = 0$ and otherwise

$$\mathcal{J}_\perp^z \sim J_\perp^z\,, \tag{1.51}$$

$$\mathcal{J}_\perp^{xy}, \tilde{\mathcal{J}}_\perp^{xy}, \mathcal{J}_{+-} \sim J_\perp^{xy}\,, \tag{1.52}$$

with some positive constants of proportionality which cannot be fixed by symmetry arguments alone. Thus the effective field theory of weakly coupled spin ladder is governed by the Hamiltonian (1.44) plus current-current interactions within the single chain that become marginal at SU(2) symmetric AFM point.

CHAPTER 2

Spin Ladder with Four Spin Ring Exchange

At half filling and in the limit of small ratio $x = t/U$ of hopping and on-site Coulomb repulsion the Hubbard model can be mapped to an effective spin exchange Hamiltonian. In the leading order in x the standard (bilinear) antiferromagnetic nearest-neighbor Heisenberg exchange interaction with the exchange constant $J = 2t^2/U$ is obtained. Terms of higher order in x yield, except bilinear exchange interactions beyond the nearest neighbors, also exchange terms containing a product of four or more spin operators[37,38] (on lattices where square paths are allowed). Those higher-order terms were routinely neglected up to recent time, when it was realized that they can be important for a correct description of many physical systems.

For the first time biquadratic exchange was used for the description of the magnetic properties of solid ^{3}He.[39] Recently it was suggested that some strongly correlated electron systems like cuprates[40,41] and spin ladders[43,44] are expected to exhibit ring exchange. The analysis of the low-lying excitation spectrum of the p-d-model shows that the Hamiltonian describing CuO_2 planes should contain a finite value of ring exchange.[40–42]

There is a number of experimental work like inelastic neutron scattering[45] and nuclear magnetic resonance[47] on $Sr_{14}Cu_{24}O_{41}$ and $Ca_8La_6Cu_{24}O_{41}$ as well as optical conductivity measurements[46,48] on $(Ca,La)_{14}Cu_{24}O_{41}$. All these substances contain spin ladders built of Cu atoms. The attempts to fit the experimental data without taking ring exchange into account yield an unnaturally large ratio[47] of $J_{\rm leg}/J_{\rm rung} \approx 2$ which is expected neither from the geometrical structure of the ladder nor from electronic structure calculations. It can be shown that inclusion of other types of interactions in particular an additional diagonal interaction does not remove this discrepancy.[44]

Apart from experimental relevance to study the effect of ring exchange on ordinary quadratically interacting antiferromagnetic spin systems is by its own interesting theoretical problem, especially, because of frustration. Very often frustrated interactions in quantum spin systems give rise to 'unpredictable' exotic phases. It is very difficult to analyze frustrated models theoretically because of the presence of several competing interactions. Typical example is isotropic spin $1/2$ Heisenberg chain with nearest and next nearest antiferromagnetic couplings. Frustration results into dimerization for sufficiently strong next nearest exchange the result difficult to predict based on classical, or quasiclassical approaches (e.g. it is well known that Kosterlitz -Thouless transition to spontaneously dimerized phase for the above mentioned model is notoriously difficult (if ever possible) to obtain by nonlinear sigma model approach). Fortunately bosonization approach appears sometimes very powerful method for studying frustrated systems. Bosonization is weak-coupling approach. So to compare the results obtained from bosonization to real world it should be accompanied by numerical studies to calculate so called nonuniversal constants, quantities, that depend on

finite bandwidth, or cutoff. Two leg ladder spin system is a 'minimal system' where effect of ring exchange could be tested. Since in one dimensional lattice (chain) no square paths are allowed four spin interactions can not be generated from reduction of Hubbard model to spin sector in strictly one dimensional case. Real two-leg ladder cuprate systems are always in the rung-singlet phase. Those, where ring exchange is believed to play important role are relatively close to quantum critical point. Therefore it is very important to understand the nature of the quantum phase transition with increasing ring interaction.

2.1 Model

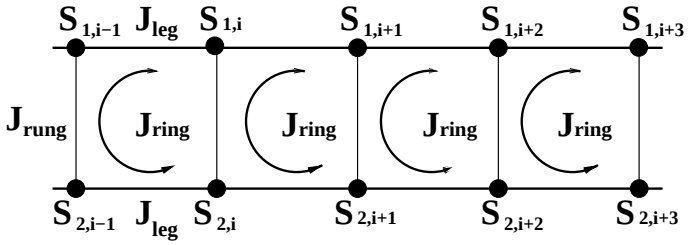

FIGURE 2.1: Structure of two leg ladder with syclic ring exchange

We consider the isotropic $S = 1/2$ antiferromagnetic spin ladder with additional cyclic four spin exchange. Fig. 2.1 illustrates the Hamiltonian, which is of the form

$$\mathcal{H} = \mathcal{H}_{\text{rung}} + \mathcal{H}_{\text{leg}} + \mathcal{H}_{\text{ring}}$$

where

$$\mathcal{H}_{\text{rung}} = J_{\text{rung}} \sum_{i=1}^{\mathcal{N}} \mathbf{S}_{1,i}\mathbf{S}_{2,i} \tag{2.1a}$$

$$\mathcal{H}_{\text{leg}} = J_{\text{leg}} \sum_{i=1}^{\mathcal{N}} \sum_{a=1,2} \mathbf{S}_{a,i}\mathbf{S}_{a,i+1} \tag{2.1b}$$

$$\mathcal{H}_{\text{ring}} = \frac{J_{\text{ring}}}{2} \sum_{\langle ijkl \rangle} \left(P_{ijkl} + P_{ijkl}^{-1} \right) \tag{2.1c}$$

In (2.1) $\langle ijkl \rangle$ labels a four spin plaquette. P_{ijkl} leads to a cyclic permutation of spin moments, i.e.

$$P_{ijkl} \left| \begin{matrix} i & j \\ l & k \end{matrix} \right\rangle = \left| \begin{matrix} l & i \\ k & j \end{matrix} \right\rangle \quad \text{and} \quad P_{ijkl}^{-1} \left| \begin{matrix} i & j \\ l & k \end{matrix} \right\rangle = \left| \begin{matrix} j & k \\ i & l \end{matrix} \right\rangle . \tag{2.2}$$

We rewrite the operator P_{ijkl} as a product of two spin permutation operators and obtain the following result which contains both bilinear and biquadratic terms of the spin-$1/2$-

operators:

$$\begin{aligned}\mathcal{H}_{\rm ring} &= \frac{J_{\rm ring}}{2}\sum_{\langle ijkl\rangle}\left[\frac{1}{4}+\mathbf{S}_i\mathbf{S}_j+\mathbf{S}_j\mathbf{S}_k+\mathbf{S}_k\mathbf{S}_l+\mathbf{S}_l\mathbf{S}_i\right]\\ &+ \frac{J_{\rm ring}}{2}\sum_{\langle ijkl\rangle}\Big[\mathbf{S}_i\mathbf{S}_k+\mathbf{S}_j\mathbf{S}_l\Big]\\ &+ 2J_{\rm ring}\sum_{\langle ijkl\rangle}\Big[(\mathbf{S}_i\mathbf{S}_j)(\mathbf{S}_k\mathbf{S}_l)\\ &+ (\mathbf{S}_i\mathbf{S}_l)(\mathbf{S}_j\mathbf{S}_k)-(\mathbf{S}_i\mathbf{S}_k)(\mathbf{S}_j\mathbf{S}_l)\Big]\end{aligned} \tag{2.3}$$

2.2 Decoupled Chains Limit of Ordinary Ladder

In this section we perform the weak-coupling analysis ($J_{\rm leg} \gg J_{\rm ring},\ J_{\rm rung}$) of our model. First we describe effective field theory for an ordinary ladder without ring exchange at $SU(2)$ AFM point and then study the effect of cyclic ring interaction. We analyze general expression of Hamiltonian (1.41). For a moment we drop current-current interaction terms since at $K = 1/2$ they are marginal, while interactions of staggered parts are relevant (the role of marginal current-current interactions will be discussed later where they will be responsible for breaking down of spurious symmetry). Dropping marginal current- current interactions (originating from both intra and interchain couplings) from Hamiltonian (1.41) makes it separate into two commuting parts in symmetric and antisymmetric basis:

$$\begin{aligned}H &= H^+ + H^-\\ H^+ &= \frac{u_+}{2}[(\partial_x\theta_+)^2+(\partial_x\phi_+)^2]-\frac{J_\perp c^2}{2\pi^2}\cos\sqrt{4\pi}\phi_+(x)\\ H^- &= \frac{u_-}{2}[(\partial_x\theta_-)^2+(\partial_x\phi_-(x))^2]\\ &+ \frac{J_\perp c^2}{2\pi^2}\cos\sqrt{4\pi}\phi_-(x)+\frac{J_\perp c^2}{\pi^2}\cos\sqrt{4\pi}\theta_-(x)\end{aligned} \tag{2.4}$$

where c stands for nonuniversal numerical constant. We see, that in antisymmetric sector Hamiltonian density contains relevant $cosine$ of bosonic field as well as its dual. Bosonic basis is unconvenient in this case and it is natural to serch for some mapping in order to render calculations tractable. Natural candidate is representation in terms of Majorana fermions. Since central charge of uncoupled chains is 2 it is clear that we have to start from 4 massless Majorana copies. Moreover since the dimensions of all kept perturbing terms are 1 it could be anticipated that they will be translated into the Majorana masses. Indeed such mapping exists and is given by inverting bosonization formulas for fermionic operators (fermionization). Following Shelton et al.[29] we introduce spinless fermions:

$$\Psi_R(x)\simeq(2\pi)^{-1/2}e^{i\sqrt{4\pi}\phi_+^R(x)},\ \Psi_L(x)\simeq(2\pi)^{-1/2}e^{-i\sqrt{4\pi}\phi_+^L(x)} \tag{2.5}$$

Under this mapping we have:

$$\frac{1}{\pi}\cos\sqrt{4\pi}\phi_+(x)=i[\Psi_R^\dagger(x)\Psi_L(x)-\Psi_L^\dagger(x)\Psi_R(x)] \tag{2.6}$$

If we pass now to real (Majorana) fermions by formulas:

$$\psi_\nu^1 = \frac{\Psi_\nu + \Psi_\nu^\dagger}{\sqrt{2}},\ \psi_\nu^2 = \frac{\Psi_\nu - \Psi_\nu^\dagger}{\sqrt{2i}},\ (\nu = R, L) \tag{2.7}$$

we will have:

$$\frac{1}{\pi}\cos\sqrt{4\pi}\phi_+(x) = i(\psi_R^1\psi_L^1 + \psi_R^2\psi_L^2) \tag{2.8}$$

We recognize that symmetric sector describes two degenerate massive Majorannas:

$$H_+ = H_{m_t}[\psi_1] + H_{m_t}[\psi_2] \tag{2.9}$$

where

$$H_m[\psi] = -\frac{v}{2}(\psi_R(x)\partial_x\psi_R(x) - \psi_L(x)\partial_x\psi_L(x)) - im_t\psi_R(x)\psi_L(x) \tag{2.10}$$

and we have introduced the notation $m_t = J_\perp c^2/2\pi$. Fortunately hamiltonian in antisymmetric sector can also be reduced to simple form in Majoranas. Introducing spinless Dirac fermion like above:

$$\chi_R(x) \simeq (2\pi)^{-1/2}e^{i\sqrt{4\pi}\phi_-^R(x)},\ \chi_L(x) \simeq (2\pi)^{-1/2}e^{-i\sqrt{4\pi}\phi_-^L(x)} \tag{2.11}$$

we get:

$$\begin{aligned}\frac{1}{\pi}\cos\sqrt{4\pi}\phi_-(x) &= i[\chi_R(x)\chi_L(x) - \chi_L^\dagger(x)\chi_R^\dagger(x)]\\ \frac{1}{\pi}\cos\sqrt{4\pi}\theta_-(x) &= -i[\chi_R^\dagger(x)\chi_L^\dagger(x) - \chi_L(x)\chi_R(x)]\end{aligned} \tag{2.12}$$

Passing again to two real fermions:

$$\psi_\nu^3 = \frac{\chi_\nu + \chi_\nu^\dagger}{\sqrt{2}},\ \rho_\nu = \frac{\chi_\nu - \chi_\nu^\dagger}{\sqrt{2i}},\ (\nu = R, L) \tag{2.13}$$

we will have:

$$\begin{aligned}\frac{1}{\pi}\cos\sqrt{4\pi}\phi_-(x) &= i(\psi_R^3\psi_L^3 + \rho_R\rho_L)\\ \frac{1}{\pi}\cos\sqrt{4\pi}\theta_-(x) &= i(-\psi_R^3\psi_L^3 + \rho_R\rho_L)\end{aligned} \tag{2.14}$$

That means in particular:

$$\frac{1}{\pi}\cos\sqrt{4\pi}\phi_-(x) + \frac{2}{\pi}\cos\sqrt{4\pi}\theta_-(x) = 3i\rho_R\rho_L - i\psi_R^3\psi_L^3 \tag{2.15}$$

From this we see that hamiltonian in antisymmetric sector will take form:

$$H_- = H_{m_t}[\psi_3] + H_{m_s}[\rho] \tag{2.16}$$

where $m_s = -3m_t = -3J_\perp c^2/2\pi$ and H_{m_t} as well as H_{m_s} represent hamiltonians for free massive Majoranas with corresponding masses $m_t, \text{and}\, m_s$. Thus the ladder problem reduced to 4 copies of massive Majoranas. Triplet of mass m and singlet of mass $-3m$. One can introduce majorana fermions for describing spin ladder system slightly in different manner. Since we start from decoupled chains we are dealing with fixed point Hamiltonian which is described in terms of two copies of WZW $SU_1(2)$ that is equivalent to $SO(4)$ WZW model that admits a representation in terms of four real fermions. This allows directly to write down expressions for generators of $SU(2)$ algebras.[13]

$$\begin{aligned}\left(J_1^{L,R}(x) + J_2^{L,R}(x)\right)^a &= -\frac{i}{2}\epsilon^{abc}\psi^b_{L,R}(x)\psi^c_{L,R}(x)\\ \left(J_1^{L,R}(x) - J_2^{L,R}(x)\right)^a &= i\psi^a_{L,R}(x)\rho_{L,R}(x)\end{aligned} \tag{2.17}$$

where $a, b, c = 1, 2, 3$. These formulas will allow to calculate various physicsl quantities in terms of majorana fermions (like susceptibility, etc.). Using above formulas one can see what corresponds in majorana formalism to neglected current current interaction.

$$J_\perp(J_1^a J_2^a + \bar{J}_1^a \bar{J}_2^a + J_1^a \bar{J}_2^a + \bar{J}_1^a J_2^a) \tag{2.18}$$

First two terms will induce velocity renormalization, the effect we are not interested in. Last two terms translate into:

$$J_\perp \left(\sum_{b<c} \frac{1}{2}(\psi_L^b\psi_R^b)(\psi_L^c\psi_R^c) - \frac{1}{2}(\psi_L^a\psi_R^a)\rho_L\rho_R\right) \tag{2.19}$$

The role of these marginal four-fermi interactions in the theory of massive fermions is described in the appendix B.2.

2.2.1 Correlation Functions for Ordinary Ladder

Apart from the correlation functions involving smooth parts of spin components (2.17) it is possible to calculate also correlation functions involving staggered components of the magnetization. It is a well known fact that massive Majorana fermion describes long- distance properties of the two-dimensional Ising model. Mass of the fermion is proportional to deviation from criticality $m \sim (T - T_c)/T_c$. So the ladder model is equivalent to four copies of two dimensional off critical Ising models. We use the following representation for total and relative staggared magnetizations $\mathbf{n}^\pm = \mathbf{n}_1 \pm \mathbf{n}_2$ in terms of ising variables[29] (see Appendix B.3):

$$\begin{aligned} n_x^+ \sim \mu_1\sigma_2\sigma_3\mu,\ n_y^+ \sim \sigma_1\mu_2\sigma_3\mu,\ n_z^+ \sim \sigma_1\sigma_2\mu_3\mu\\ n_x^- \sim \sigma_1\mu_2\mu_3\sigma,\ n_y^- \sim \mu_1\sigma_2\mu_3\sigma\ n_z^- \sim \mu_1\mu_2\sigma_3\sigma\end{aligned} \tag{2.20}$$

Let us consider: $\epsilon_{1,2}(x) = (-1)^x\mathbf{S}_{1,2}(x)\mathbf{S}_{1,2}(x + a_0)$ the dimerization operator of the first and second chain, respectively. Bosonized expression of dimerization operator is given in

appendix A.2. As explained in Appendix B.3 following representation for total and relative dimerization $\epsilon^{\pm} = \epsilon_1 \pm \epsilon_2$ is possible in Ising variables:

$$\epsilon_+ \sim \mu_1\mu_2\mu_3\mu, \;\; \epsilon_- \sim \sigma_1\sigma_2\sigma_3\sigma \tag{2.21}$$

These equivalences are crucial, since they allow to calculate dynamical staggered magnetic susceptibilities (note that in Majorana formalism we would be dealing with nonlocal operators instead), because correlation functions involving Ising order and disorder operators are known including off critically. For antiferromagnetic ladder we are considering $m_t > 0$ and $m_s < 0$, meaning in particular that in the limit $r \to \infty$:

$$\begin{aligned}
\langle \sigma_a(r)\sigma_a(0)\rangle &\simeq K_0(rm_t) + O(e^{-3rm_t}) \\
\langle \mu_a(r)\mu_a(0)\rangle &\simeq \text{const}\left[1 + \frac{e^{-2rm_t}}{8\pi(rm_t)^2} + O(e^{-4rm_t})\right] \\
\langle \sigma(r)\sigma(0)\rangle &\simeq \text{const}\left[1 + \frac{e^{-2r|m_s|}}{8\pi(rm_s)^2} + O(e^{-4r|m_s|})\right] \\
\langle \mu(r)\mu(0)\rangle &\simeq K_0(r|m_s|) + O(e^{-3r|m_s|})
\end{aligned} \tag{2.22}$$

$a = 1, 2, 3$ stands for triplet components. The leading asymptotics for the spin correlation functions obtained from (2.22) look:

$$\begin{aligned}
\left\langle \mathrm{n}^-(r)\mathrm{n}^-(0)\right\rangle &\sim K_0(rm_t)\left[1 + O(e^{-2m_t r})\right] \\
\left\langle \mathrm{n}^+(r)\mathrm{n}^+(0)\right\rangle &\sim \frac{e^{-(2m_t r + |m_s| r)}}{r^{3/2}}
\end{aligned} \tag{2.23}$$

and for dimerization- dimerization correlation functions:

$$\begin{aligned}
\langle \epsilon_-(r)\epsilon_-(0)\rangle &\sim \frac{e^{-3m_t r}}{r^{3/2}} \\
\langle \epsilon_+(r)\epsilon_+(0)\rangle &\sim K_0(|m_s|r)\left[1 + O(e^{-2rm_t})\right]
\end{aligned} \tag{2.24}$$

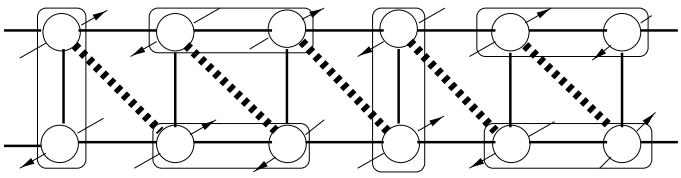

FIGURE 2.2: Typical configuration in the RVB state of AFM ladder

The ground state of the ordinary ladder system is parity symmetric, $\langle \epsilon^{\pm} \rangle = 0$. The typical configuration in the resonating valense bond state of the antiferromagnetic ladder is depicted on Fig. (2.2). Dynamical spin susceptibility calculated by Fourier transforming assymptotics of the correlation function $\langle \mathbf{n}^-(x,\tau)\mathbf{n}^-(0,0)\rangle$ exhibits the existance of a coherent $S = 1$ magnon peak at energy $\omega^2 = (\pi - q)^2 v_t^2 + m_t^2$. This is obvious, since $K_0(r|m_t|)$ is Euclidean

space propagator of a free massive bosons, after Fourier transforming and analyticaly continuing to real frequencies it contributes a δ-peak to the imaginary part of the dynamical spin susceptibility corresponding to a 'long-lived' massive triplet of magnons.

$$ImD_{-}^{(R)}(\omega, \pi - q) \simeq \left[\frac{m_t}{\pi\sqrt{v^2q^2 + m_t^2}} \delta(\omega - \sqrt{v^2q^2 + m_t^2}) + \dots \right] \tag{2.25}$$

for energies $\omega < 2|m_t| + |m_s|$. Thus at low energies ordinary two-leg ladder is in a Hal-

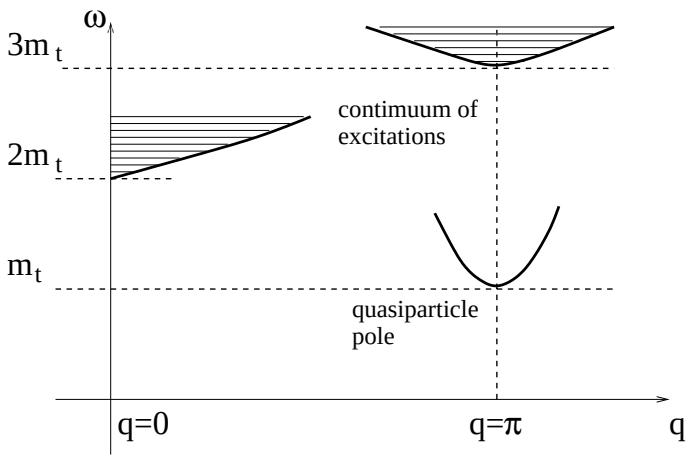

FIGURE 2.3: The area in (ω, q) plane where imaginary part of dynamical susceptibility of spin ladder in Haldane phase is finite

dane disordered spin liquid phase with relative staggered magnetization $\mathbf{n}^{-}$ playing role of staggered magnetization of Haldane chain.[29]

2.3 Bosonization of Four Spin Ring Exchange

Now we bosonize separately ring exchange. First we decompose the ring part of Hamiltonian in the following way:

$$H(x) = H_{\rm quad}(x) + H_{\rm biquad}(x) \ , \tag{2.26}$$

$H_{\rm quad}$ stands for the quadratic spin interactions and $H_{\rm biquad}$ for the four-spin interactions originating from the ring exchange term.

Neglecting renormalization of the intrachain interaction (we are in weak coupling) we first analyze the quadratic spin interactions which can be cast in the following form:

$$\begin{aligned} H_{\rm quad} &\sim (J_{\rm ring}^{\perp} + J_{\rm ring}^{\times})\mathbf{J}_1(x)\mathbf{J}_2(x) \\ &+ (J_{\rm ring}^{\perp} - J_{\rm ring}^{\times})\mathbf{n}_1(x)\mathbf{n}_2(x) \end{aligned} \tag{2.27}$$

where $J_{\rm ring}^{\perp} = J_{\rm ring}^{\times} = J_{\rm ring}$. Since the scaling dimension of the smooth part of the spin operator is 1, while the dimension of the staggered part is $1/2$, no relevant terms are generated from the quadratic part of the ring exchange, and only marginal terms are left. After bosonizing the biquadratic part only leg-leg interaction will survive, because diagonal-diagonal and

rung-rung terms give non-distinguishable relevant contributions in the infrared limit which cancel each other due to the overall opposite signs in front of them (which is fixed by the structure of the ring exchange):

$$H_{\rm biquad} \sim J^{\rm LL}_{\rm ring}\epsilon_1(x)\epsilon_2(x), \tag{2.28}$$

where $J^{\rm RR}_{\rm ring} = J^{\rm DD}_{\rm ring} = J^{\rm LL}_{\rm ring} = 2J_{\rm ring}$.

$$\begin{aligned} J^{\rm LL}_{\rm ring}\epsilon_1(x)\epsilon_2(x) &\simeq \frac{J^{\rm LL}_{\rm ring}}{\pi}\cos\sqrt{2\pi}\phi_1\cos\sqrt{2\pi}\phi_2 \\ &= \frac{J^{\rm LL}_{\rm ring}}{2\pi}(\cos\sqrt{4\pi}\phi_+ + \cos\sqrt{4\pi}\phi_-) \end{aligned} \tag{2.29}$$

using Eqs: (2.8), (2.14) we get correspondence:

$$\frac{2}{\pi}\epsilon_1(x)\epsilon_2(x) = i(\psi^1_R\psi^1_L + \psi^2_R\psi^2_L + \psi^3_R\psi^3_L + \rho_R\rho_L) \tag{2.30}$$

In the Majorana representation (retaining only relevant operators) we arrive at the following Hamiltonian:

$$H = \sum_{a=0}^{3}\int dx\left[\frac{-iv}{2}(\psi^a_R\partial_x\psi^a_R - \psi^a_L\partial_x\psi^a_L) - im\psi^a_R\psi^a_L\right] \tag{2.31}$$

above ψ_0 stands for ρ, fourth Majorana, and $m = -c^2\alpha J_{\rm ring}/2\pi$, α being non-universal cutoff dependent possitive constant. Thus in the weak-coupling limit we have effectively reduced the ring exchange to the leg-leg interaction.[72] The only difference between the bosonized forms of the ring exchange and the pure leg-leg coupling stems from the marginal current-current interaction which does not appear in the leg-leg biquadratic interaction. In contrast to the leg-leg interaction ring exchange is not invariant under independent global $SU(2)$ rotations of spins on each chain, and thus should not enjoy full $O(4)$ symmetry. This symmetry is in fact lowered by marginal operators. The refermionized version of the marginal current-current interaction contained in ring exchange will take the following form in the Majorana representation:

$$\begin{aligned} H_{\rm marg} &= J_{\rm ring}a_0\int dx[(\psi^1_R\psi^1_L)(\psi^2_R\psi^2_L) \\ &+ (\psi^2_R\psi^2_L)(\psi^3_R\psi^3_L) + (\psi^1_R\psi^1_L)(\psi^3_R\psi^3_L) \\ &- (\psi^1_R\psi^1_L + \psi^2_R\psi^2_L + \psi^3_R\psi^3_L)(\psi^0_R\psi^0_L)] \end{aligned} \tag{2.32}$$

Renormalizing the masses it weakly splits the $O(4)$ quadruplet into a triplet and a singlet, consistent with the symmetries of ring exchange:

$$\begin{aligned} \frac{m_t}{m} &\longrightarrow 1 + \frac{J_{\rm ring}a_0}{\pi v}\ln\frac{J_{\rm leg}}{|m|}, \\ \frac{m_s}{m} &\longrightarrow 1 - \frac{3J_{\rm ring}a_0}{\pi v}\ln\frac{J_{\rm leg}}{|m|}. \end{aligned} \tag{2.33}$$

The full refermionized model, including both rung and ring exchange, in the Majorana representation reads as:

$$\begin{aligned} H &= \sum_{a=1,2,3} \int dx \left[\frac{-iv_t}{2} (\psi_R^a \partial_x \psi_R^a - \psi_L^a \partial_x \psi_L^a) - im_t \psi_R^a \psi_L^a \right] \\ &+ \int dx \left[-\frac{iv_s}{2} (\rho_R \partial_x \rho_R - \rho_L \partial_x \rho_L) - im_s \rho_R \rho_L \right] \end{aligned} \tag{2.34}$$

where

$$\begin{aligned} m_t &= \frac{c^2}{2\pi} (J_{\text{rung}} - \alpha J_{\text{ring}}), \\ m_s &= -\frac{c^2}{2\pi} (3J_{\text{rung}} + \alpha J_{\text{ring}}) \end{aligned} \tag{2.35}$$

where α is nonuniversal numerical constant that is impossible to determine alone by bosonization. From the above formulas, one readily obtains the line where the triplet mass vanishes. Thus we showed that at weak coupling ring interaction induces quantum phase transition to new phase. To study the symmetry properties of the ground state of new phase we discuss the behavior of correlation functions.

2.3.1 Correlation Functions in Ring Exchange Dominated Phase

From the representation of staggered magnetization and dimerization operators resp. (2.23) and (2.24) we find, that relative staggered spin of two chains (which is the same as total staggared spin across the diagonal), as well as relative dimerization decay algebraically according to $SU_2(2)$ universality class:[30]

$$\left\langle \vec{n}^-(r) \vec{n}^-(0) \right\rangle \sim \langle \epsilon_-(r) \epsilon_-(0) \rangle \sim r^{-3/4} \tag{2.36}$$

On the line where mass of the triplet of Majoranas vanishes a quantum phase transition from conventional Haldane phase (rung exchange dominated phase) where spectrum displays coherent single-particle (magnon) excitations to non-Haldane spontaneously dimerized phase (ring exchange dominated phase) without coherent magnon modes takes place.[72] In the dimerized phase for staggered spin correlation functions we obtain following expressions:

$$\begin{aligned} \left\langle \mathrm{n}^-(r) \mathrm{n}^-(0) \right\rangle &\sim K_0^2(r|m_t|) \\ \left\langle \mathrm{n}^+(r) \mathrm{n}^+(0) \right\rangle &\sim K_0(r|m_t|) K_0(r|m_s|) \end{aligned} \tag{2.37}$$

While for dimerization correlation functions we have:

$$\begin{aligned} \langle \epsilon_-(r) \epsilon_-(0) \rangle &\sim \text{const} \left[1 + O(e^{-2rm_t}) \right] \\ \langle \epsilon_+(r) \epsilon_+(0) \rangle &\sim K_0^3(|m_t|r) K_0(|m_s|r) \end{aligned} \tag{2.38}$$

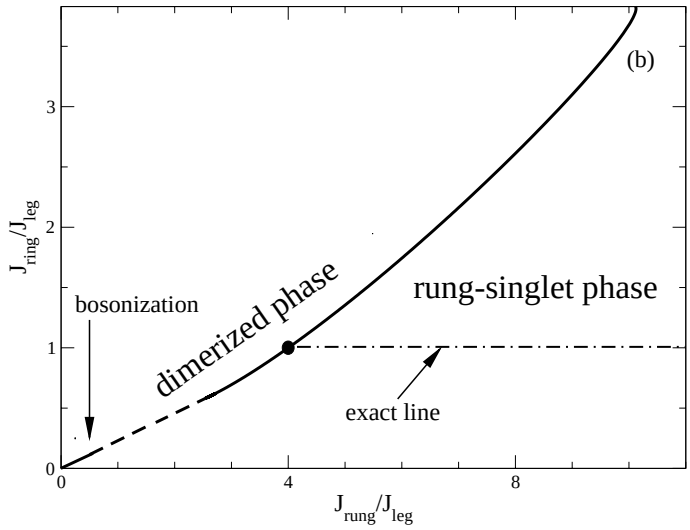

FIGURE 2.4: Phase diagram of rwo leg ladder with ring exchange

The imaginary part of the dynamical magnetic susceptibility reveals only two-magnon thresholds and complete disappearance of coherent magnon poles (see Appendix C.3):

$$ImD_{+}^{(R)}(\omega,\pi-q) \sim \frac{\theta[\omega^2-q^2-(m_t+m_s)^2]}{\sqrt{m_t m_s}\sqrt{\omega^2-q^2-(m_t+m_s)^2}}$$
$$ImD_{-}^{(R)}(\omega,\pi-q) \sim \frac{\theta[\omega^2-q^2-4m_t^2]}{m_t\sqrt{\omega^2-q^2-4m_t^2}} \qquad (2.39)$$

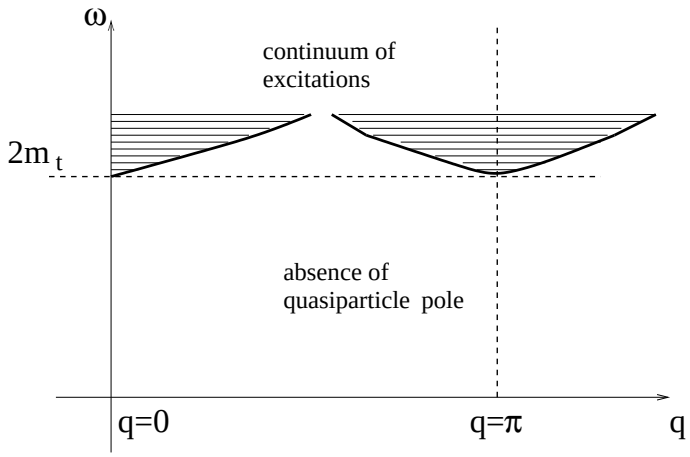

FIGURE 2.5: The area in (ω, q) plane where imaginary part of dynamical susceptibility of spin ladder in dimerized phase is finite

This transition belongs to the universality class of critical, exactly integrable, $S = 1$ spin chain (Takhtajan-Babujian point) with the central charge $c = 3/2$. The dimerization pattern emerging after crossing the critical line is the following: the chains become dimerized in a staggered way to each other with a nonzero relative dimerization. This is consistent with

the fact that for the antiferromagnetic interchain interaction effective $S = 1$ spins exhibiting nonzero string order are formed across the ladder diagonals rather than along the rungs.[34,35] On either side of this line the system is gapped, described in terms of free massive Majorana fermions with the symmetry $SU(2)\otimes Z^2$. The gap (which is the mass of the Majorana triplets 2.35) opens linearly as one deviates from the criticality. Owing to the $SU(2)$ symmetry of the model no other perturbations than mass terms of Majoranas are allowed in the vicinity of the critical line.

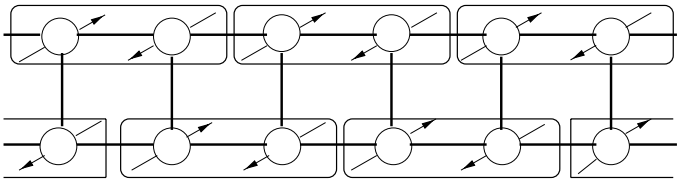

FIGURE 2.6: Dimerization pattern emerging after the phase transition

2.4 Elementary Excitations in Spontaneously Dimerized Ladder

Now we want to discuss elementary excitations in spontaneously dimerized ladder. For the sake of clarity we can switch-off rung interaction and discuss elementary excitations in purely dimerized phase. Discussion of elementary excitation will hold qualitatively valid also when rung interaction is nonzero. In this case neglecting the marginal interactions in Eq.(2.29) Hamiltonian is expressed as:[30]

$$\begin{aligned} H &= H^+ + H^- \\ H^+ &= \frac{u}{2}[(\partial_x\theta_+)^2 + (\partial_x\phi_+)^2] + \frac{J^{\mathrm{LL}}_{\mathrm{ring}}}{2\pi}\cos\sqrt{4\pi}\phi_+ \\ H^- &= \frac{u}{2}[(\partial_x\theta_-)^2 + (\partial_x\phi_-)^2] + \frac{J^{\mathrm{LL}}_{\mathrm{ring}}}{2\pi}\cos\sqrt{4\pi}\phi_- \end{aligned} \tag{2.40}$$

In the ground state plus-minus fields are pinned in one of the vacua $\left\langle\sqrt{4\pi}\phi_\pm\right\rangle = \pi + 2\pi n$. Elementary excitations could be described as free massive fermions (we remind, that $\cos\sqrt{4\pi}\phi$ is mapped to the mass term under Jordan-Wigner transformation), or kinks interpolating between the two degenerate ground states. S^z of elementary excitation is:

$$S^z = \frac{1}{\sqrt{2\pi}}\int dx(\partial_x\phi_1 + \partial_x\phi_2) = \frac{\triangle\phi_+}{\sqrt{\pi}} = 1 \tag{2.41}$$

if the kink is in symmetric sector, and otherwise zero. Since dimerization is spontaneous two nonequivalent vacuum configurations are energetically degenerate and single dimerization kink interpolates between them. At infinities fields should approach constant value $\phi_{\pm\infty} \to 2\pi n$ as a consequence only pairs of dimerization kinks can appear in each sector. Moreover, since there is no correlation between kinks (decoupling point of sine-Gordon)

once two kinks are created they propagate independently without coherence. Pictorial comparison of elementary excitation in spontaneously dimerized phase and weakly coupled ladder is on Fig. (2.7). We note peculiar difference, because of the spontaneous translational symmetry breaking only pair of solitons are allowed to appear in dimerized phase. That means at least four spins are involved in elementary excitation, as opposed to ordinary ladder, where single magnon, bound state of two spinons can propagate. As is evident from the

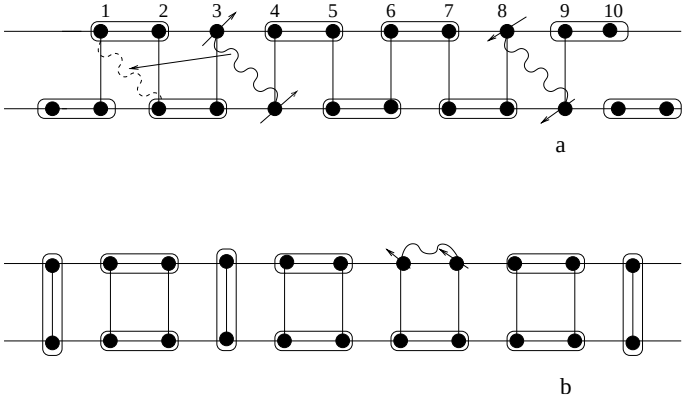

FIGURE 2.7: Elementary excitation in: a) spontaneously dimerized ladder, b) weakly coupled ladder. Arrow indicates possible hopping of the dimerization kink

Fig.(2.7) because of the doubling of the unit cell in the ground state of the dimerized phase dimerization kink hops over two lattice constants.

2.5 Thermodynamic Quantities

In this section we will extensively use fermionic representation of our model. Since low energy sector of spin ladder is described in terms of essentially free fermions we can apply free field theory methods to calculate various thermodynamical quantities. We will start from perhaps the simplest one, namely specific heat.

2.5.1 Specific Heat

Free energy of fermion systems with dispersion spectrum E_k looks:

$$F = -T \int_{-\infty}^{+\infty} \frac{dk}{2\pi} \ln\left(1 + e^{-E_k/T}\right) \tag{2.42}$$

Direct evaluation of specific heat $C = -T\frac{\partial^2 F}{\partial T^2}$ gives:

$$C = \frac{1}{T^2} \int_{-\infty}^{+\infty} \frac{dk}{2\pi} \frac{E_k^2 e^{E_k/T}}{(e^{E_k/T}+1)^2} = \frac{1}{4T^2} \int_{-\infty}^{+\infty} \frac{dk}{2\pi} E_k^2 \left(\operatorname{sech}\frac{E_k}{2T}\right)^2 \tag{2.43}$$

This expression allows to evaluate specific heat for massless fermions (at criticality) exactly, so for spectrum $E_k^2 = v^2 k^2$ we get

$$C(T) = \frac{T\pi^2}{6v} \tag{2.44}$$

On the gapless line in the space of Ring, Rung and Leg exchanges there is a special point, where ground state is an exact product of singlets[36] located along the ladder rungs. On this special point lowest excitation is propagating triplets along the ladder. The spectrum is quadratic $E \simeq q^2$, instead of linear, and thus cpecific heat will be given (using dimensional arguments for Eq. (2.43)) at this point as:[52]

$$C(T) \simeq \sqrt{T} \tag{2.45}$$

We note, that this point is in some sense pathological, the velocity of linear excitations vanishes only on this point. Thus this critical point is not described in terms of free fermions. For the off critical or massive case $E_k^2 = v^2k^2 + m^2$. At low enough temperatures when $T/m \to 0$ we can neglect 1 in denominator of the middle part of (2.43).

$$C \simeq \frac{1}{T^2}\int_{-\infty}^{+\infty}\frac{dk}{2\pi}E_k^2 e^{-E_k/T} \tag{2.46}$$

Furthermore, since at low T dominant contribution comes from small k region $v^2k^2 \ll m^2$ we can approximate

$$e^{-\frac{E_k}{T}} = e^{-\frac{\sqrt{m^2+v^2k^2}}{T}} = e^{-\frac{m}{T}\sqrt{1+\frac{v^2k^2}{m^2}}} \simeq e^{-\frac{m}{T}}e^{-\frac{v^2k^2}{2mT}} \tag{2.47}$$

Taking simple Gaussian integral finally we get:

$$C \simeq \frac{1}{T^2}\int_{-\infty}^{+\infty}\frac{dk}{2\pi}m^2 e^{-\frac{m}{T}}e^{-\frac{v^2k^2}{2mT}} = m^2 e^{-\frac{m}{T}}\frac{\sqrt{2\pi mT}}{2\pi T^2 v} = \left(\frac{m}{T}\right)^{\frac{3}{2}}\frac{m}{v\sqrt{2\pi}}e^{-\frac{m}{T}} \tag{2.48}$$

2.5.2 Static Susceptibility

Static susceptibility for the ladder system is calculated using diagrammatic methods and is explained in details in Appendix C. 6.

$$\chi(T) = \frac{1}{T}\int_0^{\infty}\frac{dk}{2\pi}\mathrm{sech}\,\frac{E_t(k)}{2T} \tag{2.49}$$

For massless case this expression can be calculated exactly and we get temperature independent constant magnetic susceptibility (characteristic to Luttinger Liquids),

$$\chi(T) = \frac{\pi}{2v} \tag{2.50}$$

On this special point where velocity of linear excitations vanishes and lowest spectrum is quadratic $E \simeq q^2$, instead of constant susceptibility applying dimensional arguments to (2.49) we have:[52]

$$\chi(T) \simeq \sqrt{T^{-1}} \tag{2.51}$$

We note, that althougth this point is not described in terms of free fermions our fomulas for specific heat and static susceptibility are equally well applicable to get their temperature behavior. We have just to replace gapless linear spectrum with gapless quadratic. The reason

why fermionic theory is so successful is that magnon, is hard core boson. In one dimension there is no difference between thermodynamical properties of fermions and bosons with infitite repulsion. For massive case making low temperature approximation as we did for calculation of the specific heat we get:

$$\chi(T) \simeq \frac{\sqrt{2\pi m_t}}{v} T^{-\frac{1}{2}} e^{-\frac{m_t}{T}} \tag{2.52}$$

2.5.3 Nuclear Magnetic Resonance Relaxation Rate

Looking on the thermodynamical quantities e.g. specific heat, static susceptibility it is impossible to distinguish conventional Haldane phase of spin ladder from the dimerised phase. The reason is that those quantities depend only on the gap magnitude and are insensitive on the mutual sign between triplet and singlet excitation masses. Peculiarly there is an interesting quantity: nuclear magnetic resonance relaxation rate that can distinguish between the Haldane like phase and dimerised phase of the ladder, but not for the spin one chain. The explanation of this puzzle is, that for spin ladder we get contribution from triplet singlet channel, which is absent for spin 1 chain. Here we write temperature dependent NMR relaxation rate, conventionally denoted by T_1. For detailed calculation we refer to Appendix C.6.

$$T_1^{-1} \simeq \frac{m_t}{2(\pi v)^2} e^{-\frac{m_t}{T}} \left(-C + \ln 4 - \ln \frac{w}{T} \right) + \frac{1}{(\pi v)^2} \sqrt{\pi |m_s|} \sqrt{\frac{|m_s + m_t|}{|m_s - m_t|}} e^{-\frac{m_s}{T}} \sqrt{T} \tag{2.53}$$

The amplitude of the second term depends on the mutual signs of singlet and triplet masses. Main charachteristics of the above expression is exponential drop in temperature, due to excitation gap. Logarithmic divergence in prefactor with vanishing nuclear resonance frequency is caused by Van Hove singularity in the density of states of free Majoranas at a bottom of the band.

2.6 Conclusions

This chapter of the thesis was concerned with the study of a $SU(2)$ antiferromagnetic ladder with additional four-spin ring interaction. Bosonization- fermionization approach was used to describe the low energy exitations of the model and determine effect of frustration produced by additional plaquette interaction on the ground state phase diagram. Weak coupling regime of the model was described in terms of the massive Majorana fermions coupled by weak four-fermi intaraction. A part of the ground state phase diagram for sufficiently strong frustration was obtained. It was shown that the ordinary rung singlet phase of the pure antiferromagnetic ladder undergoes a quantum phase transition to spontaneously dimerized phase. This phase transition was identified with the one that happens in the spin one AFM chain with additional biquadratic terms. Since in AFM ladder effective S=1 spins are formed accross the ladder diagonals dimerization pattern obtained after the phase transition was of valence bond solid structure (staggeredly dimerized chains). Transformation to the two dimensional Ising variables allowed to relate correlation functions of the model with

2D Ising correlation functions that are known analytically both at and off criticality. The single magnon that is well defined quasiparticle in the ordinary ladder disappears from the low energy excitation spectrum which is exhausted by the continuum of incoherent dimerization kinks. Finite temperature calculations were carried out using conformal field theory and Matsubara formalisms.

CHAPTER 3

Phase Diagrams of Spin Ladders with Ferromagnetic Legs

This part of the thesis is devoted to investigation of ground state phase diagram of spin ladders with ferromagnetic legs. These systems exhibit very rich ground state properties. Apart from pure academic interest in these models our motivation stems from the fact that quasi low-dimensional spin systems with ferromagnetic interactions are also realized as real crystals, as exemplified by the $S = 1/2$ chain $(C_6H_{11}NH_3)CuBr_3$ (CHAB)[59] and the $S = 1$ chain $CsNiF_3$.[60] No ladder systems with ferromagnetic interactions are known yet, but considering recent progress in material science such systems may well be synthesized in the future. In following we study ground state phase diagram of a $S = 1/2$ ladder system with ferromagnetic legs and anisotropic interleg exchange using the continuum limit bosonization approach.

The Hamiltonian of the model under consideration is given by

$$\hat{H} = H^1_{leg} + H^2_{leg} + H_\perp \,, \tag{3.1}$$

where the Hamiltonian for leg $\alpha = 1, 2$ is

$$\begin{aligned} H^\alpha_{leg} &= -J \sum_{j=1}^{N} \left(S^x_{\alpha,j} S^x_{\alpha,j+1} + S^y_{\alpha,j} S^y_{\alpha,j+1} \right. \\ &+ \left. \Delta\, S^z_{\alpha,j} S^z_{\alpha,j+1} \right) , \end{aligned} \tag{3.2}$$

and the interleg coupling is given by

$$\begin{aligned} H_\perp &= J^{xy}_\perp \sum_{j=1}^{N} \left(S^x_{1,j} S^x_{2,j} + S^y_{1,j} S^y_{2,j} \right) \\ &+ J^z_\perp \sum_{j=1}^{N} S^z_{1,j} S^z_{2,j} \,. \end{aligned} \tag{3.3}$$

Here $S^{x,y,z}_{\alpha,j}$ are spin $S = 1/2$ operators at the j-th rung. The intraleg coupling constant is chosen ferromagnetic $J > 0$. In these denotions $\Delta = 1$ corresponds to *isotropic ferromagnetic* legs , while $\Delta = -1$ corresponds to *isotropic antiferromagnetic* legs.

We will be concerned with the study of ground state phase diagram of the model for $\Delta > 0$ (ferromagnetic legs), as well as $\Delta \simeq 0$.

In section II we derive the bosonized formulation of the model in the continuum limit. In section III we discuss the weak coupling phase diagrams of the model for three different cases of anisotropic interleg coupling. Finally, we conclude and summarize our results in section IV. In the Appendix E we present the spin-wave approach to study the transition line related to the ferromagnetic instability in the system.

3.1 Bosonization

In this section we derive the low-energy effective field theory of the lattice model Eq. (3.1).

3.1.1 Separate Chains

The bosonized effective field theory of general anisotropic spin ladders is governed by Hamiltonian (1.44). However, since in this section we consider the ladder model with *ferromagnetic legs*, our bosonization conventions require some comments. The unitary transformation

$$S^{x,y}_{\alpha,j} \to (-1)^j S^{x,y}_{\alpha,j}\,, \quad S^{z}_{\alpha,j} \to S^{z}_{\alpha,j} \tag{3.4}$$

changes the sign of the intrachain transverse exchange and maps the Hamiltonian (3.1) to the Hamiltonian with *antiferromagnetic* legs. This duality transformation maps points under reflection with respect to $J_{XY} = 0$ line (Fig. 3.1). Under this mapping smooth and staggered parts of inplain components of spin operators are interchanged. Bosonization procedure of

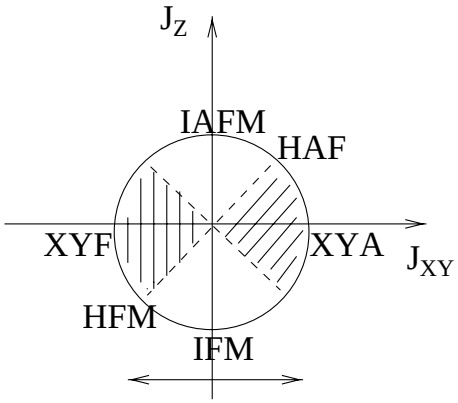

FIGURE 3.1: XXZ spin half chain phase diagram for arbitrary sign of inplain and out of plane couplings. Different regions are denoted respectively from above clockwise as: Ising antiferromagnet, Heisenberg antiferromagnet, XY (planar) antiferromagnet, Ising Ferromagnet, Heisenberg ferromagnet, and XY (planar) ferromagnet

spin system (as derived in Appendix A) is based on Jordan- Wigner transformation to spinless fermions. While for evaluating terms quadratic in fermionic operators change of sign in front of hopping term is irrelevant, terms linear in fermionic operators (e.g. $S^{\pm}$) undergo smooth - staggared part transmutation. Under this transformation left and right Fermi points of corresponding Jordan- Wigner fermionic bands are interchanged. Equivalently one can pass to Jordan- Wigner fermions in case of inplain ferro exchange with $S^{-}_{i} = \mathrm{c}_i\, exp(i\pi \sum_{j=0}^{i-1} \mathrm{c}^{+}_{j}\mathrm{c}_j)$ and for antiferro $S^{-}_{i} = (-1)^i \mathrm{c}_i\, exp(i\pi \sum_{j=0}^{i-1} \mathrm{c}^{+}_{j}\mathrm{c}_j)$, thus leaving the positions of left and right fermi points the same place, but one reads from above again extra staggering factor in $S^{\pm}$ between ferro and antiferro inplane coupling cases. So to maintain the ferromagnetic character of the in-plane correlations in the bosonization, it is convenient to implement the multiplicative factor $(-1)^j$, introduced by the unitary transformation (3.4), directly in the

bosonized expressions for the transverse components of the spin operators. Using the standard bosonization formulas (Appendix A) we obtain:

$$\begin{aligned} S^x_{j,\alpha} &\simeq \frac{c}{\sqrt{2\pi}} : \cos\sqrt{\frac{\pi}{K}}\theta_\alpha(x) : \\ &+ (-1)^j \frac{ib}{\sqrt{2\pi}} : \sin\sqrt{4\pi K}\phi_\alpha(x) \sin\sqrt{\frac{\pi}{K}}\theta_\alpha(x) : , \qquad (3.5) \\ S^y_{j,\alpha} &\simeq \frac{c}{\sqrt{2\pi}} : \sin\sqrt{\frac{\pi}{K}}\theta_\alpha(x) : \\ &- (-1)^j \frac{ib}{\sqrt{2\pi}} : \sin\sqrt{4\pi K}\phi_\alpha(x) \cos\sqrt{\frac{\pi}{K}}\theta_\alpha(x) : , \qquad (3.6) \\ S^z_{j,\alpha} &= \sqrt{\frac{K}{\pi}}\partial_x\phi_\alpha(x) + \\ &(-1)^j \frac{a}{\pi} : \sin\sqrt{4\pi K}\phi_\alpha(x) : . \qquad (3.7) \end{aligned}$$

Note that the first and the second terms in Eqs. (3.5),(3.6) are hermitian because of (1.36). Furthermore $: \mathcal{A} :$ denotes the normal ordering (in following we will omit it from operators, bur will be understood implicitely) withrespect to free bose system (1.35), α is the leg index. The non-universal real constants *a*, *b* and *c* depend smoothly on the parameter Δ,[64,65] and are nonzero for general $\Delta < 1$.

3.1.2 Coupled Spin-1/2 Chains

Effective field theory for weakly coupled spin ladder with ferromagnetic legs is obtained from general Hamiltonian (1.44):

$$\begin{aligned} \mathcal{H} &= \mathcal{H}^+ + \mathcal{H}^- + \mathcal{H}^\pm_{int} , \qquad (3.8) \\ \mathcal{H}^+ &= \frac{u_+}{2}[(\partial_x\theta_+)^2 + (\partial_x\phi_+)^2] \\ &- \frac{\mathcal{J}^z_\perp}{2\pi}\cos\sqrt{8\pi K_+}\phi_+(x) , \qquad (3.9) \\ \mathcal{H}^- &= \frac{u_-}{2}[(\partial_x\theta_-)^2 + (\partial_x\phi_-(x))^2] \\ &+ \frac{\mathcal{J}^z_\perp}{2\pi}\cos\sqrt{8\pi K_-}\phi_-(x) \\ &+ \frac{\mathcal{J}^{xy}_\perp}{2\pi}\cos\sqrt{\frac{2\pi}{K_-}}\theta_-(x) , \qquad (3.10) \\ \mathcal{H}^\pm_{int} &= \frac{\mathcal{J}_{+-}}{2\pi}\cos\sqrt{\frac{2\pi}{K_-}}\theta_-(x)\cos\sqrt{8\pi K_+}\phi_+(x) . \qquad (3.11) \end{aligned}$$

In deriving (3.8) from (1.44) a term $\sim \tilde{\mathcal{J}}^{xy}_\perp \cos\sqrt{\frac{2\pi}{K_-}}\theta_- \cos\sqrt{8\pi K_-}\phi_-$ which is strongly irrelevant at $\Delta > 0$ (ferromagnetic legs) was omitted. Plus strongly irrelevant terms, products of the current current operators along each chain (responsible to AFM transition and

becoming marginal at $SU(2)$ point) were also neglected. Thus Hamiltonian (3.8) describes effective field theory of weakly coupled ferromagnetic chains as well as antiferromagnetic chains only for $\Delta \sim 0$.

3.1.3 The Effective Continuum-Limit Model

At $J_\perp^z = J_\perp^{xy} = 0$ the Hamiltonian (3.8) describes two independent Gaussian fields, i.e. two gapless fields, each describing a critical spin S=1/2 Heisenberg chain. We will study the effects of longitudinal ($J_\perp^z$) and transverse ($J_\perp^{xy}$) part of the interleg coupling separately.
At $J_\perp^{xy} = 0$ the effective theory of the original ladder model is given by two decoupled quantum sine-Gordon models

$$\mathcal{H}_{eff} = \mathcal{H}^+ + \mathcal{H}^- \tag{3.12}$$

where

$$\begin{aligned} \mathcal{H}^\pm &= u_\pm \int dx \left[\frac{1}{2}[(\partial_x\theta_\pm(x))^2 + (\partial_x\phi_\pm(x))^2]\right. \\ &+ \left.\frac{M_\pm}{2\pi}\cos\sqrt{8\pi K_\pm}\phi_\pm(x)\right]. \end{aligned} \tag{3.13}$$

The two SG models respectively describe the symmetric (ϕ_+) and antisymmetric (ϕ_-) degrees of freedom.
The bare values of the dimensionless coupling constants $M_\pm$ and $K_\pm$ are known only in the weak-coupling limit $|J_\perp^z|/J, |\Delta| \ll 1$:

$$M_\pm = \mp\frac{J_\perp^z}{\pi J}, \tag{3.14}$$

$$K_\pm = 1 + \frac{2\Delta}{\pi} \mp \frac{J_\perp^z}{2\pi J}. \tag{3.15}$$

As $M_\pm$ follow directly from (1.48) and (1.50) some explanation needs derivation of $K_\pm$ (we remind, that at $\Delta = 0$ we have $u = J$). Part coming from linearization of (1.49) is clear, we explain how we obtain Δ dependent part. For this we consider bosonized version of separate xy chain and add $\Delta S_i^z S_{i+1}^z$ part of interaction, assuming $|\Delta| \ll J^{xy} = J$.

$$\frac{J}{2}\left[(\partial_x\theta(x))^2 + (\partial_x\phi(x))^2\right] - \frac{\Delta}{\pi}(\partial_x\phi(x))^2 + \frac{\Delta}{\pi^2} : \sin\sqrt{4\pi}\phi(x) :: \sin\sqrt{4\pi}\phi(x+a) : \tag{3.16}$$

Plus sign before the product of staggered components comes form the $(-1)^n$ factors. This time we have to restore lattice cutoff (ultraviolet regulator), otherwise product of two vertex operators at coinciding point is divergent and also we restored explicitly normal ordering signs. We have to apply the following ope:

$$\begin{aligned} &: \sin\sqrt{4\pi}\phi(x) :: \sin\sqrt{4\pi}\phi(x+a) : \\ &= \frac{1}{2}\left[: \cos\sqrt{4\pi}\left(\phi(x) - \phi(x+a)\right) : - : \cos\sqrt{4\pi}\left(\phi(x) + \phi(x+a)\right) :\right] \\ &= -\frac{1}{2} : \cos\sqrt{16\pi}\phi(x) : + \sqrt{\pi}a : \partial_x\phi(x)\sin\sqrt{16\pi}\phi(x) : - \pi a^2 : (\partial_x\phi(x))^2 : + \ldots \end{aligned} \tag{3.17}$$

The most important term is the last one, together with the term that originates from the product of smooth parts of S^z it has the form of 'kinetic energy' of the Gaussian model. All other terms including dots are irrelevant (at $\Delta = -1$ term $\cos\sqrt{16\pi}\phi(x)$ becomes marginal). Collecting all terms Eq. (3.16) will acquire the following form:

$$\frac{J}{2}\left[(\partial_x\theta(x))^2 + (1-\frac{4\Delta}{J\pi})(\partial_x\phi(x))^2\right] \tag{3.18}$$

Obtained Hamiltonian density could be diagonalized by canonical transformation (simplest manifestations of why bosonization is so efficient in 1 dimension). Passing to new canonical variables (fields):

$$(\partial_x\tilde{\theta})^2 = (\partial_x\theta)^2/\sqrt{1+\frac{4\Delta}{J\pi}},\ (\partial_x\tilde{\phi})^2 = (\partial_x\phi)^2\sqrt{1+\frac{4\Delta}{J\pi}} \tag{3.19}$$

We will get for Hamiltonian density:

$$\frac{JK}{2}\left[(\partial_x\tilde{\theta}(x))^2 + (\partial_x\tilde{\phi}(x))^2\right] \tag{3.20}$$

where

$$K = \sqrt{1+\frac{4\Delta}{J\pi}} \simeq 1+\frac{2\Delta}{J\pi} \tag{3.21}$$

Combining Eq. (3.21) with linearized expression from Eq. (1.48) we arrive at the desired first order result as in Eq. (3.15). The scaling dimensions of the *cosine* terms in (3.13) are $d^z_\pm = 2K_\pm \simeq 2$. Therefore, in the weak-coupling limit, both SG models have marginal dimension and details of their behavior should be determined within the framework of the renormalization-group analysis.

The transverse interleg exchange ($J^{xy}_\perp$) leads to the appearance of the strongly relevant operator $\mathcal{J}^{xy}_\perp \cos\sqrt{2\pi K_-^{-1}}\theta_-$ with the scaling dimension $d^{xy}_- = (2K_-)^{-1} \leq 1/2$ in the theory. Therefore, the antisymmetric sector is gapped at arbitrary $J^{xy}_\perp \neq 0$. FLuctuations of the field $\theta_-(x)$ are completely suppressed in this sector and $\theta_-(x)$ is condensed in one of its vacua. The vacuum expectation value of the *cosine* term is

$$\langle\cos\sqrt{2\pi K_-^{-1}}\theta_-\rangle = \gamma \tag{3.22}$$

with $\gamma \sim (|\mathcal{J}^{xy}_\perp|/J_{eff})^{\frac{d^{xy}_-}{2-d^{xy}_-}} \ll 1$ (see Eq. (D.15)) in weak coupling and is of the order of unity at $|\mathcal{J}^{xy}_\perp| \sim J$. If we apply dimensional analyses straightforwardly to the interaction term (3.11) it tells that in weak-coupling at $K_\pm \simeq 1$ this term is irrelevant. It is the condensation of the field θ_- that strongly influences the coupling between the symmetric and antisymmetric modes induced by $\mathcal{H}^\pm_{int}$. Taking into account that the θ_- field is frozen, fluctuates slowly aroud its vacuum expectation value, one easily finds that at $J^{xy}_\perp \neq 0$ infrared behavior of the symmetric field is governed by the following "effective" sine-Gordon theory obtained after mean-field like separation between two sectors:

$$\begin{aligned}\mathcal{H}^+_{eff} &= u_+\int dx\left[\frac{1}{2}[(\partial_x\theta_+)^2 + (\partial_x\phi_+(x))^2]\right.\\ &+ \left.\frac{M^+_{eff}}{2\pi}\cos\sqrt{8\pi K_+}\phi_+(x)\right],\end{aligned} \tag{3.23}$$

where

$$M^{+}_{eff} = -\frac{1}{\pi u_{+}} \left(\mathcal{J}^{z}_{\perp} + \gamma \cdot |\mathcal{J}_{+-}| \right) . \tag{3.24}$$

One may wonder about the self consistency of the above mean-field separation, that is about the feedback or reverse influence of symmetric sector on antisymmetric one. The effective Hamiltonian for the symmetric field is the SG model with the marginal coupling, whereas antisymmetric sector is governed by strongly relevant operator. Thus the reverse influence of the symmetric field on the antisymmetric one is negligible in the leading order RG analysis even in the case of strong coupling regime in the symmetric sector. The mapping of the initial spin $S = 1/2$ ladder model onto the quantum sine-Gordon theories (3.13) or (3.23) will allow us to extract the ground state phase diagram of the $S = 1/2$ ladder from the infrared properties of the quantum SG models.

3.1.4 The RG Analysis

All the phase transition lines determined within bosonization formalism (sometimes after mean-field like separations) will belong to the Kosterlitz-Thouless type (exeption will be transition into ferromagnetic phase). Meaning, that retained single $cosine$ perturbation changes from marginaly irrelevant to relevant one on those lines. Thus it is extremely important to analyse Kosterlitz-Thoulees transition in sine-Gordon Model. The infrared behavior of the SG Hamiltonian is described by the corresponding pair of renormalization group (RG) equations for the effective coupling constants $\mathcal{K}(l)$ and $\mathcal{M}(l)$ (for derivation see Appendix D)

$$\begin{aligned} \frac{d\mathcal{M}(l)}{dl} &= -2\left(\mathcal{K}(l) - 1\right)\mathcal{M}(l) \\ \frac{d\mathcal{K}(l)}{dl} &= -\frac{1}{2}\mathcal{M}^{2}(l) \end{aligned} \tag{3.25}$$

where $l = \ln(a_0)$ and the bare values of the coupling constants are $\mathcal{K}(l = 0) \equiv K$ and $\mathcal{M}(l = 0) \equiv M$. The pair of RG equations (3.25) describes the Kosterlitz-Thouless transition.[66] The flow lines lie on the hyperbola

$$4\left(\mathcal{K} - 1\right)^{2} - \mathcal{M}^{2} = \mu^{2} = 4(K - 1)^{2} - M^{2} \tag{3.26}$$

and exhibit two different regimes depending on the relation between the bare coupling constants (see Fig.3.2):

Weak coupling regime. For $2(K - 1) \geq |M|$ we are in the weak coupling regime: the effective mass $\mathcal{M} \to 0$. The low energy (large distance) behavior of the corresponding gapless mode is described by a free scalar field.

The vacuum averages of exponentials of the corresponding fields show a power-law decay at large distances

$$\langle\, e^{iK\phi(0)}\, e^{-iK\phi(r)} \rangle \sim \langle\, e^{iK\theta(0)}\, e^{-iK\theta(r)} \rangle \sim |r|^{-\frac{K^{*2}}{2\pi}} . \tag{3.27}$$

where K^{*} is the fixed-point value of the parameter K determined from the Eq. (3.26).

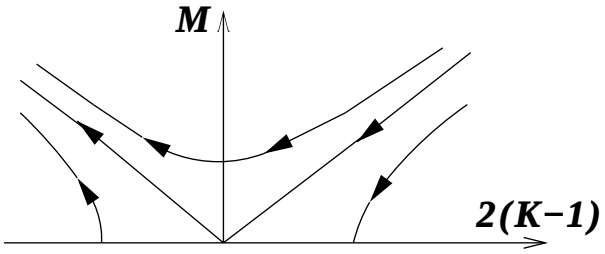

FIGURE 3.2: Renormalization-group flow diagram; the arrows denote the direction of flow with increasing length scale.

Strong coupling regime. For $2(K-1) < |M|$ the system scales to strong coupling: depending on the sign of the bare mass M, the renormalized mass $\mathcal{M}$ is driven to $\pm\infty$, signaling a crossover to one of two strong coupling regimes with a dynamical generation of a commensurability gap in the excitation spectrum. The flow of $|\ \mathcal{M}\ |$ to large values indicates that the $\mathcal{M}\cos\sqrt{8\pi K}\phi$ term in the sine-Gordon model dominates the long-distance properties of the system. Depending on the sign of the mass term, the field ϕ gets ordered with the expectation values

$$\langle\phi\rangle = \begin{cases} \sqrt{\pi/8K} & \text{at } M > 0 \\ 0 & \text{at } M < 0 \end{cases} . \tag{3.28}$$

Using this analysis for the excitation spectrum of the SG model and the behavior of the corresponding fields, Eqs. (3.27, 3.28), we will now discuss the *weak-coupling* phase diagram of the spin $S = 1/2$ *ferromagnetic ladder* model (3.1).

3.2 Ground State Phase Diagrams

In this section we discuss separately the ground state phase diagram of the *ferromagnetic ladder* coupled only by the longitudinal part of the interleg spin exchange (subsection 1), coupled only by the transverse part of the interleg spin exchange (subsection 2) and by an isotropic interleg coupling (subsection 3). At this point we note that from the structure of the interaction Hamiltonian Eq. (3.3) follows that the phase diagrams for case (1) and case (2) will be symmetric with respect to the lines $J_\perp = 0$ since a change of sign in $J_\perp$ leads to a unitary equivalent Hamiltonian. This is in contrast to case (3) where this unitary equivalence does not exist (compare corresponding Figures:(3.3),(3.4), and (3.5) with respect to the reflection symmetry around the $J_\perp = 0$ axes).

3.2.1 Chains Coupled by the Longitudinal Part of the Interleg Exchange

In this subsection we consider the weak-coupling phase diagram of the spin S=1/2 ferromagnetic ladder model (3.1) coupled by a weak longitudinal interchain exchange ($J_\perp^{xy} = 0, J_\perp^z \neq 0$). The bosonized version of the model is $\mathcal{H}_{eff} = \mathcal{H}^+ + \mathcal{H}^-$ where $\mathcal{H}^\pm$ are given by Eq. (3.13) and the bare values of the corresponding dimensionless coupling constants are

given by (3.14)-(3.15). By inspecting the initial values of the coupling constants one easily finds that:

- At $\Delta < 0$ both the symmetric and the antisymmetric sectors are gapped (except for $J_\perp^z = 0$).
- At $\Delta > 0$ the *symmetric sector is gapped* for $J_\perp^z/J > 2\Delta > 0$ while the *antisymmetric sector is gapped* for $J_\perp^z/J < -2\Delta < 0$.

This determines the following three distinct sectors of the phase diagram as traced already in the RG analysis (see also Fig. (3.3):

- Sector A: $\Delta < 0$ corresponds to the phase with gapped excitation spectrum;
- Sector B: $\Delta > 0$ and $|J_\perp^z| > 2J\Delta$ corresponds to the phase characterized by the one gapless and one gapped mode in the excitation spectrum. In particular at $J_\perp^z > 0$ the symmetric mode is gapped whereas the antisymmetric mode is gapless and vice-versa at $J_\perp^z < 0$;
- Sector C: $\Delta > 0$ and $|J_\perp^z| < 2J\Delta$ corresponds to the phase where both modes are gapless.

As we will show below, the same phases are present in the strong coupling regime. The only phase which is missed in the weak-coupling RG analysis is the ferromagnetic phase; it appears only in the strong coupling regime at $\Delta \simeq 1$ or at $\Delta \ll 1$ but $|J_\perp^z| \sim 1/\Delta \gg 1$.

To clarify the symmetry properties of the ground states of the system in the different sectors we study the large-distance behavior of the longitudinal

$$K_{\alpha\beta}^{zz}(r) := \langle S_\alpha^z(0) S_\beta^z(r) \rangle \,, \tag{3.29}$$

and the transverse

$$K_{\alpha\beta}^{xy}(r) := \langle S_\alpha^+(0) S_\beta^-(r) \rangle \,, \tag{3.30}$$

spin-spin correlation functions for intraleg ($\alpha = \beta$) and interleg ($\alpha \neq \beta$) spin pairs.

Using the results for the excitation spectrum and the behavior of the corresponding fields in the gapless and gapped phases, Eqs. (3.27)-(3.28), and the expressions for the corresponding correlation functions from bosonization, we now discuss the characteristics of the various phases in the different sectors of the *weak-coupling* ground state phase diagram.

In the sector A ($J_\perp^z < 0$) the vacuum expectation values of the fields are:

$$\langle \phi_+ \rangle = \sqrt{\pi/8K_+} \text{ and } \langle \phi_- \rangle = 0 \tag{3.31}$$

In the following we will use the following properties of the bose fields: the ordering of fields induce exponential decay of their dual fields. This non-trivial fact can be derived for special cases of anisotropy where vertex operators involving fields map to the order fields of the 2 dimensional Ising variables and dual fields map to disorder variables. In general, where such mapping does not exist this statement is expected to hold, since fileds and their duals are non-local objects to each other. Ordering of the $\phi_\pm$ suppresses transverse spin correlations

(which necessarily involve dual fields), Using Eq. (3.31) the longitudinal correlations are given by the following formula:

$$K^{zz}_{\alpha\beta}(r) \sim \langle \partial_x \phi_\alpha(r) \partial_x \phi_\beta(0) \rangle + (-1)^r \left\langle \sin\sqrt{4\pi K}\phi_\alpha(r) \sin\sqrt{4\pi K}\phi_\beta(0) \right\rangle$$
$$\sim (-1)^r \cdot const \tag{3.32}$$

For the above result we have used the following representations:

$$\sin\sqrt{4\pi K}\phi_{1,2} \to \sin\sqrt{2\pi K_+}\phi_+ \cos\sqrt{2\pi K_-}\phi_- \pm \cos\sqrt{2\pi K_+}\phi_+ \sin\sqrt{2\pi K_-}\phi_- \tag{3.33}$$

and the vacuum expectation values Eq. (3.31) from which it follows:

$$\langle \cos\sqrt{2\pi K_-}\phi_- \rangle \simeq 1 \;\; \langle \sin\sqrt{2\pi K_-}\phi_- \rangle \simeq 0$$
$$\langle \cos\sqrt{2\pi K_+}\phi_+ \rangle = 0 \;\; \langle \sin\sqrt{2\pi K_+}\phi_+ \rangle \simeq 1 \tag{3.34}$$

Therefore at $\Delta < 0$ and $J^z_\perp < 0$, the long-range ordered (LRO) antiferromagnetic phase with inphase spin ordering on the rungs is realized in the ground state of the system.
In the Sector A1 ($J^z_\perp < 0$) the vacuum expectation values of the fields are given by

$$\langle \phi_+ \rangle = 0 \text{ and } \langle \phi_- \rangle = \sqrt{\pi/8K_-}. \tag{3.35}$$

From Eq. (3.33) and (3.34) it follows that in this sector

$$K^{zz}_{\alpha\beta}(r) \sim (-1)^{\alpha+\beta} \cdot (-1)^r \cdot \text{const}$$

Therefore, at $\Delta < 0$ and $J^z_\perp > 0$ the LRO antiferromagnetic phase with antiphase intrarung spin ordering is realized in the ground state of the system.
In the sector B (B1) the antisymmetric (symmetric) field is gapped with the vacuum expectation value $\langle \phi_- \rangle = 0$ ($\langle \phi_+ \rangle = 0$). However, as can be seen from weak coupling RG analysis as well as from the strong coupling effective spin $1/2$ model (see below), at $J^z_\perp \neq 0$ the line $\Delta = 0$ is the phase transition line along which the gapped at $\Delta < 0$ symmetric (antisymmetric) mode becomes gapless. Therefore in the sector B (B1) the gapless degrees of freedom corresponding to the symmetric (antisymmetric) mode are described by the free Bose field system with the fixed-point value of the parameters $K^*_\pm$. Using Eq. (3.26) and the bare values of coupling constants (3.14)-(3.15)we get for $|\Delta|, |J^z_\perp/J| \ll 1$

$$K^*_\pm \simeq 1 + \frac{1}{\pi}\sqrt{2\Delta(2\Delta \mp J^z_\perp/J)}\,.$$

Note that at $\Delta = 0$ the fixed-point values of the spin-liquid parameters are $K^*_\pm = 1$ while at $J^z_\perp = 0$ (see Eq. (1.49)) $K^*_\pm = K$. Therefore we conclude that along the line $\Delta = 0$ the gapless sector in the system is identical to a single isotropic spin $S = 1/2$ Heisenberg chain, while along the line $J^z_\perp = 0$ we reach the limit of two decoupled spin $S = 1/2$ Heisenberg chains.

Ordering of the field ϕ_- (or ϕ_+) implies suppression of the transverse correlations (since they involve dual fields that are disorder operators and in ordered phase decay exponentially). On the other hand the presence of the gapless excitation mode leads to the power law decay

of the longitudinal spin correlations. Using representation (3.33) for sector B we get the following correlation functions:

$$K^{zz}_{\alpha\beta}(r) \simeq \frac{K^*_+}{2\pi r^2} + \frac{(-1)^r}{r^{K^*_+}},$$

while in the sector B1

$$K^{zz}_{\alpha\beta}(r) \simeq (-1)^{\alpha+\beta}\left[\frac{K^*_-}{2\pi r^2} + \frac{(-1)^r}{r^{K^*_-}}\right].$$

We denote this phase as the *spin liquid I* phase. It is interesting to note that in sector B the following operator shows quasi long range behavior:

$$\begin{aligned}\langle (S^+_1(r) &+ S^+_2(r))^2\,(S^-_1(0)+S^-_2(0))^2\rangle \\ &\simeq 4\langle S^+_1(r)S^+_2(r)\,S^-_1(0)S^-_2(0)\rangle \\ &\simeq r^{-1/K^*_+} + (-1)^r\, r^{-1/K^*_+ - K^*_+}. \end{aligned} \tag{3.36}$$

$(S^\alpha_1 + S^\alpha_2)^2$ for the $S=\frac{1}{2}$ ladder corresponds to the operator $(S^\alpha)^2$ in the $S=1$ chain and we therefore identify sector B with the $XY2$ phase for the $S=1$ chain([27]). The counterpart of this operator exists also in sector B1, al-bight, not connected with effective spin 1:

$$\langle S^+_1(r)S^-_2(r)\,S^+_1(0)S^-_2(0)\rangle \simeq r^{-1/K^*_-} + (-1)^r\, r^{-1/K^*_- - K^*_-}. \tag{3.37}$$

With increasing interleg ferromagnetic coupling we reach the line $\Delta = |J^z_\perp|/2J$ which marks the transition into the phase where both fields are gapless (sine-Gordon is marginaly irrelevant on this line). In the sector C of the phase diagram the system shows properties of two *almost independent* spin $S=1/2$ anisotropic Heisenberg chains with dominating ferromagnetic coupling. Let us calculate the transverse correlations in this phase. Since the rotational symmetry in plane is not broken it will suffice to evaluate correlation functions involving one, e.g. x component of the spin:

$$\begin{aligned}\langle S^x_1(r)S^x_1(0)\rangle &\simeq \langle \cos\sqrt{\frac{\pi}{K}}\theta_1(r)\,\cos\sqrt{\frac{\pi}{K}}\theta_1(0)\rangle \\ -(-1)^r\langle \sin\sqrt{4\pi K}\phi_1(r)\sin\sqrt{\frac{\pi}{K}}\theta_1(r)\sin\sqrt{4\pi K}\phi_1(0)\sin\sqrt{\frac{\pi}{K}}\theta_1(0)\rangle &\end{aligned} \tag{3.38}$$

We will continue with explicit calculation only for smooth part of the correlation function, for staggered part exactly the same calculation could be done:

$$\begin{aligned}&\langle S^x_1(r)S^x_1(0)\rangle_{smooth} \to \langle \cos[\sqrt{\frac{\pi}{2K_+}}\theta_+(r) + \sqrt{\frac{\pi}{2K_-}}\theta_-(r)]\cos[\sqrt{\frac{\pi}{2K_+}}\theta_+(0) + \frac{\pi}{2K_-}\theta_-(0)]\rangle \\ &= \langle (\cos\sqrt{\frac{\pi}{2K_+}}\theta_+(r)\cos\sqrt{\frac{\pi}{2K_-}}\theta_-(r) - \sin\sqrt{\frac{\pi}{2K_+}}\theta_+(r)\sin\sqrt{\frac{\pi}{2K_-}}\theta_-(r)) \\ &(\cos\sqrt{\frac{\pi}{2K_+}}\theta_+(0)\cos\sqrt{\frac{\pi}{2K_-}}\theta_-(0) - \sin\sqrt{\frac{\pi}{2K_+}}\theta_+(0)\sin\sqrt{\frac{\pi}{2K_-}}\theta_-(0))\rangle \end{aligned} \tag{3.39}$$

Taking into account following facets: 1) we are dealing with decoupled theories; 2) correlation function of $\sin$ with $\sin$ is given by the same formula as for $\cos$ with $\cos$; 3) correlation function of $\sin$ with $\cos$ is zero (neutrality condition) we will obtain following expression:

$$\begin{aligned} K^{xy}_{\alpha\beta}(r) &\simeq \delta_{\alpha\beta}\Big[r^{-1/4(1/K^*_+ + 1/K^*_-)} \\ &+ (-1)^r \cdot r^{-\left(K^*_+ + K^*_- + 1/4K^*_+ + 1/4K^*_-\right)}\Big], \end{aligned} \tag{3.40}$$

where $\delta_{\alpha,\beta}$ is the Kronecker symbol. The reason why inplain correlations between spins on different legs is zero could be seen from considering again only smooth parts:

$$\begin{aligned} &\langle S^x_1(r) S^x_2(0)\rangle_{smooth} \rightarrow \\ &= \langle (\cos\sqrt{\frac{\pi}{2K_+}}\theta_+(r)\cos\sqrt{\frac{\pi}{2K_-}}\theta_-(r) - \sin\sqrt{\frac{\pi}{2K_+}}\theta_+(r)\sin\sqrt{\frac{\pi}{2K_-}}\theta_-(r)) \\ &(\cos\sqrt{\frac{\pi}{2K_+}}\theta_+(0)\cos\sqrt{\frac{\pi}{2K_-}}\theta_-(0) + \sin\sqrt{\frac{\pi}{2K_+}}\theta_+(0)\sin\sqrt{\frac{\pi}{2K_-}}\theta_-(0))\rangle \end{aligned} \tag{3.41}$$

We see, that in this case correlation functions involving $\cos$ines are exactly cancelled by the ones involvins $\sin$es. The longitudinal correlations decay faster. In particular the intraleg longitudinal correlations could be calculated with the help of formula Eq. (3.33) and are given by:

$$K^{zz}_{\alpha\alpha}(r) \simeq \frac{K^*_+ + K^*_-}{2\pi r^2} + (-1)^r \cdot r^{-\left(K^*_+ + K^*_-\right)}. \tag{3.42}$$

From Eq. (3.33) it follows that the transverse interleg correlations are strongly suppressed in this phase, while the longitudinal part of the interleg spin-spin correlations is given by:

$$K^z_{\alpha\beta}(r) \simeq \frac{K^*_+ - K^*_-}{2\pi r^2} \tag{3.43}$$

To obtain the above result one has to reexpress ϕ_1 and ϕ_2 in terms of $\phi_\pm$ fields inverting equation (1.43) and substitute this into the correlation function:

$$\begin{aligned} &\langle S^z_1(r) S^z_2(0)\rangle_{smooth} = \frac{K}{\pi}\langle \partial_x\phi_1(r)\partial_x\phi_2(0)\rangle \\ &= \frac{K}{2\pi}\langle \left(\sqrt{\Lambda_+}\partial_x\phi_+(r) + \sqrt{\Lambda_-}\partial_x\phi_-(r)\right)\left(\sqrt{\Lambda_+}\partial_x\phi_+(0) - \sqrt{\Lambda_-}\partial_x\phi_-(0)\right)\rangle \end{aligned} \tag{3.44}$$

Since $\phi_\pm$ fields are independent and described by Gaussian free field theories, correlation functions of their currents decay quadratically, while in between plus and minus sectors there is no correlation. Finally using Eq.(1.49) we come to desired result. This phase we denote as the *spin liquid II* phase.

Strictly speaking the analysis as considered above is formally valid in the weak-coupling limit ($\Delta, |J^z_\perp| \ll J$). Still it is interesting to estimate the upper boundary for the *spin liquid II* phase, in the vicinity of the single chain ferromagnetic instability regime using the dimensionality analysis. We determine the instability curve corresponding to the transition into the gapped phase from the condition $K_\pm = 1$, where the scaling dimension of the corresponding

cosine term $d_\pm = 2K_\pm = 2$. At $J_\perp^z > 0$ the field ϕ_- is gapless, while the field ϕ_+ becomes massive for $K_+ = 1$ for which from Eq. (1.49) we find:

$$K_+ = K\left(1 - \frac{1}{2\pi}\frac{J_+^c K}{u}\right) = 1$$
$$J_+^c = 2\pi\frac{u}{K}(1 - 1/K) \tag{3.45}$$

Substituting $u/K = \mathcal{J}_{eff} = \sin\frac{\pi}{2K}/(2K-1)$ and taking the limit $K \to \infty$ we get:

$$J_+^c(\Delta) = 4J\epsilon\left(1 - \frac{\sqrt{2\epsilon}}{\pi}\right). \tag{3.46}$$

where we have introduced notation $\Delta = 1 - \epsilon$ with $\epsilon \ll 1$. For $K \to \infty$ we have $\Delta = \cos(\pi/2K) \to 1 - \pi^2/8K^2$ and consecuently $\pi^2/8K^2 = \epsilon$ in this limit.

Therefore in the vicinity of the single chain ferromagnetic instability point, at $1 - \Delta \ll 1$, the *spin liquid I* phase with only one gapless (here antisymmetric) mode reenters the phase diagram at $J_\perp^z > J_+^c(\Delta)$. (We note that the amplitude of the $cosine$ term in the limit of the single chain ferromagnetic instability point is not determined exactly, so the phase transition line determined by the dimensional analysis is of qualitative nature in this limit). For $J_\perp^z < 0$ the analysis is done in exactly the same manner with symmetric and antisymmetric modes changing roles.

At $J_\perp^z = 0$ and $\Delta > 1$ each of the decoupled legs is unstable towards the transition into a ferromagnetic phase. At $J_\perp^z \neq 0$, we can address the problem of the ferromagnetic instability in the ladder system studying the velocity renormalization of the corresponding gapless excitations. In analogy with the single chain case we mark the transition into the ferromagnetically ordered phase at $u_\pm = 0$. Using Eqs. (1.37) and (1.48) one finds by extrapolation of the result valid up to first order in $J_\perp^z$ the following estimate for the ferromagnetic transition

$$J_{FM}^z(\Delta) = 4J\epsilon\,. \tag{3.47}$$

At $|J_\perp^z| \gg J$ the boundary of the ferromagnetic instability can be established from the large rung coupling expansion approach. Let us first consider the case of strong ferromagnetic intrarung interaction $J_\perp^z < 0$. In this limit a large gap of order $|J_\perp^z|$ exists in the one-magnon excitation spectrum. Projecting the system on the subspace excluding antiparallel orientation of spins within a given rung, in the second-order perturbation expansion with respect to $J^2/|J_\perp^z|$ and up to the additive constant $E_0 = -N_0|J_\perp^z|$ we obtain the following effective spin-1/2 XXZ spin chain Hamiltonian

$$\mathcal{H} = \sum_n \left[\frac{1}{2}\lambda_{eff}^{xy}(\tau_n^+\tau_{n+1}^- + h.c.) + \lambda_{eff}^z\tau_n^z\tau_{n+1}^z\right], \tag{3.48}$$

where

$$\lambda_{eff}^{xy} = -\frac{J^2}{|J_\perp^z|}, \quad \lambda_{eff}^z = \frac{J^2}{|J_\perp^z|} - 2J\Delta \tag{3.49}$$

and the pseudospin operators are

$$\begin{aligned} \tau_n^+ &= S_{n,1}^+ S_{n,2}^+ \,, \quad \tau_n^- = S_{n,1}^- S_{n,2}^- \,, \\ \tau_n^z &= \frac{1}{2}(S_{n,1}^z + S_{n,2}^z) \,. \end{aligned}$$

In agreement with the weak-coupling bosonization analysis, at $\Delta = 0$ (XY-legs) the system is equivalent to the $S = 1/2$ isotropic antiferromagnetic chain. For arbitrary $\Delta < 0$ ($\lambda_{eff}^z > \lambda_{eff}^{xy}$) the spin chain given by the Hamiltonian (3.48) is in the *gapped Néel phase*. This phase corresponds to the LRO AFM interleg ordering with interleg phase shift equal to zero. At

$$0 < \Delta < J/|J_\perp^z|$$

($-\lambda_{eff}^{xy} < \lambda_{eff}^z < \lambda_{eff}^{xy}$) the spin chain (3.48) is in a *gapless planar* XY phase, corresponding to the "spin liquid I" phase of the bosonization studies and finally at

$$\Delta > J/|J_\perp^z|$$

($\lambda_{eff}^z < -\lambda_{eff}^{xy}$) the transition into the completely polarized ferromagnetic phase takes place. In the case of strong antiferromagnetic interleg coupling $J_\perp^z \gg J > 0$ analysis is similar. In this case the intrarung ordering of spins is antiferromagnetic. Projecting the system on the subspace excluding *parallel* orientation of spins within the same rung, and introducing a new set of spin operators

$$\begin{aligned} \tilde{\tau}_n^+ &= S_{n,1}^+ S_{n,2}^- \,, \quad \tilde{\tau}_n^- = S_{n,1}^- S_{n,2}^+ \,, \\ \tilde{\tau}_n^z &= \frac{1}{2}(S_{n,1}^z - S_{n,2}^z) \,, \end{aligned}$$

in the second-order with respect to $J^2/J_\perp^z$ we once again map the initial ladder model onto the theory of an anisotropic spin $1/2$ Heisenberg chain (3.48). One can perform the analysis as discussed above, however the ferromagnetic ordering in terms of the effective $S = 1/2$ chain, at $J_\perp^z > 0$ corresponds to an interleg ferromagnetic ordering with a phase shift of π of the order parameter along the rung.

The results obtained within the bosonization approach together with the results from the strong coupling expansion allow to draw the following phase diagram of the ladder with a longitudinal interleg coupling $J_\perp^z$ (see Fig.3.3). At $\Delta < 0$ the phase diagram consists of two gapped phases describing respectively long range ordered Néel antiferromagnetic phases with gapped excitation spectrum and inphase (at $J_\perp^z < 0$) or antiphase (at $J_\perp^z > 0$) ordering of spins within the same rung. The line $\Delta = 0$ marks the transition into the *Spin Liquid I* - phase characterized by a gapless excitation spectrum and a power law decay of the spin-spin correlation functions. The critical indices for the decay of the corresponding spin-spin correlations in the Spin Liquid I phase are $\gamma_i \simeq 1$. In the case of strong interleg exchange $|J_\perp^z| \gg J$, further increase of the interleg ferromagnetic exchange Δ leads to the transition at $\Delta_c \simeq J/|J_\perp^z|$ into the phase with ferromagnetically ordered legs. However, in the weak-coupling case, at $|J_\perp^z| \ll J$, an increase of the parameter Δ at given $J_\perp^z$ leads to the transition into the *Spin Liquid II* at $\Delta_{c(1)} = |J_\perp^z|/2J$. The Spin Liquid II phase is characterized by a

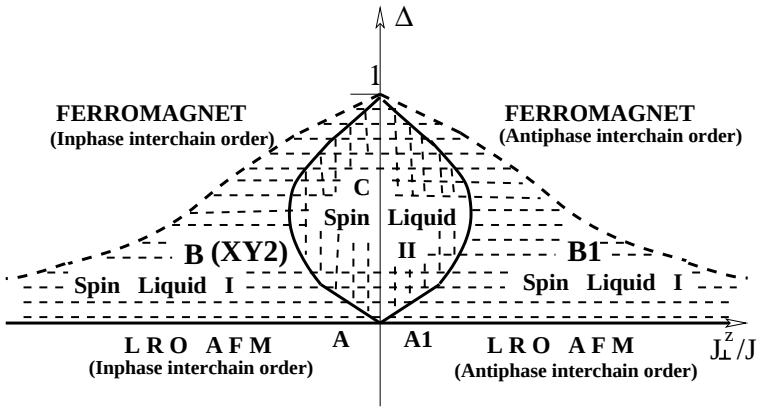

FIGURE 3.3: The groundstate phase diagram of the two-leg ladder with a longitudinal $J_{\perp}^{z} S_{j,1}^{z} S_{j,2}^{z}$ coupling between legs. For details see text.

gapless excitation spectrum and power-law decay of the spin-spin correlation functions with critical indices $\gamma_i \simeq 2$. This transition marks the development of the regime dominated by intraleg coupling, whereas the interleg longitudinal exchange plays only a rather moderate role. However, with further increase of the intraleg ferromagnetic exchange, in the vicinity of the ferromagnetic instability line the *Spin Liquid II* phase becomes unstable and the system reentres into the *Spin Liquid I* phase. This reentrance effect is connected with a sharp reduction of the bandwidth in the vicinity of the ferromagnetic transition and a subsequent increase of the potential energy of the interleg coupling. Therefore, just before the transition into the ferromagnetically ordered phase, the short range interleg fluctuations get stopped, and as in the case of the strong intrarung coupling, the *Spin Liquid I* - phase is unstable toward the transition into the phase with ferromagnetically ordered legs.

However, since the transition into the ferromagnetic phase is a typical finite bandwidth effect, the parameters determined quantitatively within the bosonization (i.e. infinite band) approach strongly depend on the way of regularization of the continuum theory on small distances. Therefore, it is useful to determine the lowest boundary of the ferromagnetic phase on the phase diagram, starting from the ferromagnetically ordered phase and using the standard spin-wave analysis (Appendix E). At $|J_{\perp}^{z}| \ll J$ ordinary spin wave calculation in the subspace of $S_{Tot}^{z} = N - 1$ gives $J_{FM}^{SW} = 2J\epsilon$. It is interesting to note, that spin wave calculation in the subspace of $S_{Tot}^{z} = N - 2$ gives following boundary for ferromagnetic phase:

$$J_{\perp,cr}^{Z} = \frac{J}{\triangle} - J\triangle \tag{3.50}$$

This formula interpolates between the results of weacly coupled and strongly coupled chains limits. We believe this simple expression (3.50) gives exact boundary of ferromegnetic phase for all interchain coupling strengths.

To conclude this subsection we note that the ground state phase diagram of the ferromagnetic ladder system coupled only by the longitudinal part of the spin-spin exchange interaction exhibits a rather rich phase diagram which consist of LRO AFM phases, a spin liquid phase with one gapped and one gapless mode, a spin liquid phase with two gapless modes and a

phase with ferromagnetically ordered legs.

3.2.2 Chains Coupled by the Transverse Part of the Ladder Exchange

In this subsection we consider the case of two critical Heisenberg chains coupled by a transverse interleg exchange interaction $J_\perp^z = 0$ and $J_\perp^{xy} \neq 0$. The particular aspects of this limiting case are the following ones:

- The antisymmetric mode is gapped at arbitrary $J_\perp^{xy} \neq 0$.
- The low energy properties of the system are determined by the behavior of the symmetric field.
- The infrared properties of the symmetric field are determined by the subtle coupling between the symmetric and antisymmetric modes.

We start our analysis from the limiting case of weakly anisotropic XY chains, coupled by the weak interleg transverse exchange, assuming $|\Delta|, |\mathcal{J}_\perp^{xy}|/J \ll 1$. At $J_\perp^{xy} \neq 0$ the antisymmetric mode is gapped and the dual antisymmetric field is "pinned" with vacuum expectation value

$$\langle \theta_- \rangle = \begin{cases} \sqrt{\pi K_-/2} & \text{at } J_\perp^{xy} > 0 \\ 0 & \text{at } J_\perp^{xy} < 0 \end{cases} . \tag{3.51}$$

Behavior of the symmetric field is governed by the SG Hamiltonian (3.23). The standard RG analysis gives that the symmetric mode is gapped at

$$\Delta < \Delta_{c1} = \frac{\gamma}{4J} \cdot |\mathcal{J}_{+-}| . \tag{3.52}$$

Therefore at $\Delta < \Delta_{c1}$ the excitation spectrum of the system is gapped. The dynamical generation of a gap in the symmetric mode leads to condensation of the field ϕ_+ with a vacuum expectation value $\langle \phi_+ \rangle = 0$. Since the dual component of the antisymmetric field is "pinned" with vacuum expectation value given by (3.51), the so-called "disordered" phase[27] is realized in the ground state. At $J_\perp^{xy} > 0$, spins on the same rung try to form a singlet and the ground state corresponds to the state with a dominant tendency of singlet pairs on each rung. Correlations between spins along the ladder decay exponentially. In the case of ferromagnetic coupling, at $J_\perp^{xy} < 0$ spins on the same rung form a state corresponding to the $S^z = 0$ component of the triplet (an "asymmetric triplet" pair) and the ground state corresponds to the state with an "asymmetric triplet" pair on each rung. In analogy to the phases of the $S = 1$ chain as discused in[27] we denote this phase as "anisotropic large D phase".

For $\Delta \geq \Delta_{c1}$ the system is in the phase where the symmetric mode is gapless. Since the antisymmetric mode is gapped the *alternating part* of the spin-spin correlations is *exponentially damped* (alternating part of spin-spin correlation functions necessarily involve antisymmetric field, that decays exponentially, since its dual field is ordered). We examine smooth part

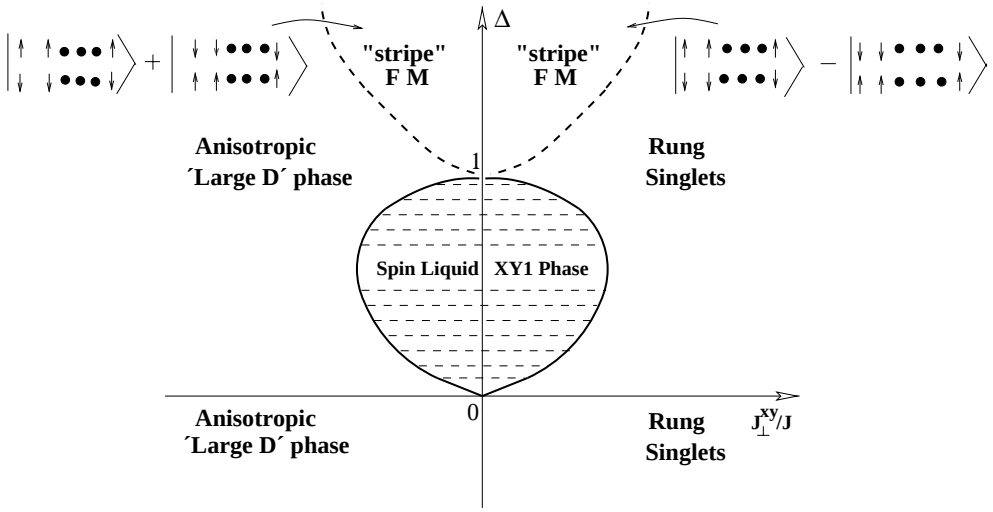

FIGURE 3.4: The groundstate phase diagram of the two-leg ladder with transverse coupling between legs.

of the in-plane correlations that are given by

$$\begin{aligned}
&\langle S_1^x(r)S_2^x(0)\rangle_{smooth} \rightarrow \\
&= \Big\langle (\cos\sqrt{\frac{\pi}{2K_+}}\theta_+(r)\cos\sqrt{\frac{\pi}{2K_-}}\theta_-(r) - \sin\sqrt{\frac{\pi}{2K_+}}\theta_+(r)\sin\sqrt{\frac{\pi}{2K_-}}\theta_-(r)) \\
&(\cos\sqrt{\frac{\pi}{2K_+}}\theta_+(0)\cos\sqrt{\frac{\pi}{2K_-}}\theta_-(0) + \sin\sqrt{\frac{\pi}{2K_+}}\theta_+(0)\sin\sqrt{\frac{\pi}{2K_-}}\theta_-(0))\Big\rangle
\end{aligned} \tag{3.53}$$

Using expectation values from Eq. (3.51)

$$\begin{cases} \langle\cos\sqrt{\frac{\pi}{2K_-}}\theta_-\rangle = 0 & \langle\sin\sqrt{\frac{\pi}{2K_-}}\theta_-\rangle \simeq 1 \quad \text{at } J_\perp^{xy} > 0 \\ \langle\cos\sqrt{\frac{\pi}{2K_-}}\theta_-\rangle \simeq 1 & \langle\sin\sqrt{\frac{\pi}{2K_-}}\theta_-\rangle = 0 \quad \text{at } J_\perp^{xy} < 0 \end{cases} . \tag{3.54}$$

and using the fact, that the symmetric mode is gapless, we get the following result for in-plane correlations:

$$K_{\alpha\beta}^{xy}(r) \simeq r^{-1/4K_+^*} \tag{3.55}$$

while the longitudinal correlations decay universally:

$$K_{\alpha\beta}^{zz}(r) \simeq \langle\partial_x\phi_+(r)\phi_+(0)\rangle \simeq \frac{1}{r^2}\,. \tag{3.56}$$

As follows from Eq. (3.55) the line $J_\perp^{xy} = 0$ marks the transition from a regime with ferromagnetic interleg order into the regime with antiferromagnetic interleg order. Following Schulz[27] who has discussed a similar phase in the context of the spin $S = 1$ chain we identify this phase as a *spin liquid XY1* phase.

We want now to discuss the phase diagram of model in the vicinity of the single chain ferromagnetic instability point $\Delta = 1$, and in particular investigate what happens with gapless

$XY1$ phase. For the moment we will forget about the antisymmetric sector, that is governed by strongly relevant operator, and concentrate only on the symmetric one. The symmetric sector is governed by the sine-Gordon model Eq.(3.23). We want to identify Kosterlitz-Thouless transition line in the symmetric field given by $K_+ \simeq 1$. For this we have to find the mechanism renormalizing K_+. As we approach ferromagnetic instability point K increases to infinity, so we need some mechanism that works in opposite direction and drives Kosterlitz-Thouless transition in the symmetric sector. We remind that we are working in the vicinity of the point where bandwidth of linear excitations collapses. So our approach can only have a qualitative nature. $\Delta \to 1$, the effective coupling constant behaves as

$$\frac{M^+_{eff}}{2\pi u} \simeq \frac{\pi^2 K \mathcal{J}_{+-}}{2J} \sim \frac{1}{\sqrt{\epsilon}}$$

where $\epsilon = 1 - \Delta$. We can make a rough estimate of the renormalization of the velocity of the symmetric mode excitations u_+. We write out Euclidean action density for the sin-Gordon model:

$$S_E[\phi(z,\bar{z})] = \partial_z\phi(z,\bar{z})\partial_{\bar{z}}\phi(z,\bar{z}) + \frac{2M}{u}\cos\sqrt{8\pi K}\phi(z,\bar{z})] \tag{3.57}$$

In the spirit of RG to obtain effective action we have to integrate out short wavelength fluctuations. In the second order of perturbation theory the effective action for sine-Gordon theory reads:[62]

$$\begin{aligned} S_{eff}[\phi_\Lambda] &= S_0[\phi_\Lambda] + \langle S_1[\phi_\Lambda]\rangle_h \\ &- \frac{1}{2}\left(\langle S_1^2[\phi_\Lambda + h]\rangle_h - \langle S_1[\phi_\Lambda + h]\rangle_h^2\right) \end{aligned} \tag{3.58}$$

Above S_0 is free part, S_1 interaction term, ϕ_Λ are slowly varying fields and h are fast modes. Averages are to be understood with respect to free part of short wave length fluctuations. For our further discussions only the last term $\langle S_1^2[\phi_\Lambda + h]\rangle$ is important. We will apply ope for the products of two cosines.

$$\begin{aligned} &:\cos\alpha\phi(z,\bar{z}) :: \cos\alpha\phi(0,\bar{0}) := \frac{1}{2}|z|^{\alpha^2/2\pi} :\cos 2\alpha\phi(0,0): -\frac{1}{2}|z|^{-\alpha^2/2\pi} \\ &-\frac{\alpha^2}{2}|z|^{\frac{4\pi-\alpha^2}{2\pi}} :\partial\phi(0)\bar{\partial}\phi(0): -\frac{\alpha^2}{4}\left[z^{\frac{4\pi-\alpha^2}{2\pi}}\Big(\bar{\partial}\phi(0)\Big)^2 + \bar{z}^{\frac{4\pi-\alpha^2}{2\pi}}\big(\partial\phi(0)\big)^2\right] \end{aligned} \tag{3.59}$$

The term $:\partial\phi(0)\bar{\partial}\phi(0):$ has the form of kinetic energy Eq. (1.5). For our case $\alpha \sim K$ and we obtain following renormalization of K:

$$K_+ = K\left(1 - \lambda K\left(\mathcal{J}_{+-}/J\right)^2\right) \tag{3.60}$$

where λ is a nonuniversal positive constant of the order of unity. Using the fact that Luttinger liquid parameter renormalization is inverse of the velocity renormalization (see Eq.(1.48) and (1.49), strictly speaking they are valid only in lowest order) for velocity renormalization we obtain:

$$u_+ = u\left(1 + \lambda K\left(\mathcal{J}_{+-}/J\right)^2\right) \tag{3.61}$$

As follows from Eqs. (3.61/3.60) the strong effective transverse coupling reduces the tendency towards ferromagnetic ordering and leads to the transition into the gapped phase at

$$\mathcal{J}_{+-} > \mathcal{J}_{+-}^{cr} \simeq J(1-\triangle)^{\frac{1}{4}}.$$

Which follows from the solution of $K_+ = K\left(1-\lambda K\left(\mathcal{J}_{+-}/J\right)^2\right) = 1$.
Equivalently we have

$$\Delta_{c2} \simeq 1-\lambda^2(\mathcal{J}_{+-}/J)^4.$$

To summarize this subsection we note that the ground state phase diagram of the ferromagnetic ladder system coupled by the transverse part of the spin-spin exchange interaction only also exhibits a rich phase diagram which consist of the "disordered rung-singlet" and "anisotropic large D" phases, the easy-plane gapless XY1 phase and the "stripe" ferromagnetic phases with dominating intraleg ferromagnetic ordering. The groundstate phase diagram of the two-leg ladder with only transverse coupling between legs is given in Fig.(3.4).

3.2.3 Chains Coupled by the Isotropic Interleg Exchange

In this subsection we consider the weak-coupling ground state phase diagram of the model (3.1) in the case of $SU(2)$ invariant interleg exchange $J_\perp^z = J_\perp^{xy} =: \mathcal{J}_\perp$.
In this case the behavior of the antisymmetric sector is completely similar to the above considered case of the ladder with transverse exchange: the antisymmetric field is gapped and the vacuum expectation value of the dual field θ_-, depends on the sign of exchange and is given by Eq. (3.51) after the substitution $\mathcal{J}_\perp^{xy} \to \mathcal{J}_\perp$.
The symmetric field is governed by the effective SG Hamiltonian (3.23) with the bare values of the model parameters given by K_+ and M_{eff}^+

$$\begin{aligned} K_+ &= K\left(1-\frac{\mathcal{J}_\perp K}{2\pi u}\right), \\ M_{eff}^+ &= -\frac{1}{\pi u_+}\mathcal{J}_\perp\left(1+\delta sign(\mathcal{J}_\perp)\right), \end{aligned} \tag{3.62}$$

(where δ is a nonuniversal positive number)
The resulting asymmetry of the model is clearly seen:

- at $\mathcal{J}_\perp > 0$, the antiferromagnetic interleg exchange reduces K_+ and increases M_{eff}^+ and therefore supports the tendencies towards development of a gap in the excitation spectrum
- at $\mathcal{J}_\perp < 0$, the ferromagnetic interleg exchange increases K_+, while with increasing $|\mathcal{J}_\perp|$ the parameter $M_{eff}^+ \simeq \mathcal{J}_\perp(1-\delta) \to 0$; therefore we expect an enlargement of the gapless section in this case.

We start our analysis from the limiting case of weakly anisotropic XY chains assuming $|\Delta|, |\mathcal{J}_\perp|/J \ll 1$. At $\Delta = 0$ we have $K = 1$ and the system shows a gap in the excitation spectrum at $\mathcal{J}_\perp > 0$ and is gapless in the case of ferromagnetic interleg exchange $\mathcal{J}_\perp < 0$.

Therefore at $\Delta = 0$, with increasing ferromagnetic interleg exchange ($\mathcal{J}_\perp < 0$, $|\mathcal{J}_\perp| \to \infty$) the system continuously evolves into the limit of the $S = 1$ XY model, which is known to be gapless.[67,68] In the case of antiferromagnetic interleg exchange $\mathcal{J}_\perp > 0$ the symmetric mode is unstable towards the Kosterlitz-Thouless type transition associated with the dynamical generation of a gap in the excitation spectrum. The weak-coupling RG analysis tells, that at $\Delta \neq 0$ and $\mathcal{J}_\perp > 0$ the gapless $XY1$ phase is realized for

$$\Delta > \Delta_{c1} = \frac{\mathcal{J}_\perp}{2J}\,(1+\delta)\ , \tag{3.63}$$

whereas in the case of ferromagnetic interrung exchange $\mathcal{J}_\perp < 0$ it is realized for

$$\Delta > \Delta'_{c1} = -\frac{\delta \mathcal{J}_\perp}{2J}\,.$$

Therefore, from the RG studies we obtain that the gapless $XY1$ phase is stable in the case of ferromagnetic exchange. At $\mathcal{J}_\perp > 0$ it is unstable towards the transition into the gapped rung-singlet phase. At $\mathcal{J}_\perp < 0$ the gapless $XY1$ phase penetrates into the $\Delta < 0$ sector of the phase diagram. However, since $M^+_{eff} \to 0$ with increasing ferromagnetic exchange, at $|\mathcal{J}_\perp| \gg J$ the gapless phase on the antiferromagnetic side ($\Delta < 0$) of the phase diagram shrinks up to a narrow stripe as $|\mathcal{J}_\perp|/J \to \infty$.

With $\Delta \to 1$ the gapless $XY1$ phase becomes unstable towards transition into the ferromagnetically ordered state. Following the route developed before, we find that at $\Delta = 1 - \epsilon$ and antiferromagnetic interleg exchange, $\mathcal{J}_\perp > 0$, the reentrance of the gapped rung-singlet phase takes place at

$$\Delta_{c2} = 1 - \frac{\mathcal{J}_\perp}{4J} + \mathcal{O}\left(\frac{\mathcal{J}_\perp}{4J}\right)^{3/2}\ . \tag{3.64}$$

This reentrance behavior of the gap is similar to the reentrance of the gap in symmetric sector for the case of chains coupled by longitudinal exchange. Here in addition antisymmetric mode is gapped, thus there are not left any soft modes. In agreement with the quasiclassical studies,[53] we obtain that two almost ferromagnetically ordered chains coupled by an isotropic interleg exchange are unstable towards formation of the gapped rung-singlet phase at $J_\perp > J^c_\perp > 0$, where $J^c_\perp \to 0$ as $\Delta \to 1$. However, in contrast to the quasiclassical case, $\mathcal{J}^{c2}$ increases linearly with ϵ in the quantum spin-ladder case.

In the case of ferromagnetic interleg exchange, $\mathcal{J}_\perp < 0$, the gapless $XY1$ phase becomes unstable towards the transition into the ferromagnetically ordered phase when Δ increases towards 1. In this case the spin-wave approach (Appendix E) gives that the boundary between the $XY1$ and the ferromagnetic phase is $\Delta = 1$.

We summarize our results considering the phase diagram of the ladder with ferromagnetic legs and an isotropic interleg exchange in Fig. 3.5.

3.3 Conclusions

We have studied the ground state phase diagram of the $S = 1/2$ ladder with ferromagnetically interacting legs using the continuum limit bosonization approach. The phase diagrams

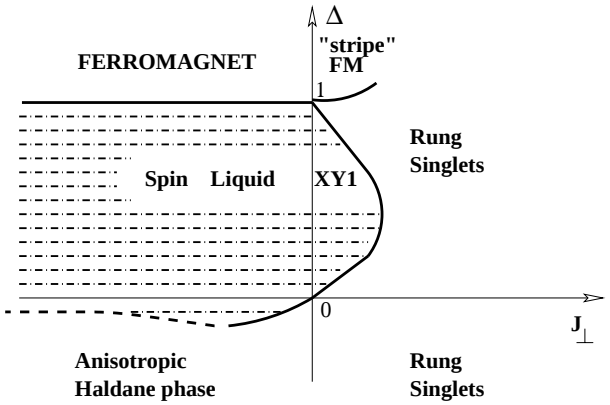

FIGURE 3.5: The ground state phase diagram of the two-leg ladder with an isotropic interleg coupling.

for the extreme anisotropic interchain coupling cases (Ising and XY interleg exchange) as well as for the $SU(2)$ symmetric case were obtained. These phase diagrams exhibit a number of interesting phases, gapped as well as gapless; some of these are familiar from well known 1D models (rung singlet phase, anisotropic Haldane phase, ferromagnetic and large D phase), in addition we revealed less conventional phases for ladders: the spin liquid phases with (i) one gapless and one gapped mode (including the known $XY1$ and $XY2$ phases) and (ii) two gapless modes. We have shown moreover that the gapped rung singlet phase found semiclassically to appear for an arbitrarily small isotropic antiferromagnetic interaction between ferromagnetic legs[53] continues to exist for $S = 1/2$ ladders and $xy-$like interactions and actually extends to small values of Δ.

The neighborhood of the single chain ferromagnetic instability point turned out to be of particular interest. We investigated the behavior of the system in this regime using the multiplicative regularization scheme. This scheme allows to extend the bosonization formalism to the limit when the bandwidth of the single chain excitations collapses and leads to the result that upon increasing the strength of ferromagnetism Δ at any moderate fixed longitudinal interleg interaction a sequence of two phase transitions occurs before the system enters the final ferromagnetically ordered phase (see Fig. (3.3).

Summary

In the present work effective field theory description was applied for studying the low temperature behavior of generalized spin $1/2$ ladder systems.
Namely two different spin ladder systems were considered. In the first part we studied the effect of an additional four-spin ring interaction on the ground state phase diagram of an antiferromagnetic spin ladder. The bosonization- fermionization approach has been used that allows us to describe the low energy excitations of the model in terms of weakly interacting massive Majorana fermions. We showed that the ordinary rung singlet phase of the pure antiferromagnetic ladder undergoes a quantum phase transition to a spontaneously dimerized phase with increasing ring exchange. Emerging quantum critical point belongs to the universality class of $SU(2)_2$ Wess-Zumino model and is described in terms of massless triplet of Majorana fermions. Due to universality quantum critical line extends from weak-coupling to strongly coupled ladder limit and moreover, phases in the vicinity of the critical line are also universal. We connected the above mentioned quantum phase transition in the ladder system due to additional four-spin exchanges to the quantum phase transition that takes place at the integrable point of the spin one chain (Takhtajan-Babujan point). From bosonization as well as from numerical works it was known that effective $S = 1$ spins (objects that exhibit well defined string order parameter) are formed across the ladder diagonals in the antiferromagnetically coupled ladder. That corresponds to the dimerization pattern emerging after the crossing the critical line to that of the valence bond solid type, i.e. chains are dimerized with nonzero relative dimerization.
Thermodynamically both phases of the ladder system – rung singlet phase and spontaneously dimerized phase are identical, since both are gapped phases. Dynamical behavior of the two phases are completely different. Using mapping to 2D Ising variables we calculated structure factors and found that magnons disappear from the low energy excitation spectrum with increasing ring interaction. Instead the low energy spectrum is exhausted by the continuum of incoherent dimerization kinks.
The temperature dependence of various response functions were calculated using Matsubara imaginary time formalism. Analytically continuing temperature Green's functions to real frequencies and extracting the imaginary parts we obtained structure factors in frequency momentum space that is directly connected to experimentally measurable quantity, namely scattering cross section of neutrons. With Matsubara formalism we also calculated spin specific heat, static susceptibility as well as the nuclear magnetic resonance relaxation rate in the gapped phases. In addition conformal mapping of an infinite plane to a finite stripe was used for obtaining the temperature dependencies of the dynamical magnetic susceptibilities at the criticalities.
In the second part of the thesis we analyzed the ground state phase diagram of two spin $1/2$ ferromagnetic chains coupled by the exchange interactions of an arbitrary sign. In particular the effects of anisotropies both in intra and interchain interactions on the ground state phase diagram were investigated. All known phases for the spin one chain with additional single ion anisotropy as well as less conventional phases were obtained for the model. Using the peculiar property of the sine-Gordon model, namely that relevancy criterion determined within the one loop R.G. becomes exact, we determined phase diagram at weak couplings in case of chains coupled only with Z part of interaction exactly. Combining exact results,

available for the single chain, with linearized expressions for interchain interaction the bosonization formalism was extended to approach the single chain ferromagnetic instability point. In addition we carried out spin wave calculations and large rung coupling expansion for determining the exact boundary of ferromagnetic phase. Superimposing the phase diagram of the chains coupled only by Z part of interaction with the phase diagram of the chains coupled only by XY part of interaction we identified Haldane phase emerging for the $SU(2)$ symmetrically coupled ladder as Néel ordered rung triplets diluted with zero components of the triplets. We have shown moreover that the gapped rung singlet phase found semiclassically to appear for an arbitrarily small isotropic antiferromagnetic interaction between ferromagnetic legs exists also for $S = 1/2$ ladders and it extends down to small values of Δ. Ground state spin correlation functions were calculated throughout the phase diagram.

APPENDIX A

Bosonization Formalism

A.1 Bosonization Dictionary for Antiferromagnetic XXZ Spin Chain

We start from antiferromagnetic S=1/2 quantum XY chain which is given by the following lattice Hamiltonian:

$$H = |J| \sum_{j=1}^{N-1} S_j^x S_{j+1}^x + S_j^y S_{j+1}^y \tag{A.1}$$

and introduce Jordan-Wigner transformation from spins to spinless fermions:

$$\begin{aligned} S_n^- &= (-1)^n \quad c_n e^{i\pi \sum_{j=1}^{n-1} c_j^+ c_j} \\ S_n^z &= \quad c_n^+ c_n - \frac{1}{2} \end{aligned} \tag{A.2}$$

Alternating factor $(-1)^n$ is implemented for convenience, to obtain Hamiltonian for free fermions with negative hopping:

$$H = -\frac{|J|}{2} \sum_{j=1}^{N-1} c_j^+ c_{j+1} + c_{j+1}^+ c_j \tag{A.3}$$

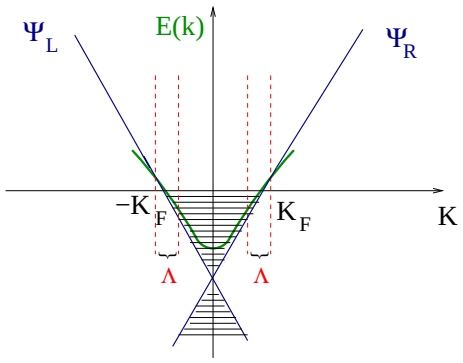

FIGURE A.1: Linearization of the spectrum of free lattice fermions

After passing to Fourier components we diagonalize Hamiltonian to obtain:

$$H = -|J| \sum_{k=-\pi}^{\pi} \cos(k) c_k^+ c_k \tag{A.4}$$

Now we pass to the continuum limit by linearizing of the cos spectrum around the fermi points. This step already tells us that if only electrons near the fermi points are involved in the physics of the model we can approximate around those points spectrum with straight lines. It is obvious that in this way we can only try to mimic the low energy behavior of the system. Introducing left and right moving fermions Fig. (A.1) we decompose fermion annihilation operator in the following way (for simplicity we have set lattice spacing to 1):

$$c(x) = i^n \psi_R(x) + (-i)^n \psi_L(x)$$

($x = na$, and $a = 1$) The low energy limit of the Hamiltonian (A.4) will look:

$$H_\Lambda = -iv_F \int dx[\psi_R^+(x)\partial_x\psi_R(x) - \psi_L^+(x)\partial_x\psi_L(x)] \tag{A.5}$$

where index Λ stands for the momentum cutoff, meaning that we are dealing with effective field theory. As wee see from Fig. (A.1) the ground state of model is equivalent to the filled Dirac vacuum, where all states below E_F are occupied. The presence of infinite vacuum is crucial to guarantee existence of anomalous commutators of the chiral density operators, providing mathematical background of the fermi-bose equivalence in one dimension. We[11] bosonize left and right fermions:

$$\psi_R(x) = \frac{1}{\sqrt{2}\pi} e^{i\sqrt{4\pi}\Phi_R(x)},\ \psi_L(x)\frac{1}{\sqrt{2}\pi} e^{-i\sqrt{4\pi}\Phi_L(x)} \tag{A.6}$$

where $\Phi_{R(L)}(x)$ is right (left) chiral bosonic field

$$\Phi_L(x) + \Phi_R(x) = \phi(x),\ \Phi_L(x) - \Phi_R(x) = \theta(x)$$

For chiral components of the bosonic field we have the following commutation relations:

$$\begin{aligned}
[\Phi_R(x), \Phi_L(y)] &= \frac{i}{4} \\
[\Phi_R(x), \Phi_R(y)] &= \frac{i}{4} sign(x-y) \\
[\Phi_L(x), \Phi_L(y)] &= -\frac{i}{4} sign(x-y)
\end{aligned} \tag{A.7}$$

One can check that the above commutation rules guarantee fulfillment of correct fermionic commutation relations. It is straightforward to bosonize S^z, since it is a local object in fermionic representation. Carrying out simple opes for chiral vertexes we get:

$$S_j^z = \frac{1}{\sqrt{\pi}}\partial_x\phi(x) + \frac{(-1)^j}{\pi}\sin\sqrt{4\pi}\phi(x) \tag{A.8}$$

Bosonized form of the Jordan-Wigner statistical factor reads:

$$\sum_{j=1}^{n-1} c_j^+ c_j = \frac{n-1}{2} + \int^{x-1} \frac{1}{\sqrt{\pi}}\partial_{x'}\phi(x')dx' \tag{A.9}$$

$$
\begin{aligned}
(-1)^n S_n^- &= \frac{1}{2}\left(i^n e^{i\sqrt{4\pi}\Phi_R(x)} + (-i)^n e^{-i\sqrt{4\pi}\Phi_L(x)}\right) \\
&\quad \left[e^{i\pi\left(\frac{n-1}{2}+\int^{x-1}\frac{1}{\sqrt{\pi}}\partial_{x'}\phi(x')\right)} + h.c.\right] \\
&= \frac{1}{2}\left(i^n e^{i\sqrt{4\pi}\Phi_R(x)} + (-i)^n e^{-i\sqrt{4\pi}\Phi_L(x)}\right) \\
&\quad \left[e^{i\sqrt{\pi}\phi(x-1)}(i)^{n-1} + e^{-i\sqrt{\pi}\phi(x-1)}(-i)^{n-1}\right]
\end{aligned} \tag{A.10}
$$

Using (A.7):

$$
[\Phi_R(x), \phi(x-1)] = [\Phi_R(x), \Phi_R(x-1) + \Phi_L(x-1)] = \frac{i}{2}
$$
$$
[\Phi_L(x), \phi(x-1)] = [\Phi_L(x), \Phi_R(x-1) + \Phi_L(x-1)] = -\frac{i}{2}
$$

and Baker-Hausdorff formula $e^A e^B = e^{A+B} e^{\frac{1}{2}[A,B]}$ we get:

$$
\begin{aligned}
(-1)^n S_n^- &= \frac{1}{2}(-1)^n e^{3i\sqrt{\pi}\Phi_R + i\sqrt{\pi}\Phi_L} \\
&+ \frac{1}{2}e^{-i\sqrt{\pi}\theta} + \frac{1}{2}(-1)^n e^{-3i\sqrt{\pi}\Phi_R - i\sqrt{\pi}\Phi_L} \\
&+ \frac{1}{2}e^{-i\sqrt{\pi}\theta} \\
&= e^{-i\sqrt{\pi}\theta} + \frac{1}{2}(-1)^n \left(e^{i2\sqrt{\pi}\phi - i\sqrt{\pi}\theta} + e^{-i2\sqrt{\pi}\phi - i\sqrt{\pi}\theta}\right) \\
&= e^{-i\sqrt{\pi}\theta} \\
&+ \frac{1}{2}(-1)^n e^{-i\sqrt{\pi}\theta}\Big(e^{i2\sqrt{\pi}\phi} e^{-\frac{1}{2}[i2\sqrt{\pi}\phi, -i\sqrt{\pi}\theta]} \\
&+ e^{-i2\sqrt{\pi}\phi} e^{-\frac{1}{2}[-i2\sqrt{\pi}\phi, -i\sqrt{\pi}\theta]}\Big) \\
&= e^{-i\sqrt{\pi}\theta} \\
&+ \frac{1}{2}(-1)^n e^{-i\sqrt{\pi}\theta}\left(e^{i2\sqrt{\pi}\phi}(-i) + (e^{-i2\sqrt{\pi}\phi} i\right) \\
&= e^{-i\sqrt{\pi}\theta} + (-1)^n e^{-i\sqrt{\pi}\theta} \sin\sqrt{4\pi}\phi
\end{aligned} \tag{A.11}
$$

There is a bit of ambiguity in the above derivation. Namely, above we used regularized on-site commutation rule:

$$
[\phi(x), \theta(x)] = i/2 \tag{A.12}
$$

Had we used instead

$$
[\phi(x), \theta(x)] \to [\phi(x), \theta(x+a)] = i \tag{A.13}
$$

we would have obtained:

$$
S^- = (-1)^n e^{-i\sqrt{\pi}\theta} + e^{-i\sqrt{\pi}\theta} \cos\sqrt{4\pi}\phi \tag{A.14}
$$

These two forms are equivalent to each other, application of each of them is a matter of convenience.

This completes bosonization dictionary of spin one half operators in case when S^z part of interaction is zero. If we add bosonized $J^z S^z S^z$ interaction we will generate (for $|J^z| < J_{xy}$) irrelevant operators. Although irrelevant operator can not modify physical behavior of the system (infrared behavior) it modifies nonuniversal constants and namely constants in bosonization expressions for spin operators will change. This change is uncontrollable from field theory point, and comparison to nonperturbative results whenever possible should be done. The spin chain is solvable by Bethe ansatz for arbitrary $J^z, J_{xy} \equiv |J|$. Comparison with Bethe ansatz solution gives the following bosonization expressions:

$$\begin{aligned}
S^x_j &\simeq (-1)^j \frac{c}{\sqrt{2\pi}} : \cos\sqrt{\frac{\pi}{K}}\theta(x) : \\
&+ \frac{ib}{\sqrt{2\pi}} : \sin\sqrt{4\pi K}\phi(x) \sin\sqrt{\frac{\pi}{K}}\theta(x) : \\
S^y_j &\simeq (-1)^j \frac{c}{\sqrt{2\pi}} : \sin\sqrt{\frac{\pi}{K}}\theta(x) : \\
&+ \frac{ib}{\sqrt{2\pi}} : \sin\sqrt{4\pi K}\phi(x) \cos\sqrt{\frac{\pi}{K}}\theta(x) : \\
S^z_j &= \sqrt{\frac{K}{\pi}}\partial_x\phi(x) \\
&+ (-1)^j \frac{a}{\pi} : \sin\sqrt{4\pi K}\phi(x) :
\end{aligned} \tag{A.15}$$

where the quantity

$$K = \frac{\pi}{2\left(\pi - \arccos\frac{J_z}{J_{xy}}\right)} \tag{A.16}$$

is the one determined from the comparison with Bethe ansatz[12] (recently it became possible to determine all the nonuniversal constants appearing in (A.15) by comparing to the scaling limit of exactly solvable XYZ chain and using conjectured exact expectation values for vertex operators in the sin-Gordon model[63,64]).

A.2 Dimerization Operator

Now we derive the continuum limit expression for the dimerization operator, that is for the staggered part of the spin energy density

$$\epsilon(x) = (-1)^j \mathbf{S}_j \mathbf{S}_{j+1} \tag{A.17}$$

To get continuum version of dimerization operator we have to carry out ope of smooth part of spin operator with its staggered part.

$$S^z(x) = a\sqrt{\frac{K}{\pi}}\partial_x\phi_(x) + \frac{(-1)^j}{\pi} : \sin\sqrt{4\pi K}\phi(x) \tag{A.18}$$

Carrying out the following ope:

$$\partial_x \phi(x+a) : \sin \sqrt{4\pi K}\phi(x) :\sim \frac{\sqrt{K}}{\sqrt{\pi}a} \cos \sqrt{4\pi K}\phi \tag{A.19}$$

and

$$: \cos \sqrt{4\pi K}\phi e^{i\sqrt{\pi/K}\theta} :: e^{-i\sqrt{\pi/K}\theta} :\sim \cos \sqrt{4\pi K}\phi + ... \tag{A.20}$$

where dots stand for less singular terms. We conclude, that continuum expression for dimerization operator reads:

$$\epsilon(x) \sim \cos \sqrt{4\pi K}\phi + \text{less singular terms} \tag{A.21}$$

APPENDIX B

Some Words on Majorana Fermions in 2D

B.1 Green's Functions for Majorana Fermions

Lagrangian for Majorana fermions reads:[21]

$$\bar{\psi}(i\rho_\alpha\partial^\alpha - m)\psi \tag{B.1}$$

Where $\bar{\psi} = \psi^\dagger\rho_0 = \psi^T\rho_0$ for Majoranas and we choose Majorana basis for Dirac matrices in 2D:

$$\rho_0 = \tau_2 = \begin{pmatrix} 0 & -i \\ i & 0 \end{pmatrix}, \qquad \rho_1 = i\tau_1 = \begin{pmatrix} 0 & i \\ i & 0 \end{pmatrix} \tag{B.2}$$

Where τ-s are Pauli matrices. We represent Majorana spinor in terms of its chiral components:

$$\psi = \begin{pmatrix} \psi_L \\ \psi_R \end{pmatrix}$$

Rewritten in chiral components Majorana Lagrangian takes form:

$$i(\psi_L\partial_t\psi_L + \psi_R\partial_t\psi_R) + iv(\psi_L\partial_x\psi_L - \psi_R\partial_x\psi_R) + im\psi_R\psi_L - im\psi_L\psi_R \tag{B.3}$$

The partition function for free Majoranas at finite temperature $T = 1/\beta$ may be represented as Berezin path integral:

$$Z = \int d[\psi_L]d[\psi_R]e^{-\int_0^\beta d\tau\int_{-\infty}^{\infty} dx[\psi_L\partial_\tau\psi_L + \psi_R\partial_\tau\psi_R + iv(\psi_L\partial_x\psi_L - \psi_R\partial_x\psi_R) + im\psi_R\psi_L - im\psi_L\psi_R]} \tag{B.4}$$

Grasman variables are assumed antiperiodic for $\tau \to \tau + \beta$. Quadratic form in the exponent can be written as a matrix:

$$S = \int_0^\beta d\tau \int_{-\infty}^{\infty} dx(\psi_L, \psi_R) \begin{pmatrix} \partial_\tau + iv\partial_x & -im \\ im & \partial_\tau - iv\partial_x \end{pmatrix} \begin{pmatrix} \psi_L \\ \psi_R \end{pmatrix} \tag{B.5}$$

Introducing finite temperature Fourier components of left and right fields:

$$\begin{aligned} \psi_L(x,\tau) &= T^{\frac{1}{2}} \sum_{w_n} \int \frac{dk}{\sqrt{2\pi}} e^{i(w_n\tau - kx)}\psi_L(k, w_n) \\ \psi_R(x,\tau) &= T^{\frac{1}{2}} \sum_{w_n} \int \frac{dk}{\sqrt{2\pi}} e^{i(w_n\tau - kx)}\psi_R(k, w_n) \end{aligned} \tag{B.6}$$

and using the following identities

$$\frac{1}{2\pi}\int_{-\infty}^{\infty} dx e^{i(kx+k'x)} = \delta(k+k')$$
$$T\int_0^{\beta} d\tau e^{i(w_n+w'_n)\tau} = \delta_{w_n,-w'_n} \tag{B.7}$$

Eq. (B.5) will take form:

$$S = \int dk \sum_{w_n} (\psi_L(k,w_n), \psi_R(k,w_n)) \begin{pmatrix} iw_n + vk & -im \\ im & iw_n - vk \end{pmatrix} \begin{pmatrix} \psi_L(-k,-w_n) \\ \psi_R(-k,-w_n) \end{pmatrix} \tag{B.8}$$

The Green's functions may be read off as matrix elements of the matrix $G(k,w_n)$ whose inverse is:

$$G^{-1}(k,w_n) = \begin{pmatrix} -iw_n - vk & im \\ -im & -iw_n + vk \end{pmatrix} \tag{B.9}$$

From above we get:

$$G_{LL}(k,w_n) = \langle \psi_L(k,w_n)\psi_L(-k,-w_n)\rangle = -\frac{iw_n - vk}{w_n^2 + v^2k^2 + m^2}$$
$$G_{RR}(k,w_n) = \langle \psi_R(k,w_n)\psi_R(-k,-w_n)\rangle = -\frac{iw_n + vk}{w_n^2 + v^2k^2 + m^2}$$
$$G_{LR}(k,w_n) = \langle \psi_L(k,w_n)\psi_R(-k,-w_n)\rangle = \frac{im}{w_n^2 + v^2k^2 + m^2}$$
$$G_{RL}(k,w_n) = \langle \psi_R(k,w_n)\psi_L(-k,-w_n)\rangle = -\frac{im}{w_n^2 + v^2k^2 + m^2} \tag{B.10}$$

We can write above in compact matrix notations:

$$\hat{G}(k,w_n) = \begin{pmatrix} G_{RR}(k,w_n), & G_{RL}(k,w_n) \\ G_{LR}(k,w_n), & G_{LL}(k,w_n) \end{pmatrix} = -\frac{iw_n I + vk\tau_3 - m\tau_2}{w_n^2 + v^2k^2 + m^2} \tag{B.11}$$

(I stands for unit two by two matrix) We note, that because of the mass of Majoranas that couples left and right sectors so called anomalous Green's functions appeared. Mass term brakes down discrete Z_2 symmetry $(\psi_L, \psi_R) \to (\psi_L, -\psi_R)$ enjoyed by massless theory. This effect rediscovers itself in spin ladders where hidden order parameter is associated with this discrete symmetry breaking.

B.2 One Loop Mass Renormalization

In quantum field theories mass corrections due to the interactions follow from the examining the dressed propagator. As a result the first order mass renormalization is expressed by the first order self-energy function which is given by the bubble diagrams, the only first order corrections to the propagator Fig. (B.1).

$$m = m_0 + \Sigma^1$$

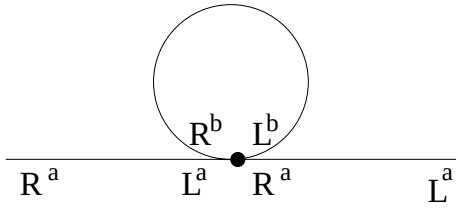

FIGURE B.1: First order correction to Majorana mass $\mathrm{a} \neq \mathrm{b}$

Σ^1 is one-loop self energy correction that could be expressed as:

$$\Sigma^1 = \frac{g}{2} \triangle_E(0,0) \tag{B.12}$$

where

$$\triangle_E(x,\tau) = \mathrm{tr} \int \frac{dkdw_n}{(2\pi)^2} \frac{e^{i(w_n\tau - k_1 x)}(w_n\rho_0 - k_1\rho_1 + m_0)}{k^2 + m_0^2} \tag{B.13}$$

(here w_n is Matsubara frequencies at zero temperature. In our notations it is related to zero component of Euclidean momentum as $k_0 = -w_n$. Using Euclidean momentum renders above expression explicitly covariant). Because ultraviolet part of the theory is cut off by itrachain scale Λ, $\triangle_E(0)$ is finite, and given by:

$$\triangle_E(0) = \frac{m_0}{\pi} \int_0^\Lambda \frac{kdk}{k^2 + m_0^2} \simeq \frac{m_0}{\pi} \ln \frac{\Lambda}{m_0} \tag{B.14}$$

From above we conclude that first order mass renormalization for the theory of massive Majoranas interacting with four-fermi interaction is given by:

$$\Sigma^1 = \frac{g m_0}{2} \ln \frac{\Lambda}{m_0} \tag{B.15}$$

B.3 Mapping to Ising Variables

This appendix is based on chapter 12 of Ref. (62). It is well known fact that two dimensional classical Ising model on a square lattice near critical line (in the parameter plane: temperature v coupling constant) in so called τ-continuum limit (when rows are squeezed) could be reduced to the one dimensional quantum Ising chain in a transverse magnetic field.[70]

$$H = -J \sum_{j=1}^{N} \left(\sigma_n^z \sigma_{n+1}^z + h\sigma_n^x \right) \tag{B.16}$$

(Starting two dimensional Ising variables have two labels, for rows and columns respectively. In reduction to one dimensional chain row label becomes continuous imaginary time, whereas column label is just site index. So for example correlation function for two Ising spins situated at different rows and columns will translate into the correlation function of the quantum chain Ising spins at different times. Roughly we can write $\sigma_{m,n} \to \sigma_n(\tau)$, where

$\tau = ma$ and $a \to 0$ corresponds to squeezing the rows. This reduction is a particular example of a general equivalence of the statistical classical models at a finite temperature and their quantum counterparts at zero temperature, but in one less spatial dimension). The transverse magnetic field plays the role of a temperature in the original two dimensional Ising lattice. For $h = 0$ system is equivalent to the classical Ising chain with the long range order (fully polarized state). It is clear that h tries to reduce the long range order and at a sufficiently large magnetic field system indeed has zero magnetization on the Z axes. This means, that for some value of h the quantum phase transition takes place. In analogy with the two dimensional case there exists a nice argument involving the duality transformation for determining the critical point. The dual spins are defined on the dual chain (shifted chain by the half of a lattice constant with respect to the original one). The duality transformation reads:

$$\mu^z_{n+1/2} = \prod_{j=1}^{n} \sigma^x_j, \quad \mu^x_{n+1/2} = \sigma^z_n \sigma^z_{n+1} \tag{B.17}$$

with the inverse transformation:

$$\sigma^z_n = \prod_{j=0}^{n-1} \mu^x_{j+1/2}, \quad \sigma^x_n = \mu^z_{n-1/2} \mu^z_{n+1/2} \tag{B.18}$$

If we apply dual spin on the ground state configuration for $h = 0$ we get:

$$\mu^z_{n+1/2} \left|+ + + + + \ldots + + +\right\rangle = \left|- - - - - + + \ldots + + +\right\rangle \tag{B.19}$$

thus dual spins create kinks in the ground state, because of this property they are called disorder operators. Under the duality transformation the analog of Kramers-Wannier duality holds:

$$H[\sigma, h] = hH[\mu, 1/h] \tag{B.20}$$

From above it is clear, that critical point is necessarily self-duality point, $h_c = 1$. Thus we have the following phase diagram:

$$\begin{array}{l} \langle \sigma^z \rangle \neq 0, \ \langle \mu^z \rangle = 0 \quad h < h_c \ \text{ ordered phase} \\ \langle \sigma^z \rangle = 0, \ \langle \mu^z \rangle \neq 0 \quad h > h_c \ \text{ disordered phase} \end{array} \tag{B.21}$$

Now we want to pass to one dimensional lattice fermions by Jordan-Wigner transformation:

$$\begin{aligned} \sigma^x_n &= 2a^+_n a_n - 1 \\ \sigma^z_n &= (-1)^n \exp\left[i\pi \sum_{j=1}^{n-1} a^+_j a_j \right] (a^+_n + a_n) \end{aligned} \tag{B.22}$$

It is easily checked, that correct fermionic anticommutation relations hold:

$$\left\{ a_n, a^+_m \right\} = \delta_{n,m} \quad \{a_n, a_m\} = 0 \tag{B.23}$$

Under this transformation quantum Ising chain is mapped to the following Hamiltonian:

$$\begin{aligned} &- \sum_n \left(J\sigma^z_n \sigma^z_{n+1} + hJ\sigma^x_n \right) \to \\ &\sum_n \left[J(a^+_n - a_n)(a^+_{n+1} + a_{n+1}) - hJ(a^+_n - a_n)(a^+_n + a_n) \right] \end{aligned} \tag{B.24}$$

Introducing two independent real fermions (Majoranas)

$$\zeta_n = \frac{a_n^+ + a_n}{\sqrt{2}}, \quad \eta_n = -i\frac{a_n^+ - a_n}{\sqrt{2}}$$
$$\{\zeta_n, \zeta_m\} = \{\eta_n, \eta_m\} = \delta_{n,m}, \;\; \{\eta_n, \zeta_m\} = 0 \tag{B.25}$$

Hamiltonian will take the following form:

$$H = \frac{i}{2}\sum_n [J\eta_n(\zeta_{n+1} - \zeta_n) - J(h-1)\eta_n\zeta_n] \tag{B.26}$$

Assuming that $h \sim 1$, so that we are close to criticality we take the continuum limit of the above Hamiltonian:

$$a \to 0, \;\; J \to \infty, \;\; Ja = v = const, \;\; 2J(h-1) = m$$
$$\zeta_n \to \sqrt{a}\zeta(x), \;\; \eta_n \to \sqrt{a}\eta(x)$$
$$\{\zeta(x), \zeta(y)\} = \{\eta(x), \eta(y)\} = \delta(x-y), \;\; \{\eta(x), \zeta(y)\} = 0 \tag{B.27}$$

In continuum limit the model Hamiltonian will look:

$$H = \int \mathrm{d}x[iv\eta(x)\partial_x\zeta(x) - im\eta(x)\zeta(x)] \tag{B.28}$$

Finally performing chiral rotation:

$$\psi_R = (\eta - \zeta)/\sqrt{2}, \;\; \psi_L = (\eta + \zeta)/\sqrt{2} \tag{B.29}$$

Hamiltonian in left right chiral components will take form:

$$H_{Majorana} = \int \mathrm{d}x \left[\frac{iv}{2}(\psi_L\partial_x\psi_L - \psi_R\partial_x\psi_R) - im\psi_R\psi_L\right] \tag{B.30}$$

with $m \sim (T - T_c)/T_c$. Duality transformation $\psi_R \to -\psi_R, \;\; \psi_L \to \psi_L$ effectively inverses sign of the mass. This corresponds to order disorder transformation in Ising variables.

$$\psi_R \to -\psi_R, \;\; \psi_L \to \psi_L \;\; \text{induces } m \to -m \;\; \text{which is equivalent to } \sigma \leftrightarrows \mu \tag{B.31}$$

Now we want to use this equivalence to derive Ising variables representation of staggered magnetization and dimerization operators of the ladder system.[62] Using bosonization formulas Eq. (A.15) and (A.21) at $K = 0.5$ we bosonize total and relative staggered magnetization and dimerization operators of the two leg ladder:

$$n_x^+ \sim \cos\sqrt{\pi}\theta_+ \cos\sqrt{\pi}\theta_-, \;\; n_x^- \sim \sin\sqrt{\pi}\theta_+ \sin\sqrt{\pi}\theta_-$$
$$n_y^+ \sim \sin\sqrt{\pi}\theta_+ \cos\sqrt{\pi}\theta_-, \;\; n_y^- \sim \cos\sqrt{\pi}\theta_+ \sin\sqrt{\pi}\theta_-$$
$$n_z^+ \sim \sin\sqrt{\pi}\phi_+ \cos\sqrt{\pi}\phi_-, \;\; n_z^- \sim \cos\sqrt{\pi}\phi_+ \sin\sqrt{\pi}\phi_-$$
$$\epsilon^+ \sim \cos\sqrt{\pi}\phi_+ \cos\sqrt{\pi}\phi_-, \;\; \epsilon^- \sim \sin\sqrt{\pi}\phi_+ \sin\sqrt{\pi}\phi_- \tag{B.32}$$

First we neglect marginal terms coupling symmetric and antisymmetric sectors. Then our Hamiltonian is decoupled sum of two sectors. We will derive Ising variables representation only for symmetric sector, for antisymmetric sector analogous expressions hold. Since

symmetric filed is equivalent to two degenerate Majoranas we consider two degenerate Ising models. To be mathematically rigorous we note, that the doublet of identical critical Ising copies is not equivalent to the CFT of free massless Dirac fermion since the two copies of Majoranas are not independent, but satisfy the same boundary conditions. On the other hand Dirac field can be bosonized using free massless scalar field of fixed compactification radius, in contrast two decoupled Ising models are described by a Bose field living on the orbifold line with the same radius.[16,17] Nonetheless as far as the bulk properties of the model under consideration are conserned this subtelty does not manifest itself and 'bosonization' of Ising variables in terms of massless scalar field can be safely applied.[15] At criticality 4 products of Ising variables

$$\sigma_1\sigma_2,\ \mu_1\mu_2,\ \sigma_1\mu_2 \text{ and } \mu_1\sigma_2$$

have the same scaling dimension $1/4$. In symmetric sector there are 4 operators with the same scaling dimension $1/4$:

$$\cos\sqrt{\pi}\phi_+,\ \sin\sqrt{\pi}\phi_+,\ \cos\sqrt{\pi}\theta_+ \text{ and } \sin\sqrt{\pi}\theta_+$$

Therefore we expect that between these two groups of operators some correspondence should hold. At $J_\perp > 0$ $(m > 0)$ in Eq. (2.4) $\left\langle\cos\sqrt{4\pi}\phi_+\right\rangle = 1$, that means $\phi_+ = \sqrt{\pi}n$ implying that

$$\left\langle\cos\sqrt{\pi}\phi_+\right\rangle \neq 0,\ \left\langle\sin\sqrt{\pi}\phi_+\right\rangle = 0 \tag{B.33}$$

at the same time, since $m > 0$ we are in disordered phase of two equivalent Ising copies:

$$\langle\sigma_1\rangle = \langle\sigma_2\rangle = 0,\ \langle\mu_1\rangle = \langle\mu_2\rangle \neq 0$$

If we invert sign to $J_\perp$, then in Eq. (2.4) $\left\langle\cos\sqrt{4\pi}\phi_+\right\rangle = -1$, that means $\phi_+ = (\sqrt{\pi}+1/2)n$, implying

$$\left\langle\cos\sqrt{\pi}\phi_+\right\rangle = 0,\ \left\langle\sin\sqrt{\pi}\phi_+\right\rangle \neq 0 \tag{B.34}$$

but at the same time two Ising copies are in ordered phase:

$$\langle\sigma_1\rangle = \langle\sigma_2\rangle \neq 0,\ \langle\mu_1\rangle = \langle\mu_2\rangle = 0$$

From above we can write following correspondence:

$$\sigma_1\sigma_2 \sim \sin\sqrt{\pi}\phi_+,\quad \mu_1\mu_2 \sim \cos\sqrt{\pi}\phi_+ \tag{B.35}$$

To obtain Ising variables representation of vertex operators involving dual symmetric field we make duality transformation in symmetric sector:

$$\phi_+ \leftrightarrow \theta_+ \text{ by } \phi_L^+ \to \phi_L^+,\ \phi_R^+ \to -\phi_R^+$$

Under the duality transformation kinetic part of Hamiltonian is invariant, but

$$\cos\sqrt{4\pi}\phi_+ \to \cos\sqrt{4\pi}\theta_+$$

from Eqs. (2.6)-(2.8) we conclude that this duality transformation is equivalent of making the duality transformation only on the first or the second Majorana copy e.g.:

$$\psi_R^1 \to \psi_R^1,\ \psi_L^1 \to \psi_L^1,\ \psi_R^2 \to -\psi_R^2,\ \psi_L^2 \to \psi_L^2,$$

or in Ising variables $\sigma_2 \leftrightarrow \mu_2$ This gives following identifications:

$$\sigma_1\mu_2 \sim \sin\sqrt{\pi}\theta_+, \quad \mu_1\sigma_2 \sim \cos\sqrt{\pi}\theta_+ \tag{B.36}$$

Analogical identifications will hold for antisymmetric field:

$$\sigma_3\sigma \sim \sin\sqrt{\pi}\phi_-, \quad \mu_3\mu \sim \cos\sqrt{\pi}\phi_- \tag{B.37}$$

and for dual field (here we can choose duality transformation on the first Ising copy $\sigma_3 \leftrightarrow \mu_3$):

$$\mu_3\sigma \sim \sin\sqrt{\pi}\theta_-, \quad \sigma_3\mu \sim \cos\sqrt{\pi}\theta_- \tag{B.38}$$

Using identification rules (B.35),(B.36), (B.37), and(B.38) and Eq. (B.32) we come to desired result Eqs. (2.20) and (2.21).[62]

APPENDIX C

Response Functions, Temperature Dependencies

C.1 Dynamical Magnetic Susceptibility for Luttinger Liquids

Dynamical susceptibility will be evaluated by general methods of conformal field theory valid for Luttinger liquids following Schulz and Bourbunais.[71] Neutron's differential cross section at energy transfer w and wave vector q is proportional to the imaginary part of the Fourier image of the dynamical spin-spin correlation function.[69]

$$\frac{d\sigma(w,q)}{d\Omega} \sim \frac{1}{1-e^{-w/T}} ImD^R(w,q) \tag{C.1}$$

In case of theory enjoying conformal symmetry thermodynamic Green's functions can be determined from conformal mapping of the infinite complex plane onto the cylinder. We will show general calculations valid for arbitrary spinfull operators. General spinfull correlation function at zero temperature has the form.

$$\frac{1}{(x+vt)^{2\triangle}(x-vt)^{2\bar{\triangle}}} \tag{C.2}$$

where $\triangle$ and $\bar{\triangle}$ are left and right or analytic and antianalytic conformal weights.

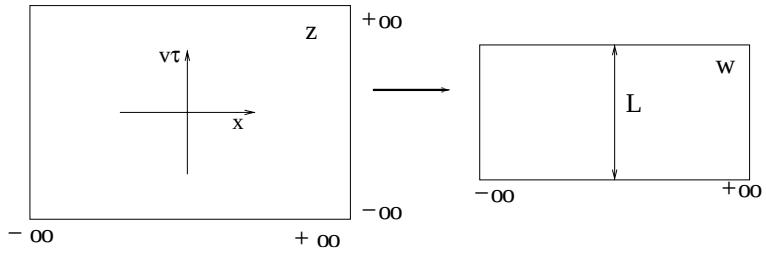

FIGURE C.1: Logarithmic transformation of the complex plane onto the strip with periodic condition (cylinder)

First step is to go to the Euclidean formalism by introducing imaginary time by $t = -i\tau$. Euclidean formalism is tightly related with the finite temperature Matsubara formalism. We remind, that in Matsubara formalism we sacrifice with time dynamics to account for non zero temperature statistical equilibrium effects. The imaginary time in Matsubara formalism runs from 0 to the inverse temperature. Thus to go from the Euclidean zero temperature

formalism to Matsubara finite temperature formalism we have to compactify the imaginary time. That is we have to translate our theory defined on the infinite complex z plane to the complex cylinder (stripe with periodic boundary conditions in imaginary time direction) with circumference $L = v/T$. Fortunately such transformation exists, and moreover belongs to the conformal transformations. Thus in theories enjoying conformal symmetries all correlation functions calculated with respect to ground state will change according to general rules of conformal transformation. Let's demonstrate the transformation of correlation function under conformal mapping on example of two point exponential correlation function(1.30). Conformal transformation that maps infinite z plane onto the cylinder w of circumference L along the imaginary axes, and infinitely extended along its real part looks:

$$w(z) = \frac{L}{2\pi} \ln z \tag{C.3}$$

From equation (1.30) we see that since correlation function is expressed in terms of Green's function of free bose field that is at the same time Green's function of Laplace equation,[62] all we need to know is how does the latter transform under mapping (C.3). For this we will use the following statement from complex analyses saying that Green's function of Laplace equation on any surface $\mathcal{A}$ is connected with Green's function of Laplace equation on infinite plane by the following formula:

$$G(w_1, w_2) = -\frac{1}{2\pi} \ln |z(w_1) - z(w_2)| + \frac{1}{4\pi} \ln |\partial_{w_1} z(w_1) \partial_{w_2} z(w_2)| \tag{C.4}$$

(where z are complex coordinate on infinite plane, and $w \in \mathcal{A}$) In case of mapping onto the cylinder $z(w) = e^{2\pi w/L}$ is the inverse of (C.3) and for the Green's function of Laplace equation on the cylinder we obtain:

$$G(w_1, w_2) = -\frac{1}{2\pi} \ln |e^{2\pi w_1/L} - e^{2\pi w_2/L}| + \frac{1}{4\pi} \ln \left(\frac{2\pi}{L}\right)^2 |e^{2\pi w_1/L} e^{2\pi w_2/L}| \tag{C.5}$$

Plugging this Green's function in the following correlation function we get:

$$\begin{aligned}
&\left\langle e^{i\alpha\phi(w_1,\bar{w}_1)} e^{-i\alpha\phi(w_2,\bar{w}_2)} \right\rangle = e^{\alpha^2 G(w_1,w_2)} \\
&= \left(\left(\frac{2\pi}{L}\right)^2 \frac{1}{|e^{2\pi w_1/L} - e^{2\pi w_2/L}|^2} |e^{2\pi(w_1+w_2)/L}| \right)^{\frac{\alpha^2}{4\pi}} \\
&= \left(\left(\frac{2\pi}{L}\right)^2 \frac{1}{(e^{2\pi w_1/L} - e^{2\pi w_2/L})(e^{2\pi \bar{w}_1/L} - e^{2\pi \bar{w}_2/L})} \left(e^{2\pi(w_1+w_2)/L} e^{2\pi(\bar{w}_1+\bar{w}_2)/L}\right)^{1/2} \right)^{\frac{\alpha^2}{4\pi}} \\
&= \left(\frac{2\pi}{L} \frac{e^{\pi(w_1+w_2)/L}}{e^{2\pi w_1/} - e^{2\pi w_2/L}} \right)^{2\triangle} \left(\frac{2\pi}{L} \frac{e^{\pi(\bar{w}_1+\bar{w}_2)/L}}{e^{2\pi \bar{w}_1/} - e^{2\pi \bar{w}_2/L}} \right)^{2\bar{\triangle}} \\
&= \left(\frac{\pi}{L} \frac{1}{\sinh \frac{\pi}{L}(w_1 - w_2)} \right)^{2\triangle} \left(\frac{\pi}{L} \frac{1}{\sinh \frac{\pi}{L}(\bar{w}_1 - \bar{w}_2)} \right)^{2\bar{\triangle}}
\end{aligned} \tag{C.6}$$

where we remind for our case $\triangle = \bar{\triangle} = \frac{\alpha^2}{8\pi}$. The above formula is applicable to general correlation functions involving operators behaving covariantly under conformal mappings.[19]

From now on for real and imaginary parts of w we will use the same notations as that for z, namely x and $v\tau$, that should not cause confusion. So we can write thermodynamic Green's function for any operator with conformal weights $(\triangle, \bar{\triangle})$(restoring $L = v/T$)

$$D(\tau, x) = \frac{(\pi T/v)^{2(\triangle+\bar{\triangle})}}{[\sinh \frac{\pi T}{v}(x - iv\tau)]^{2\triangle}[\sinh \frac{\pi T}{v}(x + iv\tau)]^{2\bar{\triangle}}} \tag{C.7}$$

It satisfies general requirements, for bosonic operators it is invariant under the shift $\tau \to \tau+T^{-1}$, while for fermionic ones, i.e. for operators with half-odd integer spin it changes sign. (This could be checked simply observing that $\triangle - \bar{\triangle} = \frac{N}{2}$ where N is even (odd) integer for bosonic (fermionic) case). We need to calculate fourier transform of thermodynamic Green's function in x as well as τ.

$$D(k, w_n) = \int_0^{T^{-1}} d\tau \int_{-\infty}^{\infty} dx e^{iw_n\tau} e^{-ikx} \frac{(\pi T/v)^{2(\triangle+\bar{\triangle})}}{[\sinh \frac{\pi T}{v}(x - iv\tau)]^{2\triangle}[\sinh \frac{\pi T}{v}(x + iv\tau)]^{2\bar{\triangle}}} \tag{C.8}$$

At the end of calculation we have to analytically continue from the set of discrete imaginary points on frequency complex plane to the real axes:

$$iw_n \to w + i\delta \tag{C.9}$$

to obtain retarded real space-time Green's function. For definiteness let's assume first that $k > 0$ in Eq. (C.8). Then we can integrate by x using branch cut as shown on the Fig. C.2. Using Jordan's lemma for this case we can bend integration contour over the imaginary axes. Integration part involving infinitesimally small circle around first branch point in the upper complex semi-plane vanishes and integral is convergent if $\triangle < 1/2$, and $\bar{\triangle} < 1/2$. For spin chains where $\triangle + \bar{\triangle} = K$ (K is a Luttinger liquid parameter) the above restriction means that we are in the repulsive regime, i.e. on antiferromagnetic side of anisotropy. This method thus is inapplicable for ferromagnetic chains. Integral has zero contribution from curves Γ_1 and Γ_2, so we have to evaluate contributions coming from contours adjacent to $Im(x)$ axe. Denoting $x - iv\tau = iy$ on the ab line on the cd line it will acquire phase $iye^{2\pi i}$. Plugging this into the integration along the ab and cd and introducing real parameter $r = y + v\tau$ we get for $\tau < \frac{1}{2T}$ where first branch point in upper semi-plane comes from $\left[\sinh \frac{\pi T}{v}(x - iv\tau]\right]^{-2\triangle}$ after the integration over x we get:

$$\begin{aligned} D(\tau, q)|_{\tau<(2T)^{-1}} \to \; - \; & \left(\int_{\infty}^{\tau} idr \frac{e^{-rk}}{[\sinh \frac{\pi T}{v}(ir - iv\tau)]^{2\triangle}[\sinh \frac{\pi T}{v}(ir + iv\tau)]^{2\bar{\triangle}}} \right. \\ + \; & \left. \int_{\tau}^{\infty} idr \frac{e^{-4\pi i\triangle} e^{-rk}}{[\sinh \frac{\pi T}{v}(ir - iv\tau)]^{2\triangle}[\sinh \frac{\pi T}{v}(ir + iv\tau)]^{2\bar{\triangle}}} \right) \end{aligned} \tag{C.10}$$

Repeating the same calculation for $\tau > (2T)^{-1}$ when the branch point of second $\sinh$ becomes the lowest one in the upper semi plane and gathering everything together we get:

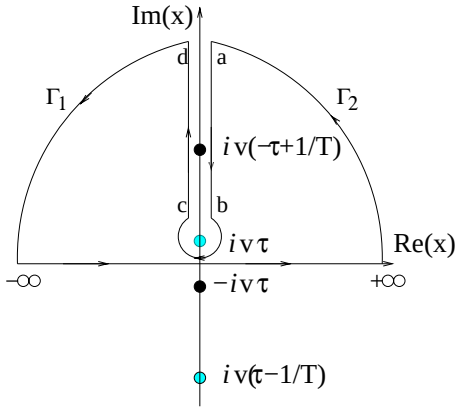

FIGURE C.2: Bending of the contour for $k > 0$.

$$D(k, w_n) =$$
$$-2\sin(2\pi\triangle)\int_0^{(2T)^{-1}} d\tau \int_{|v\tau|}^{\infty} dr e^{iw_n\tau}e^{-kr}\frac{e^{-2\pi i\triangle}(\pi T/v)^{2(\triangle+\bar{\triangle})}}{[\sinh\frac{\pi T}{v}(ir-iv\tau)]^{2\triangle}[\sinh\frac{\pi T}{v}(ir+iv\tau)]^{2\bar{\triangle}}}$$
$$+2\sin(2\pi\bar{\triangle})\int_{(2T)^{-1}}^{T^{-1}} d\tau \int_{|v(T^{-1}-\tau)|}^{\infty} dr e^{iw_n\tau}e^{-kr}\frac{e^{-2\pi i\bar{\triangle}}(\pi T/v)^{2(\triangle+\bar{\triangle})}}{[\sinh\frac{\pi T}{v}(ir-iv\tau)]^{2\triangle}[\sinh\frac{\pi T}{v}(ir+iv\tau)]^{2\bar{\triangle}}} \tag{C.11}$$

w_n represent Matsubara frequencies:

$$w_n = \begin{cases} 2n\pi T^{-1} & \text{if } \triangle - \bar{\triangle} \text{ is integer} \\ (2n+1)\pi T^{-1} & \text{if } \triangle - \bar{\triangle} \text{ is half-integer} \end{cases}$$

In the second term of (C.11) we make shift of imaginary time $\tau \to \tau - T^{-1}$. Under this shift bosonic Matsubara imaginary time Green's function as well as $e^{iw_n\tau}$ remain unchanged, while for fermionic case both change sign, so $D(k, w_n)$ will remain unaffected for both cases. Moreover, since the conformal spin of a physically measurable quantity should be half integer we see, that $\sin(2\pi\triangle)e^{-2\pi i\triangle} = \sin(2\pi\bar{\triangle})e^{-2\pi i\bar{\triangle}}$ holds as for bosonic so for fermionic cases. From above considerations we get:

$$D(k, w_n) =$$
$$-2\sin(2\pi\bar{\triangle})\int_{-(2T)^{-1}}^{(2T)^{-1}} d\tau \int_{|v\tau|}^{\infty} dr e^{iw_n\tau}e^{-kr}\frac{e^{-2\pi i\bar{\triangle}}(\pi T/v)^{2(\triangle+\bar{\triangle})}}{[\sinh\frac{\pi T}{v}(ir-iv\tau)]^{2\triangle}[\sinh\frac{\pi T}{v}(ir+iv\tau)]^{2\bar{\triangle}}} \tag{C.12}$$

Now we make approximation, assuming low enough temperature to extend the integration in τ to infinities. Extension of integration domain to infinities does not alter the result significantly, since the dominant contribution comes from small τ region because of e^{-kr} factor.

Thus the above approximation is exponentially correct.

$$D(k,w_n) = \\ -2\sin(2\pi\bar{\triangle})\int_{-(\infty)}^{\infty} d\tau \int_{|v\tau|}^{\infty} dr e^{iw_n\tau}e^{-kr}\frac{e^{-2\pi i\bar{\triangle}}(\pi T/v)^{2(\triangle+\bar{\triangle})}}{[\sinh\frac{\pi T}{v}(ir-iv\tau)]^{2\triangle}[\sinh\frac{\pi T}{v}(ir+iv\tau)]^{2\bar{\triangle}}} \tag{C.13}$$

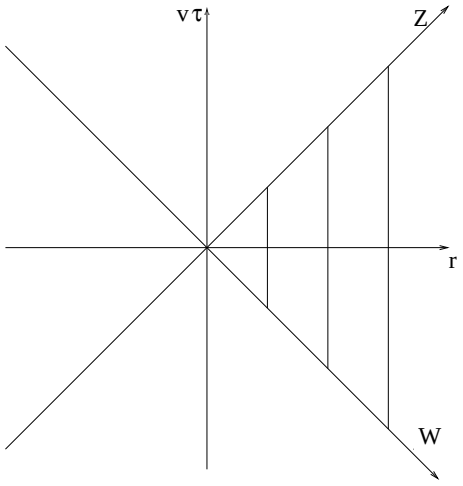

FIGURE C.3: Change of integration variables.

Passing to new coordinates $Z = r + v\tau$ and $W = r - v\tau$ we get:

$$\begin{aligned} &D(k,w_n) = \\ &-\frac{\sin(2\pi\bar{\triangle})}{v}\int_0^{\infty} dZ\int_0^{\infty} dW e^{iw_n(Z-W)/2}\frac{e^{-k(Z+W)/2}(\pi T/v)^{2(\triangle+\bar{\triangle})}}{[\sinh\frac{\pi T}{v}(iW)]^{2\triangle}[\sinh\frac{\pi T}{v}(-iZ)]^{2\bar{\triangle}}} \\ &= -\frac{\sin(2\pi\bar{\triangle})}{v}\int_0^{\infty} dZ\int_0^{\infty} dW\frac{e^{-W(\frac{vk+iw_n}{2v})}e^{-Z(\frac{vk-iw_n}{2v})}(\pi T/v)^{2(\triangle+\bar{\triangle})}}{[\sinh\frac{\pi T}{v}(iW)]^{2\triangle}[\sinh\frac{\pi T}{v}(-iZ)]^{2\bar{\triangle}}} \end{aligned} \tag{C.14}$$

Using table integral from Gradstein-Ryzhyk (3.312):

$$\int_0^{\infty} dX\frac{e^{-\mu X}e^{X(1-\nu)/2\beta}}{[\sinh(X/2\beta)]^{1-\nu}} = 2^{1-\nu}\beta\mathrm{B}(\beta\mu,\nu) \tag{C.15}$$

where B is Euler's Beta function, and making the following identification:

$$1-\nu = \begin{cases} 2\bar{\triangle} & \text{for } Z \\ 2\triangle & \text{for } W \end{cases}$$

$$\frac{1}{2\beta} = \begin{cases} -i\pi T/v & \text{for } Z \\ i\pi T/v & \text{for } W \end{cases}$$

$$\mu = \begin{cases} (vk - iw_n - 4i\pi T\bar{\triangle})/2v & \text{for } Z \\ (vk + iw_n + 4i\pi T\triangle)/2v & \text{for } W \end{cases}$$

We get:

$$D(k,w_n) = -\frac{\sin(2\pi\bar{\triangle})}{v}\left(\frac{2\pi T}{v}\right)^{2(\triangle+\bar{\triangle}-1)} \mathrm{B}(\triangle - i\frac{vk+iw_n}{4\pi T}, 1-2\triangle)\mathrm{B}(\bar{\triangle}+i\frac{vk-iw_n}{4\pi T}, 1-2\bar{\triangle}) \tag{C.16}$$

analytically continuing to real frequencies $iw_n \to w + i\delta$ (and forgetting for the moment about $\delta \to 0^+$) we arrive at following beautiful expression first obtained by Schulz and Bourbunnais:

$$D^{(R)}(k,w) = -\frac{\sin(2\pi\bar{\triangle})}{v}\left(\frac{2\pi T}{v}\right)^{2(\triangle+\bar{\triangle}-1)} \mathrm{B}(\triangle - i\frac{w+vk}{4\pi T}, 1-2\triangle)\mathrm{B}(\bar{\triangle}-i\frac{w-vk}{4\pi T}, 1-2\bar{\triangle}) \tag{C.17}$$

Expression (C.15) for B function allows to study zero temperature limit of expression (C.17).

$$D^{(R)}(k,w)|_{T=0} = -\frac{\sin(2\pi\triangle)}{v^{2(\triangle+\bar{\triangle})+1}}\Gamma(1-2\triangle)\Gamma(1-2\bar{\triangle})[vk-(w+i\delta)]^{\triangle-1}[vk+(w+i\delta)]^{\bar{\triangle}-1} \tag{C.18}$$

For the spinless operators for imaginary part of the above expression we get:

$$ImD^{(R)}(k,w)|_{T=0} \simeq sign(w)\frac{\theta(w^2-v^2k^2)\sin[\pi(1-\triangle)]}{|w^2-v^2k^2|^{1-\triangle}} \tag{C.19}$$

Let's apply above formulas to the structure factor for spin-spin correlation function for spin $1/2$ chain in the Luttinger liquid regime. The structure factor at $k=0$ (for Z component of spin) is given by the correlation function of $\partial_x\phi$ that is sum of left current $\partial\phi$ (with conformal weights $(\triangle = 1, \bar{\triangle} = 0)$) and right current $\bar{\partial}\phi$ (with conformal weights $(\triangle = 0, \bar{\triangle} = 1)$). From the property: $B(-ia,1) = \frac{i}{a}$ we see that the delta- function peak at zero momentum that follows from (C.19) survives even at finite temperatures. (Reflecting that uniform component of total S^z is conserved quantity).

$$S(k,w) \simeq \delta(w - v|k|)\theta(w) \tag{C.20}$$

While for the structure factor for transfer momentum near π ($k \sim \pi$) (for simplicity we assume $SU(2)$ symmetry) that is given by correlation function involving $\sin\sqrt{2\pi}\phi$ we get at $T=0$:

$$S(k,w) \simeq \frac{\theta(w-|vk-\pi|)}{\sqrt{w^2-(k-\pi)^2}} \tag{C.21}$$

For the latter expression momentum was shifted by π for absorbing oscillating Néel factor coming from staggered component of spin operator. So we receive expected V -shaped region $|w| \geq v|k|$ where finite imaginary part of retarded Green's function exist, in accordance with the famous picture of Bethe ansatz two spinon continuum.

C.2 Dynamical Susceptibility of Spin Ladder with Ring Exchange at Criticality

One can apply general formula (C.17) to write Fourier transform of the relative staggered magnetization operators at critical point (we remind, that the relative staggered magnetiza-

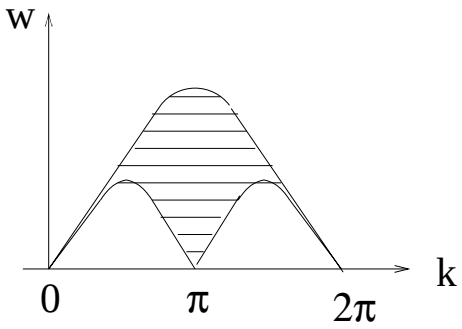

FIGURE C.4: Spin structure factor of Spin $\frac{1}{2}$ Heisenberg chain from Bethe anzats

tion decays algebraically at criticality):

$$\left\langle \mathbf{n}^{-}(\mathbf{r})\mathbf{n}^{-}(\mathbf{0})\right\rangle \sim \frac{1}{(x^2-v^2t^2)^{3/8}} \tag{C.22}$$

From this expression we read conformal weights of $n^{-}(\triangle = 3/16, \bar{\triangle} = 3/16)$. Using equation (C.19) and above given conformal weights we get the following dominant contribution to structure factor at $k \simeq \pi$ at $T \to 0$

$$ImD^{(R)}(k \simeq \pi, w) \simeq \frac{\theta(w^2-v^2k^2)}{|w^2-v^2k^2|^{13/16}} \tag{C.23}$$

C.3 Dynamical Susceptibility for Dimerized Spin Ladder

We wish to evaluate Fourier transforms of Euclidean space correlation functions of the total and relative staggered magnetization operators in the dimerized phase:

$$\left\langle \mathbf{n}^{-}(\mathbf{r})\mathbf{n}^{-}(\mathbf{0})\right\rangle \sim K_0^2(|m_t|r) \tag{C.24}$$

and

$$\left\langle \mathbf{n}^{+}(\mathbf{r})\mathbf{n}^{+}(\mathbf{0})\right\rangle \sim K_0(|m_t|r)K_0(|m_s|r) \tag{C.25}$$

We will carry out explicit calculation only for the Fourier transform of the relative magnetization, because for the total magnetization exactly similar calculation is applicable. We use the long-distance asymptotics of the Bessel function :

$$K_0(r) = \sqrt{\frac{\pi}{2r}}e^{-r}\left(1-0(1/r)\right) \tag{C.26}$$

Furthermore, since the correlation function is Lorenz invariant we will set $q = 0$ and at the end will restore the q dependence by replacement $w^2 \to w^2 - v^2q^2$.

$$\begin{aligned}\int_{-\infty}^{\infty}d\tau\int_{-\infty}^{\infty}dxe^{iW\tau}\left\langle \mathbf{n}^{-}(\mathbf{r})\mathbf{n}^{-}(\mathbf{0})\right\rangle &\sim \frac{\pi}{2|m_t|}\int_{-\infty}^{\infty}d\tau\int_{-\infty}^{\infty}dxe^{iW\tau}\frac{e^{-\sqrt{x^2+\tau^2}2|m_t|}}{\sqrt{x^2+\tau^2}}\\ =\frac{\pi}{2|m_t|}\int_0^{2\pi}d\phi\int_0^{\infty}dre^{iWr\cos\phi-r2|m_t|} &\sim \frac{1}{|m_t|\sqrt{W^2+4m_t^2}}\end{aligned} \tag{C.27}$$

Continuing analytically to real frequencies $iW \to w + i\delta$ we come to the desired expression for imaginary part Eq.(2.39). We note that considerable simplification which occured due to the Lorenz invariance of the correlation functions involving staggered components of spin operators does not occur for calculating e.g. correlation function of smooth parts. Of course only conformally scalar operators (that is operators with conformal spin equal to zero) enjoy Lorenz symmetry.

C.4 Spin Structure Factor near $q = 0$

In this section we would like to study correlation function of spin densities at small wave vectors $q \sim 0$ at zero temperature. Our purpose is to show whether coherent propagation of quasi particle like excitations are possible at small wave vectors or not. For this purpose we will calculate imaginary part of the retarded spin spin correlation function, which at zero temperature up to normalization coincides with structure factor. We will calculate Euclidean Green's function by zero temperature Matsubara (Euclidean space) formalism. As usually at the end we will make analitic continuation to real frequencies to recover retarded Green's function. So the quantity of the interest looks:

$$D(q, W) = \int_{-\infty}^{\infty} d\tau \int_{-\infty}^{\infty} dx e^{iW\tau} e^{-ikx} \left\langle S_+^z(x, \tau) S_+^z(0, 0) \right\rangle \tag{C.28}$$

τ is imaginary time, W continuous imaginary frequency, S_+ stands for total spin, that is summed spin on one rung, averaging with respect to the ground state is implied and we are interested in small wave vector behavior. To study small wave vector behavior we have to substitute total spin by its smooth part:

$$S_+^z(x) \to \sum_{\nu} J_1^{z,\nu}(x) + J_2^{z,\nu}(x) \tag{C.29}$$

$\nu = L, R$ Using formulas from Eq. (2.17) we can express Z component of total current in terms of doublet of Majoranas:

$$\sum_{\nu} J_1^{z,\nu}(x) + J_2^{z,\nu}(x) = -i \sum_{\nu} \psi_\nu^1 \psi_\nu^2 \tag{C.30}$$

Using Euclidean Green's functions for Majorana fermions Eq. (B.10) we reduce evaluation of the Euclidean Green's function Eq.(C.28) to the sum of simple bubble diagrams depicted on £g. C.5 involving only doublet of Majoranas. Why only first doublet of Majoranas are involved is easy to understand within linear response theory. If we apply magnetic field in Z direction it couples to symmetric sector, thus only Majoranas corresponding to symmetric sector will react on its application.

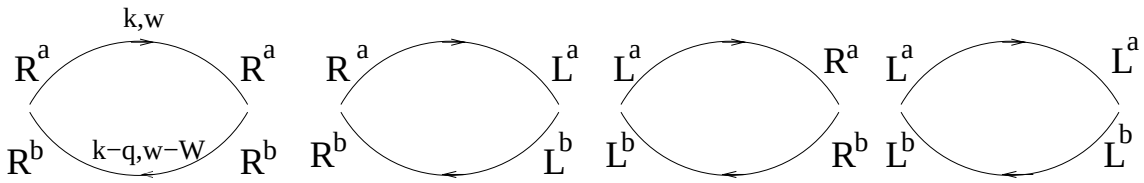

FIGURE C.5: Contribution to polarization function (a=1,b=2)

$$
\begin{aligned}
&D(q,W) = \\
&\int \frac{dk}{2\pi}\frac{dw}{2\pi}\left[G^1_{RR}(w,k)G^2_{RR}(w-W,k-q) + G^1_{RL}(w,k)G^2_{RL}(w-W,k-q) + (R \rightleftarrows L)\right] \\
&= 2\int \frac{dk}{2\pi}\frac{dw}{2\pi}\frac{-w(w-W) + v^2k(k-q) + m^2}{[w^2+v^2k^2+m^2][(w-W)^2+v^2(k-q)^2+m^2]} \\
&= 2\int_0^\infty dt\,ds \int \frac{dk}{2\pi}\frac{dw}{2\pi}[-w(w-W) + v^2k(k-q) + m^2]e^{-s[w^2+v^2k^2+m^2]} \\
&\qquad\qquad \times e^{-t[(w-W)^2+v^2(k-q)^2+m^2]} \\
&= 2\int_0^\infty dt\,ds \int \frac{dp_1}{2\pi}\frac{dp_0}{2\pi}e^{-v^2p_1^2(s+t)}e^{-p_0^2(s+t)}e^{-m^2(s+t)}e^{-(W^2+v^2q^2)st/(s+t)} \\
&\times\left[m^2 - \left(p_0 + \frac{tW}{s+t}\right)\left(p_0 + \frac{tW}{s+t} - W\right) + v^2\left(p_1 + \frac{tq}{s+t}\right)\left(p_1 + \frac{tq}{s+t} - q\right)\right]
\end{aligned}
\tag{C.31}
$$

where we have introduced notations:

$$
\begin{aligned}
p_0 &= w - \frac{tW}{s+t} \\
p_1 &= k - \frac{tq}{s+t}
\end{aligned}
\tag{C.32}
$$

after Gaussian integration over p_0 and p_1 we get:

$$
D(q,W) = \frac{1}{2\pi v}\int_0^\infty dt\,ds e^{-m^2(s+t)}e^{-(v^2q^2+W^2)\frac{st}{s+t}}\left[(W^2-v^2q^2)\frac{st}{(s+t)^2} + m^2\right]\frac{1}{s+t}
\tag{C.33}
$$

Passing to polar coordinates:

$$
t = r\sin\phi \text{ and } s = r\cos\phi
\tag{C.34}
$$

$$D(q,W) = \frac{1}{2\pi v}\int_0^\infty dr \int_0^{\pi/2} d\phi \frac{\exp\left\{\frac{-r\left[m^2(\sin\phi+\cos\phi)^2+\sin\phi\cos\phi(W^2+v^2q^2)\right]}{sin\phi+\cos\phi}\right\}}{\sin\phi+\cos\phi}$$
$$\times\left[(W^2-v^2q^2)\frac{\sin 2\phi}{2(1+\sin 2\phi)}+m^2\right]$$
$$= \frac{1}{2\pi v}\int_0^{\pi/2} d\phi\, \frac{\sin 2\phi\,[m^2+(W^2-v^2q^2)/2]+m^2}{m^2+\sin 2\phi\,[m^2+(W^2+v^2q^2)/2]}\,\frac{1}{(1+\sin 2\phi)} \tag{C.35}$$

So we have reduced our problem to the calculation of the table integral. The answer is:

$$\frac{1}{4\pi v}\frac{m^2(b-a)\left[\ln(b+\sqrt{b^2-m^4})-\ln(b-\sqrt{b^2-m^4})\right]+2(a-m^2)\sqrt{b^2-m^4}}{(b-m^2)\sqrt{b^2-m^4}} \tag{C.36}$$

With following notations:

$$b = m^2+\frac{1}{2}(W^2+v^2q^2)$$
$$a = m^2+\frac{1}{2}(W^2-v^2q^2) \tag{C.37}$$

After analytical continuation to real frequencies $W^2 \to -w^2 - i\delta\mathrm{sign}(w)$, for imaginary part of the above expression we get:

$$ImD^R(q,w) = \frac{m^2q^2v}{(w^2-v^2q^2)^{3/2}\sqrt{w^2-v^2q^2-4m^2}}\mathrm{sign}(w)\Theta(w^2-v^2q^2-4m^2) \tag{C.38}$$

Therefore dynamical magnetic susceptibility at small wave vectors has a threshold at $2m$. As can be seen $ImD^R(0,w)=0$ corresponds to the conservation of the total magnetization of the ladder system (conserved quantity does not experience spontaneous fluctuations since it is a definite number).

(In fact direct analytic continuation to real frequencies in final formula (C.36) may seem a bit tedious. In order to obtain imaginary part one can analytically continue directly before taking the angular integral in the last part of Eq. (C.35). Appearance of sign function in the final expression is evident in this case, while Θ threshold comes from the fact that $\sin(2\phi)$ is non negative for $\phi \in [0,\pi/2]$).

C.5 Matsubara Frequency Sums

We recapitulate on some basics from finite temperature field theory formalism for free fermion (boson) systems. Typical problem we will encounter is evaluation of the frequency sums of the type:

$$\sum_{w_n} f(w_n) \tag{C.39}$$

Where w_n are Matsubara frequencies, that take following values:

$$w_n = \begin{cases} (2n+1)\pi T & \text{for fermions} \\ 2n\pi T & \text{for bosons} \end{cases} \tag{C.40}$$

Introducing complex variable z one checks, that in case of fermi statistics sum (C.39) could

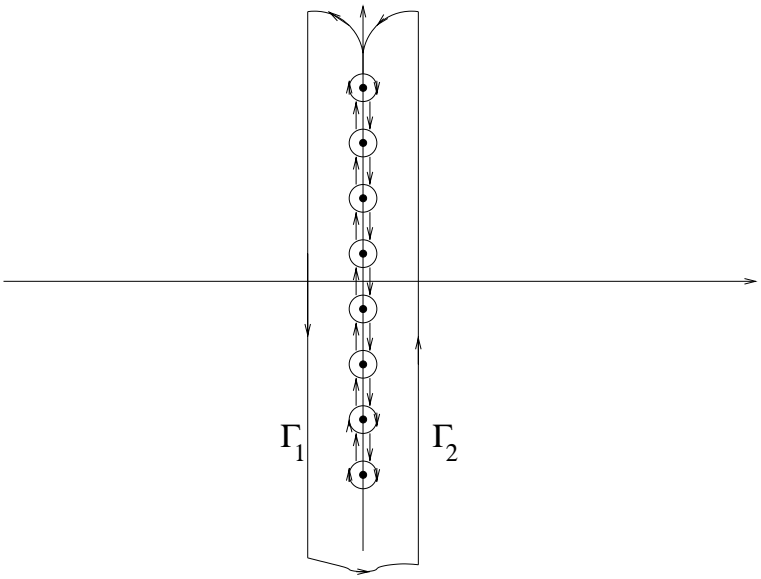

FIGURE C.6: Passing from infinite sum to contour integration

be represented as:

$$\sum_{w_n} f(w_n) = \frac{1}{4\pi i T} \int_{\Gamma_1+\Gamma_2} \tanh \frac{z}{2T}\, f(-iz) \tag{C.41}$$

whereas one has to use $\coth$ in case of bose statistics. (appearance of $\tanh$ and $\coth$ respectively in cases of fermi and bose statistics are not incidental, this could be seen just by following representation:

$$\tanh \frac{E_k}{2T} = 1 - 2n^f(E_k)$$
$$\coth \frac{E_k}{2T} = 1 - 2n^b(E_k)$$

where $n^f(E_k)$ and $n^b(E_k)$ are fermi and bose distribution functions). Indeed, poles of $\tanh \frac{z}{2T}$ are points $z_0^{(n)} = i\pi T(2n+1)$ and they are simple ones, close to them $\tanh \frac{z}{2T} \simeq \frac{2T}{z - z_0^{(n)}}$. Matsubara frequencies are recovered by $w_n = -iz_0^{(n)}$, so one has to make substitution $w_n \to -iz$ in $f(w_n)$. Last step is to deform contours so to encircle only finite number of poles coming from $f(z)$ and use residue methods. Possible deformation is indicated on figure (C.7).

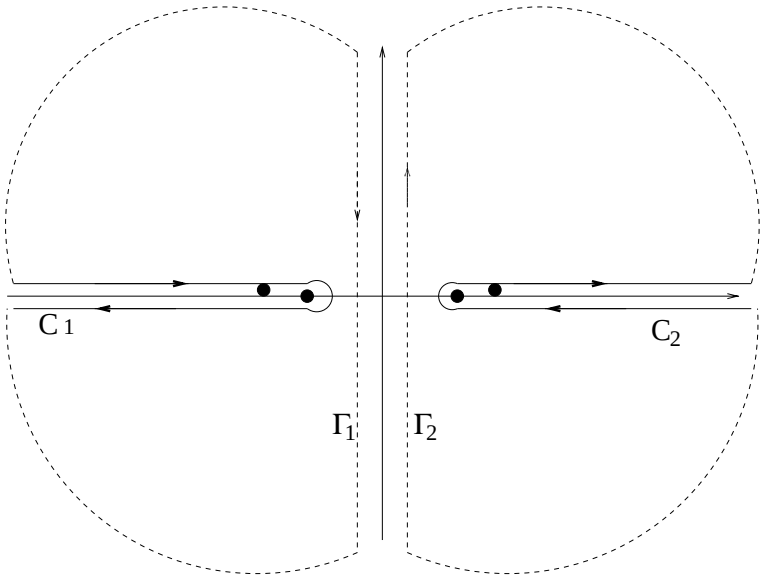

FIGURE C.7: Possible deformation of integration contour

C.6 Nuclear Magnetic Resonance Relaxation Rate

Next we consider the NMR longitudinal relaxation rate T_1^{-1}. Nuclear spins probe local spin environment. Experiments on the spin- lattice relaxation rate yield information on the dynamic spin susceptibility. The analysis of the NMR experiments begins with the magnetic hyperfine hamiltonian, which couples nuclear spins and electron spins:

$$H_{HyperFine} = \sum_{\alpha,i,j} A_{\alpha}^{ij} I_{i\alpha} S_{j\alpha} \tag{C.42}$$

α stands for spin projection, while i, j are latice cites. Nuclear spins relax througth hyperfine interactions with the fluctuating local moments of the spin ladder. The nuclear spin- lattice relaxation rate T_1^{-1} is given:

$$T_1^{-1} \sim \sum_q A_q S(q, w) \tag{C.43}$$

Where we have introduced following quantities: $A_q \simeq A_{\perp}^2(q)$ is the nuclear form factor, with $A_{\perp}(q)$ hyperfine coupling perpendicular to the applied magnetic field averaged over various nuclei, $S(q, w)$ is the dynamical spin structure factor, and w is the nuclear resonance frequency which is negligibly small compared to the other relevant energy scales (excitation gap, temperature). In the limit $w \ll T$ fluctuation dissipation relation between spin structure factor and imaginary part of the retarded spin spin correlation function will look:

$$\mathrm{Im}D^R(q, w) \simeq \frac{w}{T} S(q, w) \tag{C.44}$$

Also the q dependence arising from appropriate form factors is smooth and we replace A_q by A_0 and in the following suppress this constant. We have reduced calculation of NMR relaxation rate T_1^{-1} to the calculation of imaginary part of retarded spin- spin correlation

function:

$$T_1^{-1} \simeq T \sum_{\alpha,\beta} \lim_{w\to 0} \int \frac{dq}{2\pi} \frac{\mathrm{Im}\Gamma_{\alpha,\beta}(q,w)}{w} \tag{C.45}$$

where

$$\sum_{\alpha,\beta} \mathrm{Im}\Gamma_{\alpha,\beta}(q,w) = \mathrm{Im}D^R(q,w) \tag{C.46}$$

and indeces α, β are Majorana flavor indices, see (C.50).

We will concentrate on calculation of $1/T_1$ in the low T limit, assuming T much less than gap in the excitation spectrum. In this limit there are contributions in $1/T_1$ from $q \sim 0$ and $q \sim \pi$. Although we evaluate T_1^{-1} only by taking into account slowly varying spin-spin correlation function ($q \sim 0$) it turns out that this approach is reasonable, since exact diagonalization studies on ladders[23] as well as other theoretical calculations[24] shows that at low temperatures the contribution from staggered spin components in T_1^{-1} is less dominant and can be absorbed into the prefactor which can be determined by fitting it to the experimental data. We will calculate Matsubara finite temperature spin- spin correlation function and then apply analitic continuation to extract imaginary part of the retarded spin- spin Green's function, althought direct calculation in real time formalism is also possible. Matsubara finite temperature spin- spin correlation function in imaginary frequency momentum space is:

$$D(q,W_n) = \int_0^{T^{-1}} d\tau \int_{-\infty}^{\infty} dx e^{iW_n\tau} e^{-ikx} \left\langle S_1^z(x,\tau) S_1^z(0,0) \right\rangle \tag{C.47}$$

where we choose for definiteness spins on the first chain and averaging at finite temperature is implied. Representing smooth parts of spin operators in temrs of Majorana fermions

$$J_1^z(x) = J_{1,L}^z(x) + J_{1,R}^z(x) \tag{C.48}$$

where from (2.17) we have:

$$J_{1,\nu}(x) = -i\psi_\nu^1(x)\psi_\nu^2(x) + i\psi_\nu^3(x)\rho_\nu(x) \tag{C.49}$$

with $\nu = L, R$.

Plugging these expressions into the (C.47) and using Green's functions for Majorana fermions (B.10) we reduce calculation of NMR relaxation rate to calculation of bubbles in Majorana formalism. Unlike structure factor and uniform susceptibility calculations (see bellow) where only processes with $q_\perp = 0$ contributed ($q_\perp$ being momentum perpendicular to chains) for the NMR relaxation process we must take into account processes both with $q_\perp = 0$ and $q_\perp = \pi$, since we are calculating longitudinal NMR relaxation rate. In Majorana formalism that means we have to sum triplet-singlet bubble together with triplet- triple bubbles. Denoting a bubble (or pollarization bubble) made of one Green's function of α Majorana and second Green's function β Majorana by $\Gamma_{\alpha,\beta}(q,W_m)$ we get:

$$\Gamma_{\alpha,\beta}(q,W_m) = -T\sum_{w_n} \int \frac{dk}{2\pi} \left(\frac{iw_n + vk}{w_n^2 + v^2k^2 + m_\alpha^2} \frac{i(w_n - W_m) + v(k-q)}{(w_n - W_m)^2 + v^2(k-q)^2 + m_\beta^2} \right.$$
$$\left. + \Big[(k,q) \to (-k,-q)\Big] + \frac{2m_\alpha m_\beta}{\left[w_n^2 + v^2k^2 + m_\alpha^2\right]\left[(w_n - W_m)^2 + v^2(k-q)^2 + m_\beta^2\right]} \right) \tag{C.50}$$

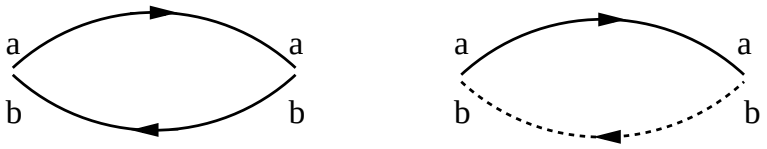

FIGURE C.8: Full propagator corresponds to triplet, while dashed to singlet Majorana. a,b=L,R

First term giving (R,R) bubble, second (L,L) and final includes (R,L)=(L,R) bubbles.

$$\Gamma_{\alpha,\beta}(q,W_m) = -\frac{1}{4\pi i}\int_{C_1+C_2} dz \int \frac{dk}{2\pi}\tanh\frac{z}{2T}\left(\frac{z+vk}{z^2-v^2k^2-m_\alpha^2}\,\frac{iW_m+v(k-q)}{(z-iW_m)^2-v^2(k-q)^2-m_\beta^2} + \Big[(k,q)\to(-k,-q)\Big] + \frac{2m_\alpha m_\beta}{\left[z^2-v^2k^2-m_\alpha^2\right]\left[(z-iW_m)^2-v^2(k-q)^2-m_\beta^2\right]}\right) \tag{C.51}$$

Using residue methods (Appendix C 5) we evaluate this integral. Poles of the integrand inside contours C_1 and C_2 are:

$$z = E_\alpha(k),\ -E_\alpha(k),\ E_\beta(k-q)+iW_m,\ -E_\beta(k-q)+iW_m \tag{C.52}$$

$$\begin{aligned}
&\Gamma_{\alpha,\beta}(q,W_m) = \\
-\ &\frac{1}{2}\int\frac{dk}{2\pi}\left(\tanh\frac{E_\alpha(k)}{2T}\,\frac{E_\alpha(k)+vk}{2E_\alpha(k)}\,\frac{E_\alpha(k)+v(k-q)}{\left(E_\alpha(k)-iW_m\right)^2-E_\beta^2(k-q)}\right.\\
+\ &\tanh\frac{-E_\alpha(k)}{2T}\,\frac{-E_\alpha(k)+vk}{-2E_\alpha(k)}\,\frac{-E_\alpha(k)+v(k-q)}{\left(-E_\alpha(k)-iW_m\right)^2-E_\beta^2(k-q)}\\
+\ &\tanh\frac{E_\beta(k-q)+iW_m}{2T}\,\frac{E_\beta(k-q)+iW_m+vk}{\left(E_\beta(k-q)+iW_m\right)^2-E_\alpha^2(k)}\,\frac{E_\beta(k-q)+v(k-q)}{2E_\beta(k-q)}\\
+\ &\tanh\frac{-E_\beta(k-q)+iW_m}{2T}\,\frac{-E_\beta(k-q)+iW_m+vk}{\left(-E_\beta(k-q)+iW_m\right)^2-E_\alpha^2(k)}\,\frac{-E_\beta(k-q)+v(k-q)}{2\left(-E_\beta(k-q)\right)}\\
+\ &\Big[(k,q)\to(-k,-q)\Big]\\
+\ &\tanh\frac{E_\alpha(k)}{2T}\,\frac{2m_\alpha}{2E_\alpha(k)}\,\frac{m_\beta}{\left(E_\alpha(k)-iW_m\right)^2-E_\beta^2(k-q)}\\
+\ &\tanh\frac{-E_\alpha(k)}{2T}\,\frac{2m_\alpha}{-2E_\alpha(k)}\,\frac{m_\beta}{\left(-E_\alpha(k)-iW_m\right)^2-E_\beta^2(k-q)}\\
+\ &\tanh\frac{E_\beta(k-q)+iW_m}{2T}\,\frac{2m_\alpha}{\left(E_\beta(k-q)+iW_m\right)^2-E_\alpha^2(k)}\,\frac{m_\beta}{2E_\beta(k-q)}\\
+\ &\left.\tanh\frac{-E_\beta(k-q)+iW_m}{2T}\,\frac{2m_\alpha}{\left(-E_\beta(k-q)+iW_m\right)^2-E_\alpha^2(k)}\,\frac{m_\beta}{2\left(-E_\beta(k-q)\right)}\right)
\end{aligned}$$

$$
\begin{aligned}
= & -\frac{1}{2}\int\frac{dk}{2\pi}\left(\tanh\frac{E_\alpha(k)}{2T}\,\frac{E_\alpha^2(k)+v^2k(k-q)+m_\alpha m_\beta}{E_\alpha(k)\left[\left(E_\alpha(k)-iW_m\right)^2-E_\beta^2(k-q)\right]}\right.\\
+ & \tanh\frac{E_\alpha(k)}{2T}\,\frac{E_\alpha^2(k)+v^2k(k-q)+m_\alpha m_\beta}{E_\alpha(k)\left[\left(E_\alpha(k)+iW_m\right)^2-E_\beta^2(k-q)\right]}\\
+ & \tanh\frac{E_\beta(k-q)+iW_m}{2T}\,\frac{E_\beta^2(k-q)+v^2k(k-q)+m_\alpha m_\beta}{E_\beta(k-q)\left[\left(E_\beta(k-q)+iW_m\right)^2-E_\alpha^2(k)\right]}\\
+ & \left.\tanh\frac{E_\beta(k-q)-iW_m}{2T}\,\frac{E_\beta^2(k-q)+v^2k(k-q)+m_\alpha m_\beta}{E_\beta(k-q)\left[\left(E_\beta(k-q)-iW_m\right)^2-E_\alpha^2(k)\right]}\right)
\end{aligned}
\tag{C.53}
$$

In deriving above formula we have suppressed terms proportional to W_m in numerator, since we are going to take the limit $W_m \to 0$. Using formula

$$
\mathrm{Im}\frac{1}{x\pm i\delta}=\mp\pi\delta(x)
$$

we extract the imaginary part of the above expression after analytic continuation $iW_m \to w+i\delta$ and taking the limiting procedure $w \to 0$. First two terms cancel each others contribution to the imaginary part and we are left with the expression:

$$
\begin{aligned}
&\mathrm{Im}\Gamma_{\alpha,\beta}(q,w)=\\
&\frac{1}{2}\int\frac{dk}{2\pi}\partial_E\left(\tanh\frac{E_\beta(k-q)}{2T}\right)w\frac{E_\beta^2(k-q)+v^2k(k-q)+m_\alpha m_\beta}{E_\beta(k-q)}\times\\
&\qquad\qquad\delta\left((E_\beta(k-q)-w)^2-E_\alpha^2(k)\right)\\
&+\frac{1}{2}\int\frac{dk}{2\pi}\partial_E\left(\tanh\frac{E_\beta(k-q)}{2T}\right)w\frac{E_\beta^2(k-q)+v^2k(k-q)+m_\alpha m_\beta}{E_\beta(k-q)}\times\\
&\qquad\qquad\delta\left((E_\beta(k-q)+w)^2-E_\alpha^2(k)\right)
\end{aligned}
\tag{C.54}
$$

We consider two cases separately. When $m_\alpha = m_\beta = m_t$ (triplet- triplet contribution and $m_\alpha = m_t \neq m_\beta = m_s$ (triplet-singlet contribution). For the latter case calculation is rather easier, since we can put w equal to zero in (C.54), while for triplet-triplet contribution because of logarithmic divergence special treatment is necessary. For triplet-singlet channel we have to evaluate the following integral:

$$
\begin{aligned}
&T\int\frac{dq}{2\pi}\int\frac{dk}{2\pi}\partial_E\left(\tanh\frac{E_s(k-q)}{2T}\right)\frac{E_s^2(k-q)+v^2k(k-q)+m_tm_s}{E_s(k-q)}\times\\
&\qquad\qquad\delta\left(E_s^2(k-q)-E_t^2(k)\right)\\
&=T\int\frac{dq}{2\pi}\int\frac{dk}{2\pi}\partial_E\left(\tanh\frac{E_s(k-q)}{2T}\right)\frac{E_s^2(k-q)+v^2k(k-q)+m_tm_s}{E_s(k-q)}\times\\
&\qquad\qquad\frac{\delta(q-q_1)+\delta(q-q_2)}{|v\sqrt{k^2v^2-(m_s^2-m_t^2)}|}
\end{aligned}
\tag{C.55}
$$

where $q_{1,2} = k \pm v^{-1}\sqrt{k^2v^2 - (m_s^2 - m_t^2)}$.
Using $E_s(k-q) = E_t(k)$ and passing to energy variables:

$$dE(k) = \frac{2|k|v^2 dk}{E(k)} \tag{C.56}$$

we get:

$$\begin{aligned} & \frac{T}{\pi}\int \frac{dk}{2\pi}\partial_E\left(\tanh\frac{E_t(k)}{2T}\right)\frac{E_t^2(k)+m_tm_s}{E_t(k)v\sqrt{E_t^2(k)-m_s^2}} \\ = \quad & \frac{T}{(2\pi v)^2}\int_{m_{max}}^{\infty} dE\partial_E\left(\tanh\frac{E}{2T}\right)\frac{E^2+m_tm_s}{\sqrt{E^2-m_t^2}\sqrt{E^2-m_s^2}} \end{aligned} \tag{C.57}$$

Taking into consideration:

$$\partial_E\left(\tanh\frac{E}{2T}\right) = \partial_E\left(1-\frac{2}{e^{E/T}+1}\right) = \frac{\left(\operatorname{sech}\frac{E}{2T}\right)^2}{2T} \tag{C.58}$$

We get for triplet singlet channel following contribution:

$$\frac{1}{2(2\pi v)^2}\int_{m_{max}}^{\infty} dE\left(\operatorname{sech}\frac{E}{2T}\right)^2\frac{E^2+m_tm_s}{\sqrt{E^2-m_t^2}\sqrt{E^2-m_s^2}} \tag{C.59}$$

where $m_{max} = Max(|m_s|,|m_t|)$ Assuming $|m_s| > |m_t|$ as is the case in ladders we can take above integral making the same approximations as for (C.65).

$$T_1^{-1}|_{ts} \simeq \frac{1}{(\pi v)^2}\sqrt{2|m_s|}\sqrt{|m_s+m_t|}e^{-\frac{|m_s|+|m_t|}{2T}}K_0\left(\frac{|m_s-m_t|}{2T}\right) \tag{C.60}$$

For the low temperature, when $T \ll |m_s - m_t|$ we can use asymptotic form of Bessel function and get:

$$T_1^{-1}|_{ts} \simeq \frac{1}{(\pi v)^2}\sqrt{\pi|m_s|}\sqrt{\frac{|m_s+m_t|}{|m_s-m_t|}}e^{-\frac{m_s}{T}}\sqrt{T} \tag{C.61}$$

Now we are in a position to evaluate triplet-triplet contribution to NMR relaxation rate. For this we go back to the general formula (C.54) and treat accurately w in the delta function.

$$\begin{aligned} & T_1^{-1}|_{tt} \simeq \frac{T}{2}\int\frac{dq}{2\pi}\int\frac{dk}{2\pi}\partial_E\left(\tanh\frac{E(k-q)}{2T}\right)\frac{E^2(k-q)+v^2k(k-q)+m^2}{E(k-q)} \\ & \left[\delta\left((E(k-q)-w)^2-E^2(k)\right)+\delta\left((E(k-q)+w)^2-E^2(k)\right)\right] \\ = \quad & \frac{T}{2}\int\frac{dq}{2\pi}\int\frac{dk}{2\pi}\partial_E\left(\tanh\frac{E(p)}{2T}\right)\frac{E^2(p)+v^2p(p+q)+m^2}{E(p)} \\ & \left[\delta\left((E(p)-w)^2-E^2(p+q)\right)+\delta\left((E(p)+w)^2-E^2(p+q)\right)\right] \\ & = \frac{T}{2}\int\frac{dq}{2\pi}\int\frac{dk}{2\pi}\partial_E\left(\tanh\frac{E(p)}{2T}\right)\frac{E^2(p)+v^2p(p+q)+m^2}{E(p)} \\ & \left[\frac{\delta(q-q_1^1)+\delta(q-q_2^1)}{|2v\sqrt{(E-w)^2-m^2}|}+\frac{\delta(q-q_1^2)+\delta(q-q_2^2)}{|2v\sqrt{(E+w)^2-m^2}|}\right] \end{aligned} \tag{C.62}$$

We have introduced the following notations: $p = k - q$, $q^1_{1,2} = -p \pm v^{-1}\sqrt{(E-w)^2 - m^2}$, and $q^2_{1,2} = -p \pm v^{-1}\sqrt{(E+w)^2 - m^2}$ Changing again to energy variables we get:

$$\begin{aligned} T_1^{-1}|_{tt} &\simeq \frac{1}{4(2\pi v)^2}\int_m^\infty dE \left(\text{sech}\ \frac{E}{2T}\right)^2 \frac{E^2+m^2}{\sqrt{E^2-m^2}\sqrt{(E+w)^2-m^2}} \\ + \quad & \frac{1}{4(2\pi v)^2}\int_{m+w}^\infty dE \left(\text{sech}\ \frac{E}{2T}\right)^2 \frac{E^2+m^2}{\sqrt{E^2-m^2}\sqrt{(E-w)^2-m^2}} \\ &\simeq \frac{1}{2(2\pi v)^2}\int_m^\infty dE \left(\text{sech}\ \frac{E}{2T}\right)^2 \frac{E^2+m^2}{\sqrt{E^2-m^2}\sqrt{(E+w)^2-m^2}} \end{aligned} \tag{C.63}$$

To calculate the above integral at $T \ll m$ we can make the following substitution:

$$\left(\text{sech}\ \frac{E}{2T}\right)^2 \simeq 4e^{-\frac{E}{T}} \tag{C.64}$$

$$\begin{aligned} T_1^{-1}|_{tt} &\simeq \frac{1}{2(\pi v)^2}\int_m^\infty dE e^{-\frac{E}{T}} \frac{E^2+m^2}{\sqrt{E^2-m^2}\sqrt{(E+w)^2-m^2}} \\ &\simeq \frac{1}{2(\pi v)^2}\int_m^\infty dE e^{-\frac{E}{T}} \frac{E^2+m^2}{(E+m)\sqrt{E-m}\sqrt{(E+w)-m}} \\ &\simeq \frac{m}{2(\pi v)^2}\int_m^\infty dE \frac{e^{-\frac{E}{T}}}{\sqrt{E-m}\sqrt{(E+w)-m}} \\ &= \frac{m}{2(\pi v)^2} e^{-\frac{m}{T}} K_0\left(\frac{w}{2T}\right) \end{aligned} \tag{C.65}$$

In evaluating above integral we used the fact that integrand is peaked at $E \sim m$ and used the formula 3.364(3) from Gradshteyn and Ryzhik. Finally using asymptotic expression for Bessel function of imaginary argument from Gradshteyn and Ryzhik 8.447(3) we get the following estimation for relaxation rate

$$T_1^{-1}|_{tt} \simeq \frac{m}{2(\pi v)^2} e^{-\frac{m}{T}}(-C + \ln 4 - \ln\frac{w}{T}) \tag{C.66}$$

with C standing for Euler's constant.

C.7 Static Susceptibility

For determining the static susceptibility we have to take into account only the triplet-triplet bubble, since the singlet Majorana does not carry spin. Moreover, since the uniform magnetic field applied in the direction of Z axes couples only to the symmetric sector it involves only the doublet from the Majorana triplet. We can start from equation (C.53), in the limit $q \to 0$

and take again another limit $w \to 0$.

$$\begin{aligned}\Gamma_{z,z}(q \to 0, w) &= -\frac{1}{2}\int \frac{dk}{2\pi}\left(\tanh\frac{E_t(k)}{2T}\,\frac{2E_t(k)}{\left[(E_t(k)+w+i\delta)^2 - E_t^2(k)\right]}\right. \\ &+ \tanh\frac{E_t(k)}{2T}\,\frac{2E_t(k)}{\left[(E_t(k)-w-i\delta)^2 - E_t^2(k)\right]} \\ &+ \tanh\frac{E_t(k)-w}{2T}\,\frac{2E_t(k)}{\left[(E_t(k)-w-i\delta)^2 - E_t^2(k)\right]} \\ &+ \left.\tanh\frac{E_t(k)+w}{2T}\,\frac{2E_t^2(k)}{\left[(E_t(k)+w+i\delta)^2 - E_t^2(k)\right]}\right) \end{aligned} \tag{C.67}$$

$$\begin{aligned}\Gamma_{z,z}(q \to 0, w \to 0) &= \chi(T) = -\frac{1}{2}\int \frac{dk}{2\pi}\left(\tanh\frac{E_t(k)}{2T}\,\frac{1}{w+i\delta}\right. \\ &+ \tanh\frac{E_t(k)}{2T}\,\frac{1}{-w-i\delta} \\ &+ \tanh\frac{E_t(k)-w}{2T}\,\frac{1}{-w-i\delta)} \\ &+ \left.\tanh\frac{E_t(k)+w}{2T}\,\frac{1}{w+i\delta}\right) \end{aligned} \tag{C.68}$$

As is clear from the above expression first two terms completely cancel each other. What survives the limit $w \to 0$ is the real part after the expansion of third and fourth terms, and we get the final answer:

$$\chi(T) = \frac{1}{T}\int_0^\infty \frac{dk}{2\pi}\mathrm{sech}\,\frac{E_t(k)}{2T} \tag{C.69}$$

For the massless case this expression can be calculated exactly and we get temperature independent constant magnetic susceptibility (characteristic to Luttinger Liquids),

$$\chi(T) = \frac{\pi}{2v} \tag{C.70}$$

while for the massive case making the low temperature approximation as we did for calculation of the specific heat we get:

$$\chi(T) \simeq \frac{\sqrt{2\pi m_t}}{v} T^{-\frac{1}{2}} e^{-\frac{m_t}{T}} \tag{C.71}$$

APPENDIX D

Renormalization Group Analysis

D.1 Perturbative Renormalization Group

We consider the two-dimensional Euclidean scale invariant action S_0 (fixed point action) perturbed by the operators $O_i(r)$ of conformal dimension d.

$$\langle O_i(r)O_i(0)\rangle = |r|^{-2d_i} \tag{D.1}$$

Correlation function is evaluated with respect to the fixed point action. Partition function of the theory looks:

$$Z = \int D\phi e^{-S[\phi]} \tag{D.2}$$

Where the Euclidean action reads:

$$S = S_0 + \sum_i g_i \int d^2 r a^{d_i-2} O_i(r) \tag{D.3}$$

The microscopic short distance cut-off a (e.g. the lattice spacing) is needed to make action dimensionless. We remind, that coupling constants g_i are dimensionless (small numbers), and from (D.1) dimension of perturbing operators are $(\text{length})^{-d_i}$. Let us expand the partition function in powers of g_i.

$$\begin{aligned} Z &= Z^* \Bigg[1 - \sum_i g_i \int d^2 r a^{d_i-2} \langle O_i(r)\rangle \\ &+ \frac{1}{2}\sum_{i,j} g_i g_j \int d^2 r_1 d^2 r_2 a^{d_i+d_j-4} \langle O_i(r_1)O_j(r_2)\rangle \\ &- \frac{1}{3!}\sum_{i,j,k} g_i g_j g_k \int d^2 r_1 d^2 r_2 d^2 r_3 a^{d_i+d_j+d_k-6} \langle O_i(r_1)O_j(r_2)O_k(r_3)\rangle \ldots \Bigg] \end{aligned} \tag{D.4}$$

All correlation functions are evaluated with respect to the fixed point action. The idea of renormalization is to start moving towards larger distances (lower energies) by integrating out the short-distance degrees of freedom. If the action is renormalizable, the effective action, which incorporates physics at larger distances, will have the same structure as the original one, (up to irrelevant terms) but with a new set of coupling constants. Such a procedure is repeated many times and at each RG step the form of original action is recovered. Relations between the bare and renormalized couplings then lead to the differential RG equations. Their

solution reveals the dominant tendencies developing in the system on increasing the length scale (decreasing energy, temperature). Let us rescale short distance cut-off infinitesimally $a \to (1 + d\Lambda/\Lambda)a = (1 + \delta l)a$, with $\delta l \ll 1$, and $\Lambda \sim 1/a$ is high frequency cut-off. There are two effects needed to take into account on changing the cut-off. First is trivially handled, that is explicit dependence on the cut-off from divisors in (D.4) could be compensated by rescaling coupling constants oppositely.

$$g_i \to e^{\delta l(2-d_i)} g_i \sim g_i + (2 - d_i) g_i \delta l \tag{D.5}$$

There is also implicit dependence on the cut-off in (D.4). Since integrals have potential short-distance divergences as points approach each other all integrals should be restricted to $|r_i - r_j| > a$. The effect of changing the cut-off may be evaluated by the use of operator product expansion. Consider the second order term in (D.4). After rescaling $a \to (1 + \delta l)a$ we break up the integral as:

$$\int_{|r_1 - r_2| > a(1+\delta l)} = \int_{|r_1 - r_2| > a} - \int_{a(1+\delta l) > |r_1 - r_2| > a} \tag{D.6}$$

First term gives back the original contribution to Z. It is the second term where we can use operator product expansions (ope) from underlying conformal field theory that represents ultraviolet fixed point of the model (operator product expansions are strictly valid at short distances, before the nearest additional insertion). The fact that the model under consideration in ultraviolet limit scales to fixed point theory is guaranteed from the requirement of its renormalizability. We write out ope:

$$O_i(r_1) O_j(r_2) \simeq \sum_k c_{ijk}(|r_1 - r_2|) O_k(\frac{r_1 + r_2}{2}) = \sum_k \frac{c_{ijk}}{|r_1 - r_2|^{d_i + d_i - d_k}} O_k(\frac{r_1 + r_2}{2}) \tag{D.7}$$

Above c_{ijk} are numbers. Plugging this ope in the second part of (D.6) and approximating $|r_1 - r_2| \simeq a$ we get:

$$\frac{1}{2} \sum_{ij} \sum_k c_{ijk} a^{d_k - d_j - d_i} \int_{a(1+\delta l) > |r_1 - r_2| > a} \frac{d^2 r_1 d^2 r_2}{a^{4 - d_i - d_j}} \left\langle O_k(\frac{r_1 + r_2}{2}) \right\rangle \tag{D.8}$$

Integration with relative coordinate gives factor of $2\pi a^2 \delta l$, while the remaining term may be compensated by making the change:

$$g_k \to g_k - \pi \sum_{ij} c_{ijk} g_i g_j \delta l \tag{D.9}$$

Putting together contributions from (D.5) and (D.9) to the renormalization of the coupling constants we get:

$$\frac{dg_k}{dl} = (2 - d_i) g_k - \pi \sum_{ij} c_{ijk} g_i g_j + \dots \tag{D.10}$$

Before we apply this mechanism to the concrete example represented by sine-Gordon theory we want to discuss simple (based on dimensional analyses) consequences of (D.10). First consider situation when dimension of the perturbing operator is other than 2. In this case

second term could be neglected compared to first and we can appreciate mass generated by perturbing operator. Using $\delta l = d\Lambda/\Lambda$ (dΛ being energy shell eliminated at a given step of RG) we get:

$$\mathrm{d}\ln g = (2-d)\mathrm{d}\ln\Lambda \tag{D.11}$$

From above follows:

$$\frac{g}{g_0} = \left(\frac{\Lambda_0}{\Lambda}\right)^{d-2} = \left(\frac{\xi_0}{\xi}\right)^{2-d} \tag{D.12}$$

Above $g_0,\ \Lambda_0,\ g,$ and Λ are bare and renormalized values of coupling constant and high frequency cut-offs and ξ-s are correlation lengths associated with two cutoffs. First we see, that perturbation is relevant if $d < 2$, and irrelevant if $d > 2$ (we remind, that $\Lambda/\Lambda_0 \to 0$). In Lorenz invariant system finite correlation length means a mass gap $m \sim \xi_0^{-1}$. Mass gap can be calculated from (D.12) if we assume, that correlation length is of the order of lattice spacing when coupling constant reaches value of order of unity. Then from (D.12) putting $g = 1$ and $\xi = a$ we evaluate:

$$m \sim a^{-1} g_0^{1/(2-d)} \tag{D.13}$$

If the perturbation is marginal $d = 2$, than first order term in (D.10) is zero. Repeating the same calculation for mass gap associated with marginally relevant perturbation we get:

$$m \sim a^{-1} e^{-\frac{\mathrm{const}}{g_0}} \tag{D.14}$$

Since we know how mass gap is connected with the bare value of perturbation we can evaluate by dimensional arguments alone expectation values of any operator of scaling dimension d_i in the vacuum governed by relevant perturbation of scaling dimension d.

$$\langle O_i(r)\rangle \sim m^{d_i} \sim a^{-d_i} g_0^{d_i/(2-d)} \tag{D.15}$$

D.2 One Loop RG Equations for Sine-Gordon Model

In this section we derive one loop Renormalization Group (RG) equations for sine-Gordon model. We treat sine-Gordon Hamiltonian as Gaussian conformal field theory perturbed by two marginal operators. The fact that sine-Gordon model in ultraviolet limit scales to free field theory is guaranteed from its renormalizability (this fact is responsible for the mystery why at high energies experimentlists see single chain physics in experiments on ladder systems).

$$\begin{aligned} H &= \frac{v}{2}\left[\,(\partial_x\phi(x))^2 + (\partial_x\theta(x))^2\,\right] \\ &+ \alpha\partial_x\phi_L(x)\partial_x\phi_R(x) + g\cos\sqrt{8\pi}\phi(x) \end{aligned} \tag{D.16}$$

We note, that both perturbations have scaling dimension 2, therefore first terms in (D.10) will vanish. Denoting $\alpha = g_1$ and $g = g_2$ we write one loop Renormalization Group equations from (D.10):

$$\frac{dg_k}{dl} = -\pi \sum_{i,j} c_{ijk} g_i g_j \tag{D.17}$$

where c_{ijk} numerical constants are obtained from the operator product expansion Eq. (D.7). For our case $O_1 = \partial_x\phi_L(x)\partial_x\phi_R(x) = \partial\phi(z)\bar{\partial}\phi(\bar{z})$ and $O_2 = \cos\sqrt{8\pi}\phi(z,\bar{z})$ where z and $\bar{z}$ represent conformal coordinates on Euclidean plane (see Eq. (1.3)). Writing out relevant opes for our case:

$$\begin{aligned}\cos\sqrt{8\pi}\phi(z,\bar{z})\cos\sqrt{8\pi}\phi(w,\bar{w}) &\sim -4\pi\frac{\partial_w\phi(w)\partial_{\bar{w}}\phi(\bar{w})}{|z-w|^2}\\ \cos\sqrt{8\pi}\phi(z,\bar{z})\partial_w\phi(w)\partial_{\bar{w}}\phi(\bar{w}) &\sim -\frac{1}{2\pi}\frac{\cos\sqrt{8\pi}\phi(w,\bar{w})}{|z-w|^2}\end{aligned} \tag{D.18}$$

From (D.18) we read off following nonzero ope numerical constants:

$$c_{221} = -4\pi \tag{D.19}$$

and

$$c_{122} = c_{212} = -\frac{1}{2\pi} \tag{D.20}$$

One loop RG equations will look:

$$\begin{aligned}\frac{d\alpha}{dl} &= 4\pi^2\frac{g^2}{v}\\ \frac{dg}{dl} &= \frac{\alpha g}{v}\end{aligned} \tag{D.21}$$

Noting that

$$\partial_x\phi_L(x)\partial_x\phi_R(x) = \frac{1}{4}\big((\partial_x\phi)^2 - ((\partial_x\theta)^2\big)$$

Hamiltonian (D.16) could be equivalently rewritten as:

$$H = \frac{v}{2}\int\left[\,(\partial_x\phi(x))^2 + (\partial_x\theta(x))^2\,\right] + \frac{vm}{2\pi}\cos\sqrt{8\pi K}\phi(x) \tag{D.22}$$

where $K = 1 - \alpha/2v$ and $m = \frac{2\pi g}{v}$ and we can write RG equations for running coupling constant and mass of sine-Gordon:

$$\begin{aligned}\frac{dK}{dl} &= -\frac{m^2}{2}\\ \frac{dm}{dl} &= -2m(K-1)\end{aligned} \tag{D.23}$$

One obtains following pictorial solution of RG flow diagram Fig. (3.2): For $2(K-1) \geq |m|$ we are in the weak coupling regime: the effective mass vanishes. The low energy (large distance) behavior of the corresponding gapless mode is described by a free scalar field.

For $2(K-1) < |m|$ the system scales to strong coupling: depending on the sign of the bare mass m, the renormalized mass is driven to $\pm\infty$, signaling a crossover to one of the two strong coupling regimes with a dynamical generation of a commensurability gap in the excitation spectrum.

APPENDIX E

Spin Wave Calculation

E.1 Spin Wave Calculation in $S^z_{tot} = N - 1$ Subspace

In this appendix we perform the spin wave analyses for the Hamiltonian

$$\hat{H} = H_\perp + H_{leg,1} + H_{leg,2} \tag{E.1}$$

where

$$H_\perp = -J^Z_\perp \sum_{j=1,N} S^Z_{j,1} S^Z_{j,2} - \frac{J^{XY}_\perp}{2} \sum_{j=1,N} \left[S^+_{j,1} S^-_{j,2} + S^-_{j,1} S^+_{j,2} \right] \tag{E.2}$$

$$H_{leg,\alpha} = \sum_{j=1}^{N} \left[\frac{S^+_{j,\alpha} S^-_{j+1,\alpha} + S^-_{j,\alpha} S^+_{j+1,\alpha}}{2} - \triangle S^z_{j,\alpha} S^z_{j+1,\alpha} \right] - \sum_{j=1}^{N} h S^z_{j,\alpha} \tag{E.3}$$

The strategy is to start from the region of phase diagram where we expect ground state to be fully polarized state in direction of Z axes and to identify transition line from fully polarized ground state to some other state as instability in spin wave excitation spectrum. We denote by

$$|0\rangle = \left| \begin{array}{cccccccc} \uparrow_1 & \uparrow_2 & \cdots & \uparrow_{n-1} & \uparrow_n & \uparrow_{n+1} & \cdots & \uparrow_N \\ \uparrow_1 & \uparrow_2 & \cdots & \uparrow_{n-1} & \uparrow_n & \uparrow_{n+1} & \cdots & \uparrow_N \end{array} \right\rangle \tag{E.4}$$

fully polarized configuration. As usually in the ferro state lowest excitations are spin waves, obtained from ground state configurations by inverting one spin on upper or lower chains. Those states we denote respectively:

$$|1\rangle_n = \left| \begin{array}{cccccccc} \uparrow_1 & \uparrow_2 & \cdots & \uparrow_{n-1} & \downarrow_n & \uparrow_{n+1} & \cdots & \uparrow_N \\ \uparrow_1 & \uparrow_2 & \cdots & \uparrow_{n-1} & \uparrow_n & \uparrow_{n+1} & \cdots & \uparrow_N \end{array} \right\rangle \tag{E.5}$$

and

$$|2\rangle_n = \left| \begin{array}{cccccccc} \uparrow_1 & \uparrow_2 & \cdots & \uparrow_{n-1} & \uparrow_n & \uparrow_{n+1} & \cdots & \uparrow_N \\ \uparrow_1 & \uparrow_2 & \cdots & \uparrow_{n-1} & \downarrow_n & \uparrow_{n+1} & \cdots & \uparrow_N \end{array} \right\rangle \tag{E.6}$$

What does Hamiltonian produce acting on this basis states:

$$
\begin{aligned}
H_{\perp}\left|1\right\rangle_n &= -\frac{1}{2}J_{\perp}^{XY}\left|2\right\rangle_n + \frac{1}{4}J_{\perp}^{Z}\left|1\right\rangle_n - \frac{1}{4}J_{\perp}^{Z}(N-1)\left|1\right\rangle_n \\
H_{\perp}\left|2\right\rangle_n &= -\frac{1}{2}J_{\perp}^{XY}\left|1\right\rangle_n + \frac{1}{4}J_{\perp}^{Z}\left|2\right\rangle_n - \frac{1}{4}J_{\perp}^{Z}(N-1)\left|2\right\rangle_n \\
H_{leg,1}\left|1\right\rangle_n &= \frac{1}{2}(\left|1\right\rangle_{n-1} + \left|1\right\rangle_{n+1}) \\
&+\frac{\triangle}{2}\left|1\right\rangle_n - \frac{\triangle}{4}(N-2)\left|1\right\rangle_n - \frac{h(N-2)}{2}\left|1\right\rangle_n \\
H_{leg,2}\left|1\right\rangle_n &= -\frac{\triangle}{4}N\left|1\right\rangle_n - \frac{hN}{2}\left|1\right\rangle_n \\
H_{leg,1}\left|2\right\rangle_n &= -\frac{\triangle}{4}N\left|2\right\rangle_n - \frac{hN}{2}\left|2\right\rangle_n \\
H_{leg,2}\left|2\right\rangle_n &= \frac{1}{2}\left(\left|2\right\rangle_{n-1} + \left|2\right\rangle_{n+1}\right) \\
&+\frac{\triangle}{2}\left|2\right\rangle_n - \frac{\triangle}{4}(N-2)\left|2\right\rangle_n - \frac{h(N-2)}{2}\left|2\right\rangle_n
\end{aligned}
\tag{E.7}
$$

Collecting all terms we get:

$$
\begin{aligned}
\hat{H}\left|1\right\rangle_n &= -\frac{1}{2}J_{\perp}^{XY}\left|2\right\rangle_n + (\triangle + h + \frac{1}{2}J_{\perp}^{Z})\left|1\right\rangle_n \\
&+ \frac{1}{2}(\left|1\right\rangle_{n-1} + \left|1\right\rangle_{n+1}) + E_{ferro}\left|1\right\rangle_n
\end{aligned}
\tag{E.8}
$$

where

$$
E_{ferro} = -\frac{N}{4}J_{\perp}^{Z} - \frac{N}{2}\triangle - Nh \tag{E.9}
$$

stands for Ferromagnetic state energy. (and the same holds for $\hat{H}\left|2\right\rangle_n$ with interchange $\left|1\right\rangle_n \leftrightarrow \left|2\right\rangle_n$) Now we create spin waves from $\left|1\right\rangle_n$ and $\left|2\right\rangle_n$ states:

$$
\left|\psi(q)\right\rangle = \sum_n (\gamma\left|1\right\rangle_n + \beta\left|2\right\rangle_n)e^{iqn}
$$

$$
\begin{aligned}
(\hat{H} - E_{ferro})\left|\psi(q)\right\rangle &= \sum_n e^{iqn}\{[(\triangle + h + \frac{J_{\perp}}{2} + \cos q)\gamma \\
&- \frac{J_{\perp}^{XY}}{2}\beta]\left|1\right\rangle_n \\
&+ [(\triangle + h + \frac{J_{\perp}^{Z}}{2} + \cos q)\beta \\
&- \frac{J_{\perp}^{XY}}{2}\gamma]\left|2\right\rangle_n\}
\end{aligned}
\tag{E.10}
$$

$$
(\hat{H} - E_{ferro})\left|\psi(q)\right\rangle = \omega\left|\psi(q)\right\rangle
$$

instability line is given by $\omega = 0$

$$(\triangle + h + \frac{J_\perp^Z}{2} + \cos q)\gamma - \frac{J_\perp^{XY}}{2}\beta = 0$$
$$(\triangle + h + \frac{J_\perp^Z}{2} + \cos q)\beta - \frac{J_\perp^{XY}}{2}\gamma = 0 \tag{E.11}$$

There are two cases: $\gamma = \pm\beta$ to which correspond two frequencies:

$$\gamma = -\beta : \ \omega_q^1 = \triangle + h + \frac{J_\perp^Z}{2} + \cos q + \frac{J_\perp^{XY}}{2}$$
$$\gamma = \beta : \ \omega_q^2 = \triangle + h + \frac{J_\perp^Z}{2} + \cos q - \frac{J_\perp^{XY}}{2} \tag{E.12}$$

There are following relevant cases we are interested in:

1. $h = 0$, $J_\perp^{XY} = 0$, in this case for transition line we get:

$$\triangle = 1 - \frac{1}{2J} J_\perp^z \, . \tag{E.13}$$

   where we have restored intraleg exchange ($J > 0$).

2. for the case of $SU(2)$ symmetric ferromagnetic interleg exchange $J_\perp^{XY} = J_\perp^Z > 0$, $h = 0$ we get:

$$\triangle = |J| \tag{E.14}$$

E.2 Spin Wave Calculation in $S_{tot}^z = N - 2$ Subspace

In this appendix we consider separately the case of ferromagnetic chains coupled by ZZ interchain ferromagnetic exchange. Spin wave calculation close to decoupled chains limit gave phase transition line (E.13) from fully polarized state to XY state that behave linearly with interchain exchange. On the other hand in strong rung coupling limit we determined the same boundary and it behaved as 1 over interchain exchange. Our spin wave calculation was done by searching the instability in the spin wave spectrum in the subspace of $S_{tot}^z = N - 1$ on the other hand it is clear, that when we pass to the strong rung coupling limit to invert two spins simultaneously on the same rung will cost less energy, than inverting only one spin on one of the legs. Thus it is natural to repeat spin wave calculation in the subspace of $S_{tot}^z = N - 2$. Let's start from Hamiltonian (E.1) and put $h = 0$ and $J_\perp^{XY} = 0$. We introduce the following basis of states in the subspace of $S_{tot}^z = N - 2$:

$$|n, m\rangle = S_{1,n}^- S_{2,m}^- |0\rangle = \left| \begin{array}{ccccccccccc} \uparrow_1 & \cdots & \uparrow_{m-1} & \uparrow_m & \uparrow_{m+1} & \cdots & \uparrow_{n-1} & \downarrow_n & \uparrow_{n+1} & \cdots & \uparrow_N \\ \uparrow_1 & \cdots & \uparrow_{m-1} & \downarrow_m & \uparrow_{m+1} & \cdots & \uparrow_{n-1} & \uparrow_n & \uparrow_{n+1} & \cdots & \uparrow_N \end{array} \right\rangle \tag{E.15}$$

Acting by Hamiltonian on these states we get:

$$\hat{H} \, |n, m\rangle = (E_0 - J_\perp^Z \delta_{n,m}) + \frac{1}{2} \left(|n+1, m\rangle + |n-1, m\rangle + |n, m+1\rangle + |n, m-1\rangle \right) \tag{E.16}$$

where $E_0 = E_{ferro} + 2\triangle + J_\perp^Z$ with E_{ferro} as in (E.9). Constructing spin waves:

$$|\psi\rangle = \sum_{n=1}^{N} e^{iqn} \sum_{m=1}^{N} \alpha_{n-m} |n, m\rangle \tag{E.17}$$

We search for instability line as:

$$\hat{H} |\psi\rangle = E |\psi\rangle = E_{ferro} |\psi\rangle \tag{E.18}$$

After some simple algebra we get:

$$\sum_{n=1}^{N} e^{iqn} \sum_{m=1}^{N} \Big[\left(E_0 - J_\perp^Z \delta_{n,m} - E\right) \alpha_{n-m} + \frac{1}{2} \left(e^{-iq} + 1\right) \alpha_{n-m-1} + \frac{1}{2} \left(e^{-iq} + 1\right) \alpha_{n-m+1} \Big] |n, m\rangle = 0 \tag{E.19}$$

denoting $n - m = p$ we get the following system of equations:

$$(E_0 - J_\perp^Z \delta_{p,0} - E)\alpha_p + e^{-iq/2} \cos\frac{q}{2} \alpha_{p-1} + e^{-iq/2} \cos\frac{q}{2} \alpha_{p+1} = 0 \tag{E.20}$$

for all values of p. Redefining amplitudes

$$\tilde{\alpha}_p = e^{ipq/2} \alpha_p \tag{E.21}$$

we rewrite the above system as:

$$\begin{cases} . \\ . \\ \cos\frac{q}{2}\tilde{\alpha}_{-i} + (E_0 - E)\tilde{\alpha}_{-i+1} + \cos\frac{q}{2}\tilde{\alpha}_{-i+2} = 0 \\ . \\ \cos\frac{q}{2}\tilde{\alpha}_{-2} + (E_0 - E)\tilde{\alpha}_{-1} + \cos\frac{q}{2}\tilde{\alpha}_0 = 0 \\ \cos\frac{q}{2}\tilde{\alpha}_{-1} + (E_0 - J_\perp^Z - E)\tilde{\alpha}_0 + \cos\frac{q}{2}\tilde{\alpha}_1 = 0 \\ \cos\frac{q}{2}\tilde{\alpha}_0 + (E_0 - E)\tilde{\alpha}_1 + \cos\frac{q}{2}\tilde{\alpha}_2 = 0 \\ . \\ \cos\frac{q}{2}\tilde{\alpha}_i + (E_0 - E)\tilde{\alpha}_{i+1} + \cos\frac{q}{2}\tilde{\alpha}_{i+2} = 0 \\ . \\ . \end{cases} \tag{E.22}$$

To solve the above system we take the following 'confinement' ansatz:

$$\tilde{\alpha} = \alpha e^{-\kappa|p|} \tag{E.23}$$

Plugging this Ansatz into above system we get:

$$\begin{cases} E_0 - J_\perp^Z - E + 2\cos\frac{q}{2} e^{-\kappa} = 0 \\ 2\cos\frac{q}{2}\cosh\kappa + E_0 - E = 0 \end{cases} \tag{E.24}$$

Remembering instability condition: $E_0 - E = 2\triangle + J^Z_{\perp,cr}$ we get

$$\begin{cases} \triangle + \cos\frac{q}{2} e^{-\kappa} = 0 \\ 2\cos\frac{q}{2}\cosh\kappa + 2\triangle + J^Z_{\perp,cr} = 0 \end{cases} \tag{E.25}$$

which we solve:

$$J^Z_{\perp,cr} = \frac{-\triangle^2 + \cos^2\frac{q}{2}}{\triangle} \tag{E.26}$$

Since $\triangle = 1$ is instability point for $J^Z_\perp = 0$ (decoupled chains) we deduce $q/2 = \pi$ and finally restoring intrachain coupling we get:

$$J^Z_{\perp,cr} = \frac{J}{\triangle} - J\triangle \tag{E.27}$$

This formula interpolates between the results of weakly coupled and strongly coupled chains limits. We believe this simple expression (E.27) gives exact transition line for all interchain coupling strengths.

Bibliography

[1] J. G. Bednorz and K. A. Müller, Z. Phys. B **64**, 189 (1986)

[2] N. M. Plakida, in *Lectures on the Physics of Highly Correlated Electron Systems V*, Fifth Training Course in the Physics of Correlated Electron Systems and Higt T_c Superconductors, Salerno, Italy 2000, AIP Conference Proceedings, 580.

[3] H. F. Fong, et al. Phys. Rev. B **61**, 14773 (2000).

[4] P. W. Anderson, Science **235**, 1196 (1987).

[5] M. Sigrist, T.M. Rice and F.C. Zhang, Phys. Rev. B **49**, 12058 (1994).

[6] V. Khveshchenko and T.M. Rice, Phys. Rev. B **50**, 252 (1994).

[7] For a review see E. Dagotto, Rep. Prog. Phys. **62**, 1525 (1999); E. Dagotto and T.M. Rice, Science **271**, 618 (1996).

[8] P. Jordan and E. Wigner, T. Phys. **47**, 631 (1928).

[9] P. W. Anderson Phys. Rev. Lett. **18**, 1049 (1967).

[10] S. Tomonaga, Prog. Theor. Phys. **5**, 4, 63, 1950.

[11] S. Coleman, Phys. Rev. D **11**, 2088 (1975); S. Mandelstam, Phys. Rev. D **11**, 3026 (1975).

[12] A. Luther and I. Peschel, Phys. Rev. B **12**, 3908 (1975).

[13] D. Allen and D. Sénéchal, Phys. Rev. B **55**, 299 (1997).

[14] H.Schulz, G. Cuniberti, and P. Pieri, in Fermi liquids and Luttinger liquids, lecture notes of the Chia Laguna (Italy) summer school, september 1997. cond-mat/9807366.

[15] J.B. Zuber and C. Itzykson, Phys. Rev. D **15**, 2875, 1977.

[16] P. Ginsparg, in *Champs, Cordes et Phénomènes Critiques/ Fields, strings and critical phenomena*, Eds. E. Brézin and J. Zinn-Justin, Elsevier, Amsterdam, (1990).

[17] P. Di Francesco, P. Mathieu, and D. Sénéchal, *Conformal Field Theory*, Springer Verlag, New Yourk, 1997.

[18] J. Cardy, *Scaling and Renormalization in Statistcal Physics*, Cambridge university Press, 1996.

[19] M. Henkel *Conformal Invariance and Critical Phenomena*, Springer Verlag,Berlin Heidelberg, 1999.

[20] J. Polchinski, *String Theory*, Vol. 1, Cambridge university Press, 1998.

[21] M.B. Green, J.H. Schwarz, E. Witten, *Superstring Theory*, Vol. 1, Cambridge university Press, 1987.

[22] M. Le Bellac *Thermal Field Theory*, Cambridge university Press, 1996.

[23] M. Troyer et al. Phys. Rev. B **50**, 13515 (1994).

[24] J. Sagi, I. Affleck, Phys. Rev. B **53**, 9188 (1996).

[25] J. Kishine and H. Fukuyama, J. Phys. Soc. Jpn. **66**, 26 (1997).

[26] R. Citro and E. Orignac, Phys. Rev. B **65**, 134413 (2002).

[27] H.J. Schulz, Phys. Rev. B **34**, 6372, (1986).

[28] I. Affleck, J. Phys. Condens. Matter **1**, 3047 (1991).

[29] D.G. Shelton, A.A. Nersesyan and A.M. Tsvelik, Phys. Rev. B **53**, 8521 (1996).

[30] A.A. Nersesyan and A.M. Tsvelik, Phys. Rev. Lett. **78**, 3939 (1997).

[31] A.K. Kolezhuk and H.-J. Mikeska, Phys. Rev. B **56**, R11380 (1997).

[32] F.D.M. Haldane, Phys. Rev. Lett. **50**, 1153 (1983); Phys. Lett. A **93**, 464 (1983).

[33] D. Poilblanc, H. Tsunetsugu and T.M. Rice, Phys. Rev. B **50**, 6511 (1994).

[34] S.R. White, Phys. Rev. B. **53**, 52, (1996).

[35] Y. Nishiyama, N. Hatano, adn M. Suzuki, J. Phys. Soc. Jpn. **64**, 1967 (1995).

[36] A.K. Kolezhuk and H.-J. Mikeska, Int. J. Mod. Phys. B **12**, 2325 (1998).

[37] A. H. MacDonald, S. M. Girvin, and D. Yoshioka, Phys. Rev. B **37**, 9753 (1988), **41**2565 (1990).

[38] M. Takahashi, J. Phys. C **10**, 1289, (1977).

[39] M. Roger, J. H. Hetherington, and J.M. Delrieu, Rev. Mod. Phys. **55**,1 (1983).

[40] H. J. Schmidt and Y. Kuramoto, J. Phys. C **167**, 263 (1990).

[41] Y. Honda, Y. Kuramoto, and T. Watanabe, Phys. Rev. B **47**, 11329 (1993).

[42] R. Coldea et al. Phys. Rev. Lett. **86**,5377 (2001).

[43] S. Brehmer et al.Phys. Rev. B **60**, 329 (1999).

[44] M. Matsuda et al.J. Appl. Phys. **87**, 6271 (2000).

[45] R. S. Eccleston et al. Phys. Rev. Lett. **81**, 1702 (1998).

[46] M. Windt et al. Phys. Rev. Lett. **87**, 127002 (2001).

[47] T. Imai et al. Phys. Rev. Lett. **81**, 202 (1998).

[48] T. S. Nunner et al. cond-mat /0203472.

[49] K. Hijii and K. Nomura, Phys. Rev. B **65**, 104413 (2002).

[50] T. Hikihara, T. Momoi, and X. Hu, Phys. Rev. Lett. **90**, 087204 (2003).

[51] A. Läuchli, G. Schmid, and M. Troyer, Phys. Rev. B **67**, 100409 (2003).

[52] A. Bühler, U. Löw, K. Schmidt, and G. Uhrig, Phys. Rev. B **67**, 134428 (2003).

[53] A.K. Kolezhuk and H.-J. Mikeska, Phys. Rev. B **53**, R8848 (1996).

[54] M. Roji and S. Miyashita, J. Phys. Soc. Jap. **65**, 883 (1996)

[55] A.A. Nersesyan, A.O. Gogolin and F.H.L. Essler, Phys. Rev. Lett. **81**, 910 (1998).

[56] E.H. Kim and J. Sólyom Phys. Rev. B **60**, 15230 (1999).

[57] D. Allen, F.H.L. Essler and A.A. Nersesyan, Phys. Rev. B **61**, 8871 (2000).

[58] E.H. Kim, G. Fáth, J. Sólyom and D.J. Scalapino, Phys. Rev. B **62**, 14965 (2000).

[59] K. Kopinga, A.M.C. Tinus and W.J.M. deJonge, Phys. Rev. B **25**, 4685 (1982); Phys. Rev. B **29**, 2868 (1984).

[60] C. Dupas and J.P. Renard, J. Phys C **10**, 5057 (1977).

[61] I. Affleck, in *Champs, Cordes et Phénomènes Critiques/ Fields, strings and critical phenomena*, Eds. E. Brézin and J. Zinn-Justin, Elsevier, Amsterdam, (1990).

[62] A.O. Gogolin, A.A. Nersesyan and A.M. Tsvelik, *Bosonization and Strongly Correlated Systems*, Cambridge University Press (1999).

[63] For exact vacuum expectation values of vertex operators in sine-Gordon model see S. Lukyanov and A. Zamolodchikov, Nucl.Phys. B **493**, 5121(1997).

[64] S. Lukyanov, V. Terras, Nucl.Phys. B **645**, 323 (2003).

[65] T. Hikihara and A. Furusaki, Phys. Rev. B **58**, R583 (1998).

[66] J.M. Kosterlitz and D.J. Thouless, J. Phys. C **6**, 1186 (1973).

[67] K. Kubo, Phys. Rev. B **46**, 866 (1992).

[68] A. Kitazawa, K. Nomura and K. Okamoto, Phys. Rev. Lett. **76**, 4038 (1996).

[69] S. W. Lovesey, *Theory of neutron scattering from condensed matter*, Oxford University Press, 1984.

[70] E. Fradkin and L. Susskind, Phys. Rev. D**17**, 2637 (1978).

[71] H. J. Schulz and C. Bourbonnais, Phys. Rev. B **27**, 5856 (1993).

[72] M. Müller, T. Vekua, and H.-J. Mikeska, Phys. Rev. B **66**, 134423 (2002).

[73] T. Vekua G. I. Japaridze, and H.-J. Mikeska, Phys. Rev. B **67**, 064419 (2003).

Thanks

I am grateful to Prof. Dr. H.-J. Mikeska for interesting topic, his guidance and for his permanent support.

I thank G. Japaridze for acquainting me with 1D physics, for collaboration and support at various levels of my studies.

I thank A. Kolezhuk for always being available for valuable discussions.

I thank K. Totsuka for active discussions while his stay at Hanover.

I thank Abdus Salam international center of theoretical physics for opportunity to stay and carry out part of my work in Trieste where fruitful discussions with A. Nersesyan and Y.-J. Wang are gratefully acknowledged.

I want to express my sincere thanks to Prof. Dr. H.-U. Everts, and Prof. Dr. H. Schulz for the discussion on Luttinger liquids and other interesting topics.

I want to thank M. Müller and C. Luckmann for their help with preparing manuscript and for helping with German.

Finally I acknowledge financial support from Graduiertenkolleg ”Quantenfeldtheoretische Methoden in der Teilchenphysik, Gravitation und Statistischen Physik”during 3 years of my Ph.D. studies and for allowing me to participate in various summer schools and workshops across the Europe.

Curriculum Vitae

Date/Place of Birth May 23, 1976/ Tbilisi, Georgia

Education

1981-1993	Tbilisi 53-rd School of general education
1993-1997	Bachelor Degree student at Tbilisi State University, Physics Faculty
1997- 1999	Masters Degree student at Tbilisi State University, Physics Faculty, Department of Theoretical Physics. Master´s Thesis: “Strongly correlated 1D electronic systems”
02.2000- 07.2000	Graduate guest student at Theoretisch- Physikalisches Institut, Friedrich- Shiller Universität Jena
From 07.2000-	Ph.D. Student, Institut Für Theoretische Physik, Uni- Hannover, member of Graduiertenkolleg ”Quantenfeldtheoretische Methoden in der Teilchenphysik, Gravitation und Statistischen Physik”

Publications

F. Bruckmann, T. Heinzl, T. Vekua, A. Wipf:
“Magnetic monopoles vs. Hopf defects in the Laplacian (Abelian) gauge”,
Nucl. Phys. B **593**, 545 (2001).

M. Müller, T. Vekua, and H.-J. Mikeska:
“Perturbation theories for S=1/2 spin ladder with a four-spin ring exchange ”,
Phys. Rev. B **66**, 134423 (2002).

T. Vekua, G.I. Japaridze, and H.-J. Mikeska:
“Phase diagrams of spin ladders with ferromagnetic legs”,
Phys. Rev. B **67**, 064419 (2003).